# MODELING LONG-TERM DYNAMIC EFFECTS OF BRAIN INJURY ON BIOLOGICAL MECHANISMS OF POTENTIAL PARKINSON'S DISEASE PROGRESSION

by

Nezihe Nazlı Gül

B.S., Industrial Engineering, Yıldız Technical University, 2019

Submitted to the Institute for Graduate Studies in
Science and Engineering in partial fulfillment of
the requirements for the degree of
Master of Science

Graduate Program in Industrial Engineering

Boğaziçi University

2023

# ACKNOWLEDGEMENTS

First and foremost, I would like to thank my supervisor Assoc. Prof. Gönenç Yücel for his continuous support in coordination and administration issues. I would like to express my gratitude to my co-supervisor Prof. Yaman Barlas for his guidance and inspiration throughout my studies. His intellectual enthusiasm has played a significant role in shaping my academic career. For their contribution with their insightful suggestions from various perspectives, I am grateful to Assist. Prof. Özge Karanfil and Assoc. Prof. Aybek Korugan as members of my thesis committee, and Prof. Başar Bilgiç.

I would like to thank all of my dear friends who have appointed themselves in charge of the morale. Special thanks to my dear housemate Eda Özden for her unwavering friendship and Yunus Emre Kırlı for brightening my life by being by my side whenever and wherever I need him.

Last but not least, I express my very profound gratitude to my family members, my dear mother Ferhan Gül for her unfailing motivation and positive energy, and my dear brother Denizhan Gül for providing me with continuous encouragement and guidance throughout my life. I would also like to thank my lovely cat Bambu for all the entertainment and emotional assistance. I could not have completed this study without the invaluable support of my family and friends.

I dedicate this thesis to my beloved father Ayhan Gül, who passed away during my graduate studies, for his endless support and love I feel every moment.

# ABSTRACT


## MODELING LONG-TERM DYNAMIC EFFECTS OF BRAIN INJURY ON BIOLOGICAL MECHANISMS OF POTENTIAL PARKINSON'S DISEASE PROGRESSION

Parkinson's disease (PD), the second most common neurodegenerative disorder affecting over ten million people worldwide, is a multifactorial disease influenced by several biological and environmental factors. Complex interactions controlled by feedback relationships between neuroinflammation, oxidative damage, mitochondria, protein accumulation, and neuron sub-systems are at the center of the brain. While some lifestyle elements reduce vulnerability, head trauma raises the risk for PD. Trauma-induced neuroinflammation is the most prominent short-term consequence, and due to the intricate structure of the brain, multiple variables are affected in the long-term. To study those impacts on potential PD progression, we constructed an individual-level system dynamics model of a specific brain region where dopamine-producing neurons reside. After obtaining the normal aging dynamics, various brain injury scenarios are investigated to see whether healthy individuals would exhibit PD-like behaviors. Then, possible genetic variation and/or lifestyle factors such as healthy diet and exercise are tested on both healthy and PD-prone people. The difficulties in monitoring and quantifying brain-related variables are the primary challenges for this research because only post-mortem analysis allows for neuropathological diagnosis. The model is structurally and behaviorally validated using the qualitative and quantitative knowledge of autopsy reports and animal experiments. In scenario runs, we observed the impact of several external and internal factors. The research aims to provide a comprehensive understanding of relevant brain dynamics in interaction with external factors and identify effective mechanisms for treatment and prevention strategies for PD. This work is open to development by including discoveries from field data and empirical studies.

# ÖZET

## BEYİN HASARININ OLASI PARKİNSON HASTALIĞI OLUŞUMUNDAKİ BİYOLOJİK MEKANİZMALAR ÜZERİNDE UZUN DÖNEMLİ DİNAMİK ETKİLERİNİN MODELLENMESİ

Dünya çapında on milyondan fazla kişiyi etkileyen en yaygın ikinci nörodejeneratif hastalık olan Parkinson hastalığı (PH), biyolojik ve çevresel faktörlerden etkilenir. Nöroinflamasyon, oksidatif hasar, mitokondri, protein birikimi ve nöron alt sistemleri arasındaki geri besleme ilişkileri tarafından kontrol edilen karmaşık etkileşimler beynin yapıtaşlarını oluşturur. Bazı yaşam tarzı unsurları PH riskini azaltırken, kafa darbesi riski artırır. Travmaya bağlı nöroinflamasyon kısa dönemde gözlenen en belirgin sonuçtur. Beynin karmaşık yapısı, uzun vadede çeşitli değişkenlerin etkilenmesine sebep olur. Bu çalışmada, beyin hasarının PH gelişimi üzerindeki uzun vadeli etkilerini incelemek için, dopamin üreten nöronların bulunduğu beyin bölgesinin sistem dinamiği modeli kurulmuştur. Normal yaşlanma dinamikleri elde edildikten sonra, bireylerin PH benzeri davranışlar sergileyip sergilemediği darbe senaryoları ile incelenmiştir. Sonrasında, sağlıklı beslenme ve egzersiz gibi yaşam tarzı faktörleri ve/veya genetik çeşitlilik unsurları, normal ve PH-yatkın kişi senaryoları üzerinde test edilmiştir. Beyinle ilgili değişkenlerin ölçülmesi ve gözlemlenmesi araştırmanın temel zorluklarıdır. Yalnızca ölüm sonrası analiz nöropatolojik tanıya izin vermektedir. Böylece, otopsi raporları ve hayvan deneylerinden elde edilen nitel ve nicel veriler kullanılarak modelin yapısal ve davranışsal geçerliliği test edilmiştir. Senaryo koşumlarında, çeşitli iç ve dış faktörlerin etkileri gözlemlenmiştir. Araştırmanın amacı, dış etkenlerle etkileşimde ilgili beyin dinamiklerinin kapsamlı şekilde anlaşılmasını sağlamak ve PH tedavi/önleme stratejileri için etkili mekanizmaları belirlemektir. Bu çalışma, saha verilerinden ve ampirik çalışmalardan elde edilecek bulguları içerecek şekilde geliştirilmeye açıktır.

# TABLE OF CONTENTS

# LIST OF FIGURES

# LIST OF TABLES

# LIST OF ACRONYMS/ABBREVIATIONS

| | |
|---|---|
| AD | Alzheimer's Disease |
| ATP | Adenosine Triphosphate |
| BDNF | Brain-Derived Neurotrophic Factor |
| FU | Fluorescence Unit |
| GSH | Glutathione |
| HNE | 4-hydroxy-2-nonenal |
| IL-10 | Interleukin 10 |
| LB | Lewy Body |
| M1 Microglia | Classical Microglia |
| M2 Microglia | Alternative Microglia |
| MCIA | Mitochondrial Complex I Activity |
| mg | Milligram |
| $\mu$g | Microgram |
| mtDNA | Mitochondrial DNA |
| ND | Neurodegenerative Disease |
| PD | Parkinson's Disease |
| PGPH | Peptidyl glutamyl-peptide hydrolytic |
| ROS | Reactive Oxygen Species |
| SN | Substantia Nigra |
| pg | Picogram |
| PGPH | Peptidyl glutamyl-peptide hydrolytic |
| TBI | Traumatic Brain Injury |
| TNF-$\alpha$ | Tumor Necrosis Factor Alpha |
| UPS | Ubiquitin–Proteasome System |
| WHO | World Health Organization |

# 1. INTRODUCTION

The most complex entity in the human body, brain, governs several essential biological mechanisms. It serves as the control center of the nervous system, therefore, its functions are tightly regulated. To protect brain, the blood-brain barrier separates serum factors and neurotoxins [1]. This characteristic property makes it challenging to study changes in brain metabolites and functions. Because neuropathological diagnosis can only be carried out through an autopsy after death [2]. Neurons are the building blocks of brain, however, they are post-mitotic cells. It means destroyed neurons cannot be renewed, and the average number of neurons inevitably decreases during aging [3], which results in anatomical and chemical changes in the brain [4]. Consequently, the burden of neurodegenerative disorders and the difficulties in maintaining brain health rise as the population ages [5].

Disorders of the nervous system that are characterized by the death of neurons over time are referred to as neurodegenerative diseases (NDs). The inability of neurons to regenerate themselves ultimately leads to cell death [6]. Some well-recognized forms of NDs are Alzheimer's disease, Parkinson's disease, multiple sclerosis, Huntington's disease, and amyotrophic lateral sclerosis. These diseases' pathophysiologies vary, some of them lead to problems with cognition while others impair one's mobility abilities [7–9]. A report conducted in 2006 by World Health Organization (WHO) indicates that the neurological burden will continue to worsen and pose an unmanageable public health threat unless global action is taken immediately [10]. In 2022, WHO supported the "Intersectoral global action plan on epilepsy and other neurological illnesses 2022-2032" [11]. Available medications for NDs only help relieve symptoms and cannot prevent or cure diseases. Therefore, early diagnosis is crucial, as it can slow down further progression [12].

Parkinson's disease (PD), an idiopathic condition with motor and non-motor symptoms, is the second most common ND after Alzheimer's disease [13]. According

to Parkinson's Foundation, in the United States, one million people are living with PD, and 90,000 new cases are diagnosed annually. The total number of affected people is expected to be more than 10 million worldwide [14]. In developed nations, about 1% of people over the age of 60 are impacted by PD [15]. The affected population percentage rises dramatically and reaches more than 4% after the age of 60 years [16]. Based on PD-related mortality from 114 different nations from 1994 to 2019, an estimated 1,064,753 people died [17]. According to the global incidence and prevalence data, the risk of developing PD is higher in men than women. This disparity widens with age. While the prevalence of PD is 2,000 per 100,000 individuals for the 80+ age group in men, it is approximately 1,500 in women of the same age. In terms of incidence rates for this age range, men are approximately 2.5 times more at risk [18].

The age-standardized prevalence of PD differs more than five times by country, with sub-Saharan Africa having the lowest rates while high-income North America has the highest rates [19]. In addition to health risks, PD poses a great economic threat since it cost the United States economy $51.9 billion in 2017, including direct costs ($37.7 billion) and indirect costs ($14.2 billion). The total economic burden in the United States is expected to increase to about $79.1 billion in 2037 [20].

Disease symptoms include bradykinesia, tremor, gait abnormalities, postural instability, and lack of facial expression. Unilateral symptoms develop into bilateral ones over time. Additionally, non-motor brain regions are affected, leading to cognitive decline, depression, and sleep disorders in later phases [21]. The time course of PD is long including several stages with a variety of motor and non-motor symptoms. The most frequently cited study for estimates of neuronal loss shows that the amount of neurons lost at symptom onset for PD is approximately 31% [22]. Given the absence of a particular clinical diagnosis for the disease, 50-60% of dopaminergic neurons are already lost before the diagnosis [23].

In the prodromal stage, individuals exhibit non-motor symptoms such as sleep disturbances, constipation, depression, and anxiety. As the prodromal stage nears its

end, characteristic motor symptoms including bradykinesia, tremor, and rigidity become evident. These symptoms are further accentuated during the early stage, enabling the diagnosis of the disease. While the early stage is marked by the exacerbation of these symptoms, the later stages of PD witness the emergence of additional motor and non-motor symptoms, which further complicate the disease progression and contribute to the severity of the condition [18].

Reduced dopamine levels resulting from the loss of dopaminergic (dopamine-producing) neurons in the substantia nigra of brain and the emergence of abnormal aggregates known as Lewy bodies are the pathological definitions of PD. Lewy bodies are primarily composed of toxic and insoluble forms of alpha-synuclein proteins [24]. PD is a multifactorial ND that is influenced by many mechanisms [25]. The accumulation of misfolded alpha-synuclein proteins, disruption of protein clearance pathways, mitochondrial dysfunction, oxidative damage, and neuroinflammation are the most prominent factors that contribute to the progression of PD [26, 27]. Vicious cycles result from the positive feedback mechanisms among these variables, and PD permanently impairs a person's brain functions.

The majority of PD cases have a complex etiology that involves a combination of genetic and environmental determinants. According to a study comparing the susceptibility of twins to PD, environmental and behavioral variables played a significantly larger role in the etiology of this disease than inherited ones [28]. While some lifestyle elements such as a healthy diet and regular exercise reduce the risk, exposure to toxic substances and head trauma raise the risk [29]. Several NDs have been linked to brain injury, but the greatest evidence points to the development of PD [30]. Trauma-induced neuroinflammation is the most reasonable explanation for the connection between brain injury and PD [31]. Following the initial injury, neuroinflammation might last for years in the damaged regions [32].

A disruption in brain function driven by an external factor, such as falls, accidents, or sports-related injuries, is known as traumatic brain injury (TBI). Concussion is the

most widespread TBI and its symptoms range from mild to severe. The majority of brain injuries are repetitive and mild, therefore, neuroimaging cannot detect them [33]. The risk of having PD in later life is 56% greater for veterans with a history of TBI [30]. The high proportion of TBIs in the United States occurs in men, who are also two times more likely to have PD diagnosed than women [34,35]. Athletes participating in contact sports are frequently at risk of brain injuries and suffering cognitive impairment [36]. The link between TBI and PD gained more attention when the world-famous boxer Muhammed Ali was diagnosed with this condition.

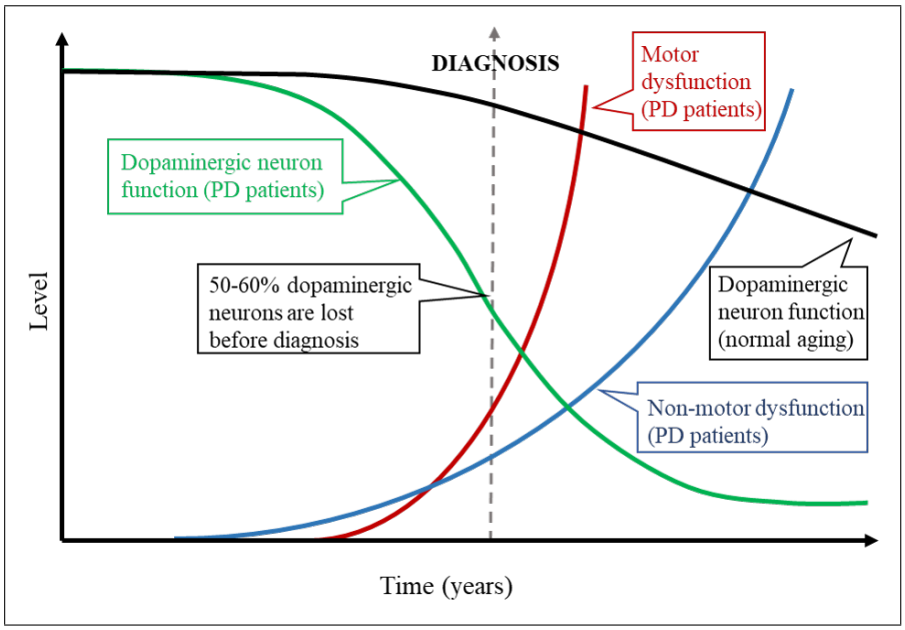


Figure 1.1. Clinical dysfunctions in Parkinson's disease (based on [23, 37]).

This study aims to construct an individual-level model of substantia nigra, a region in the brain where dopaminergic neurons reside, to capture the long-term effects of brain injury on potential pathways leading to PD progression. After obtaining the normal aging dynamics of a brain, injury scenarios with different characteristics are examined to see whether healthy individuals develop PD-like behavior. Finally, possible lifestyle factors such as a healthy diet and regular exercise, and potential protective strategies are evaluated on both normal and PD-prone (due to brain injuries) individuals. Future research on successful therapies and preventative measures is likely

to benefit from an understanding of the potential link between PD and TBI, thanks to dynamic simulation models with a systemic approach.

In the second chapter, the literature about ND, PD, and TBI modeling is summarized. Next, the objective of the study and research methodology are explained. The compatibility of the system dynamics approach for individual-level health modeling is emphasized. The fourth chapter provides an overview of the model and the key causalities between different mechanisms. In the fifth chapter, stock-flow diagrams are developed together with mathematical equations of variables based on medical studies and assumptions. The sixth chapter examines, tests, and validates the model. After obtaining the base behavior (normal aging), the seventh chapter investigates the model sensitivity to different parameter values and initial conditions. The eighth chapter focuses on the association between various properties of brain traumas and PD. Later, possible genetic variance and/or lifestyle elements such as a healthy diet and regular exercise are tested on both healthy and PD-prone people. Finally, a summary of the findings appears in the conclusion chapter.

# 2. LITERATURE REVIEW

This section presents an overview of the existing mathematical models established in the field of neurodegenerative diseases (NDs), especially for Parkinson's disease (PD). Publications on these topics have covered the issue in various scopes and methodologies. After highlighting the importance of a holistic approach in health systems modeling, some mathematical models in the field of PD will be discussed. These studies are critical for comprehending key variables and expressing how they affect the human body. Later, ND models employing the system dynamics technique will be summarized. Finally, traumatic brain injury (TBI)-related system dynamics models are presented.

For researchers to gain a good understanding of the whole system, many pieces of information need to be integrated with a more holistic approach, as the Greek philosopher Aristotle said, "The whole is more than the sum of its parts". For this purpose, the development of many system-level models in the field of human health has been studied by scientists [38]. Recently, systems biology approaches have provided a lot of experimental data. However, due to the complexity of the neurodegeneration process, the underlying molecular mechanisms of NDs are still not fully understood [39]. An integrative strategy incorporating empirical and modeling research is necessary. In parallel with the collection of new data, mathematical models of PD have been constructed, and they address a number of the mechanistic facets of disease pathogenesis [40].

In 2019, Bakshi and coworkers constructed a simplified version of the complex network of interactions underlying PD pathogenesis from their existing knowledge. This map provides viewpoints for PD investigation, however, it appears to concentrate on one-level connections. Thus, several causal links and feedback loops are lacking. Further, they classified the mathematical biology of mechanistic PD models into three groups: (1) alpha-synuclein aggregation, (2) pathogenesis, and (3) pathology propagation. The size of mechanistic models varies depending on the investigated molecular pathways and feedback relations [40].

Alpha-synuclein models try to derive parameters involved in the protein aggregation process. For this purpose, the impact of temperature and pH [41], metal ions [42], lipid membranes [43], and mutations [44] are examined. These studies implement mathematical models to fit kinetic data of experimental accumulation. To obtain a quantifiable amount of aggregated alpha-synuclein, they use high concentrations, whereas it is unclear if the aggregation kinetics vary at lower levels as in the human brain. These models have the disadvantage of assessing disease only through alpha-synuclein toxicity, however, there are other sources of toxicity such as reactive species and inflammatory mediators involved in PD pathogenesis.

Existing pathogenesis models of PD focus on some or all interactions between toxic alpha-synuclein protein, dopamine metabolism, and reactive species in various levels of detail. Raichur and colleagues built the first ordinary differential equations model for PD pathogenesis. They studied the different pathways for the generation of reactive species [45]. By including mitochondrial dysfunction and glutathione metabolism, this model was expanded. It is hypothesized that a decline in mitochondrial efficiency has an impact on glutathione production via reduced levels of Adenosine triphosphate (ATP), the source of energy for use and storage at the cellular level in human body. This may then lead to an increase in reactive species and a subsequent failure in mitochondria [46]. In another study, alpha-synuclein aggregation and its association with protein degradation mechanisms are theoretically modeled. The authors anticipated that persistent reduction of protein clearance systems may result in alpha-synuclein accumulation [47].

According to the research conducted by Braak and colleagues, misfolded alpha-synuclein aggregations spread across regions connected to the brain [48]. This propagation of pathological alpha-synuclein aggregates has received less attention compared to previously proposed models, likely due to the complex nature of brain geometry and anatomical connections. In a study, alpha-synuclein transport mechanisms are modeled to study PD [49]. Instead of PD-specific models, there exist several generic models for pathology propagation.

System dynamics studies have generally focused on examining the Alzheimer's disease (AD) population changes over time in terms of ND modeling. One paper focused on the Czech population to predict the AD population until 2100 [50]. Also, the spread of AD in the European Union population until 2080 has been modeled [51]. Another study used system dynamics modeling approach to examine the interaction of many key factors on the life course of individuals, including vascular, lifestyle, and psychological aspects, to better understand the incidence rate of AD [52]. In China, the world's largest population is aging rapidly, consequently, AD-related dementia patients are expected to rise. A multi-state dynamic population model is developed up to the year 2060 with age and gender-specific transition rates to project this rise [53]. A brain aging and/or PD pathogenesis model using system dynamics methodology is not present in the literature to our current knowledge.

Depending on the modeling purpose, TBI-related system dynamics models are classified into three categories: (1) acute injury dynamics, (2) complex recovery dynamics, and (3) care delivery [54]. Acute injury models focus on the short-term acute phase of the brain injury up to 10 days post-injury, whereas recovery models take into consideration longer periods to capture the potential recovery trajectories. On the other hand, the main focus of care delivery models is identifying the affected population.

Kochis et al. developed a computational model for the bloodstream over time following a TBI to identify the time course of potential biomarkers for the first 7-10 days [55]. Vaughan et al. constructed a differential equations model of the interactions between pro- and anti-inflammatory mediators, microglia, and tissue damage for the first 5 days post-injury [56]. To define the complex recovery dynamics, a causal loop diagram of mild TBI recovery through literature review, group modeling, and individual interviews with experts is presented across cellular, network, experimental, and social levels [57]. The same authors presented a computational model based on this causal loop diagram simulated up to 42 days post-injury to estimate recovery trajectories for various severities of TBIs [58]. The impact of patient flow [59] and the current and future prevalence of affected people [60] are studied in the scope of care delivery models.

In summary, the neurological mechanisms underlying PD are not yet fully understood or modeled. AD obtains the main focus in the context of neurodegeneration models, and ordinary differential equations represent the majority of these methods. The developed mathematical models often only include one feedback loop, hence they are unable to represent the dynamics of the whole system. To capture the multifactorial nature of PD, related components should be integrated to include synergistic impacts. In addition, models in the literature often perform analyses by creating PD individuals with excessive alpha-synuclein load, rather than associating the disease state with potential factors. When examined in terms of system dynamics methodology, there is very limited research. All ND papers utilize population-level AD models that focus on the size of the affected population rather than the underlying biological mechanisms. Individual (patient)-level TBI-related system dynamics models are short-term. They focus on the dynamics in the acute and recovery phases post-injury and do not consider the potential connection between PD and TBI-induced neuroinflammation.

# 3. PROBLEM DEFINITION AND RESEARCH METHODOLOGY

The human body in general, and brain in particular, are extremely dynamic closed systems that are internally driven by several positive and negative feedback loops and have delays with nonlinearities by their nature. Negative (balancing) loops try to keep the system at equilibrium. Thus, these loops are activated when there are abnormal levels of biological materials or activities with hazardous impacts. Neuroprotection is triggered as a result of damaged neurons to prevent further neuronal damage and death. Antioxidant system mediators are used to neutralize oxidative damage. Protein degradation and neuroinflammation are two separate negative feedback mechanisms used in the destruction of toxic proteins accumulated in the brain. While negative feedback mechanisms function effectively in young individuals to balance the system, their performance declines as people age and results in irreversible brain damage. Compared to normal people, the changes that take place in Parkinson's disease (PD) patients are considerably more drastic, which poses a serious threat to aged individuals.

Positive (reinforcing) feedback loops, on the other hand, lead to a variety of alterations in the aging brain. Especially in PD patients, those alterations are more prominent and result in severe damage to brain functions related to the dopamine system. As the human brain ages, the substantia nigra cannot remain at equilibrium because of the decrease in the functions of regulatory systems, mitochondrial DNA mutations that occur over time, accumulation of oxidative stress, and the complex network in which these changes affect each other simultaneously. In addition, some protective mechanisms become dangerous due to their excessive functioning such as neuroinflammation. Normally, acute neuroinflammation protects neurons from further damage by clearing toxic proteins and dead neurons. However, their functions also produce oxidative stress which has toxic effects. Therefore, in the presence of chronic neuroinflammation with insufficient antioxidant activity, oxidative damage triggers more disruption to dopaminergic neurons.

The biological processes in the brain are interconnected through a variety of non-linear relationships. Therefore, it is crucial to comprehend the progressive alterations as individuals age and to observe how these changes accelerate in patients with PD. As the human lifespan gets longer, the population affected by such neurological disorders increases. Future research on successful therapies and preventative measures is likely to benefit from gaining more insight into these incurable diseases.

In the literature, there is no individual (patient)-level system dynamics model focusing on the relationship between PD and traumatic brain injury (TBI). The proposed models for PD pathogenesis are far from a holistic approach. They are short-term and study the relationship of one or few mechanisms within a limited scope. They tend to have a partial understanding of the system by only focusing on one-way cause-and-effect relationships between variables rather than circular causalities. Additionally, most models analyze the condition by developing hypothetical patients instead of examining pathways that may lead to disease conditions. By simulating the problem using system dynamics method, this study aims to close this gap in the literature. Future research on effective therapeutics and prevention measures is anticipated to gain from a better understanding of the probable relationship between PD and TBI.

This work focuses on simulating substantia nigra alterations that impair the dopamine system in elderly people with system dynamics approach. A long-term quantitative model at individual (patient)-level is constructed. The scope of the study is framed around the altered biological mechanisms with aging that have been consistently at the center of PD pathogenesis research and simulating whether exposure to external TBIs may cause individuals to exhibit Parkinsonian-like behaviors in long-term. In the literature, most papers investigate the PD condition with pooled analyzes without the distinction between men and women. Therefore, the values of a 30-year-old healthy person are utilized as the initial parameters. Some age-related abnormalities which are considered normal aging dynamics can be seen when parameters are fed into the model. However, these changes are significantly pronounced in people with PD, as evidenced by toxic protein aggregation and the rapid depletion of dopaminergic neurons. After

establishing a model that exhibits normal brain aging dynamics, it is validated by comparing the results with real data and cases.

Using the values of brain-related variables with autopsy reports poses a great challenge for this study. To overcome this, post-mortem analyses of normal individuals of various ages are investigated to depict real-life behaviors. When those analyses are inadequate, the fold changes specified during aging in rodent experimental studies or expert reviews are utilized. Thus, by putting together all available knowledge, reference behaviors for the stock variables are established.

Many subsystems are involved in the progression of biological changes in the brain. It is quite challenging to predict how this complex system, which contains many nonlinear dynamics in its structure, would behave. Instead of making point estimates, the goal is to project the dynamic patterns. System dynamics methodology is thus a promising tool for studying brain aging and scenarios including external and/or internal factors to go beyond qualitative study. This methodology is based on direct causalities focusing on feedback mechanisms and their resulting dynamics. It is appropriate for large-scale systems with many causal loops, nonlinearities, accumulations, and delays. It enables simulating feedback loops in interaction and provides a holistic representation of complex models whose behaviors cannot be obtained by mathematical analysis. It helps us conduct tests on systems, understand their structure, and develop better policies. Furthermore, we can conduct experiments with different external and internal conditions which are neither practical nor ethical to carry out on a real human body.

# 4. OVERVIEW OF THE MODEL

Physiological systems are coordinated through feedback loops. Homeostasis is lost if one of those mechanisms fails to sustain the desired level of activity. We modeled the interactions among factors underlying the depletion of dopaminergic neurons in substantia nigra during aging. It is intended to investigate the impact of brain traumas on the development of Parkinson's disease (PD) after acquiring the dynamics of healthy normal aging. Considering the purpose of our model, we have determined the key variables that have been at the center of PD pathogenesis.

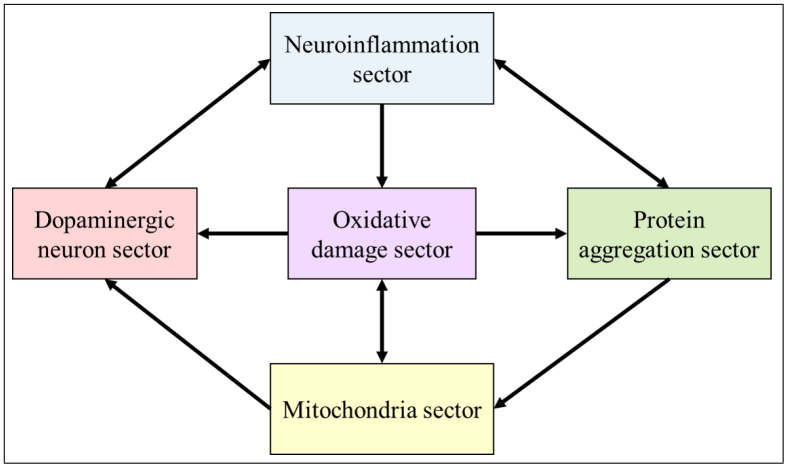


Figure 4.1. Interactions between model sectors.

Our model has five sectors: (1) neuroinflammation, (2) protein aggregation, (3) dopaminergic neuron, (4) oxidative damage, and (5) mitochondria. Intersectoral feedback mechanisms are illustrated in Figure 4.1. These causal relationships generate the dynamic behavior of the whole system. Inflammation in the brain or spinal cord is referred to as neuroinflammation. The production and release of pro- and anti-inflammatory mediators control this process [61]. Alpha-synuclein is an unfolded protein predominantly expressed in neurons. Its fibrillization results in pathological forms which are linked to neurodegeneration [62]. Dopaminergic neurons are the primary source of dopamine in the central nervous system [63]. The disequilibrium between the

levels of reactive oxygen species (ROS) and the ability to detoxify them is called oxidative stress. Proteins, DNAs, and organelle activities are damaged by oxidative stress [64]. Mitochondria are the main source of energy for the metabolic pathways [65].

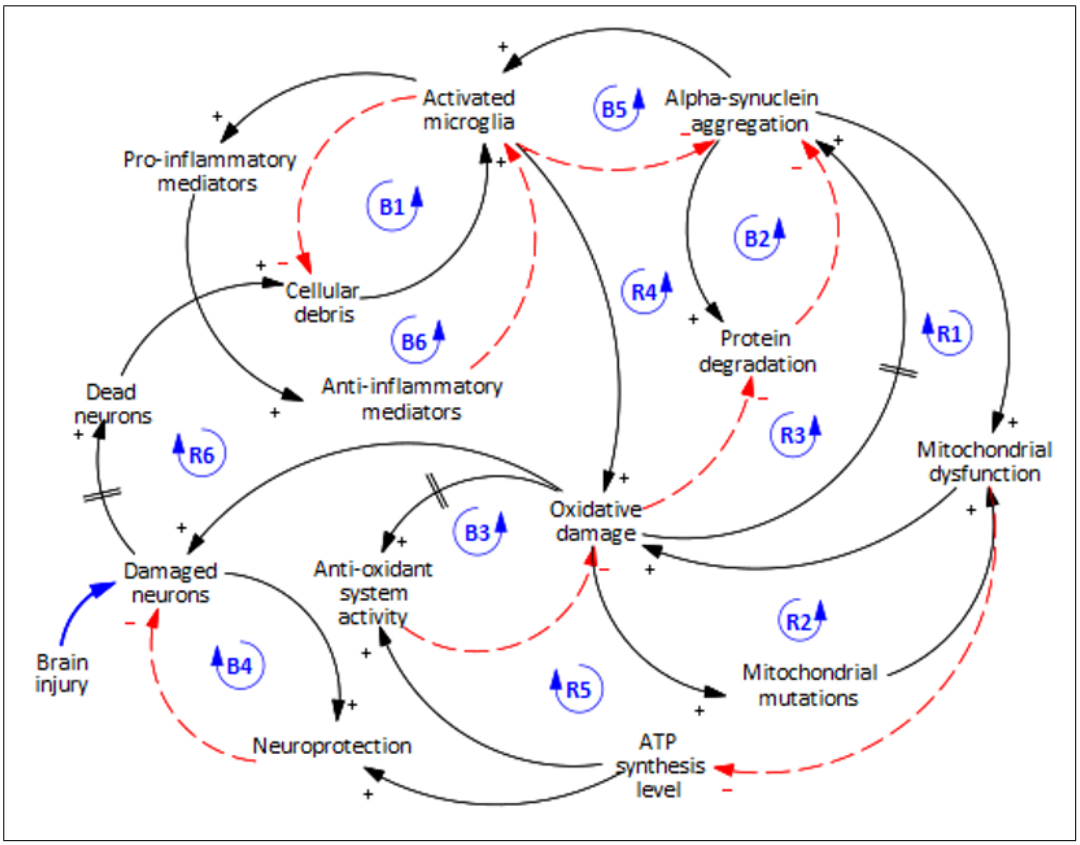


Figure 4.2. Causal loop diagram of the model.

The causal loop diagram in Figure 4.2 summarizes the interactions between the main variables in the system. An arrow linking two variables represents a causal link, while the sign of an arrow indicates the direction of the causality. A feedback loop provides either reinforcing (+) or balancing (-) dynamics, depending on the multiplication of all its signs. Changes in biological mechanisms trigger balancing (negative) loops, allowing the system to return to its normal values. Reinforcing (positive) loops, in contrast, create dynamics like growth or collapse. In the case of a disorder, the system is dominated by one or more reinforcing loops. The letters B and R stand for balancing and reinforcing, respectively.

Neuronal phagocytosis loop (B1) (Figure 4.3a) enables activated microglia to remove the cellular debris of dead neurons. To restore homeostasis in the brain, microglia cells are in charge of clearing out toxicity resulting from dead neurons [66]. These cells sense molecules released by dying neurons and become activated [67].

There are two balancing loops controlling the toxic alpha-synuclein protein levels: (1) protein degradation, and (2) alpha-synuclein phagocytosis. The protein degradation activity implied in the model stands for the ubiquitin–proteasome system (UPS) which is considered to degrade soluble, misfolded, or damaged proteins [68]. This relationship is depicted in the protein degradation loop (B2) (Figure 4.3b). One of the primary pathophysiological mechanisms of PD neurodegeneration is increased alpha-synuclein aggregations that exceed the cell's ability to eliminate them [69]. Misfolded alpha-synuclein proteins are not successfully removed in the presence of overloaded UPS and transform into insoluble forms. These substances induce microglial activation and phagocytosis [67]. This second line of defense is called the alpha-synuclein phagocytosis loop (B5) (Figure 4.3e).

In response to oxidative stressors, the brain has several antioxidant defense systems [70]. Glutathione (GSH) is one of the most abundant antioxidants in the brain [71] which is utilized in our model for antioxidant regulation. This antioxidant reduces ROS by binding to those metabolites and provides protection [72]. Oxidative stress lowers the level of GSH through this chemical reaction, in response, antioxidant activity increases to restore GSH levels to the proper amount. At the same time, oxidative stressors are neutralized. These are the mechanisms of the antioxidant regulation loop (B3) (Figure 4.3c).

Neuronal protection is essential for maintaining brain health because neurons are post-mitotic cells and cannot be reproduced. Brain-derived neurotrophic factor (BDNF) is a key molecule involved in the survival of dopaminergic neurons and protection against neurotoxic effects in substantia nigra in human brain [73], thus, it is studied in the neuroprotection loop (B4) (Figure 4.3d). BDNF is expressed prominently

by dopaminergic neurons and its release rises along with the number of damaged neurons. PD patients have significantly reduced amounts of BDNF which deteriorates the disease condition. PD patients have fewer healthy neurons, consequently, lower neuroprotection capacity [74].

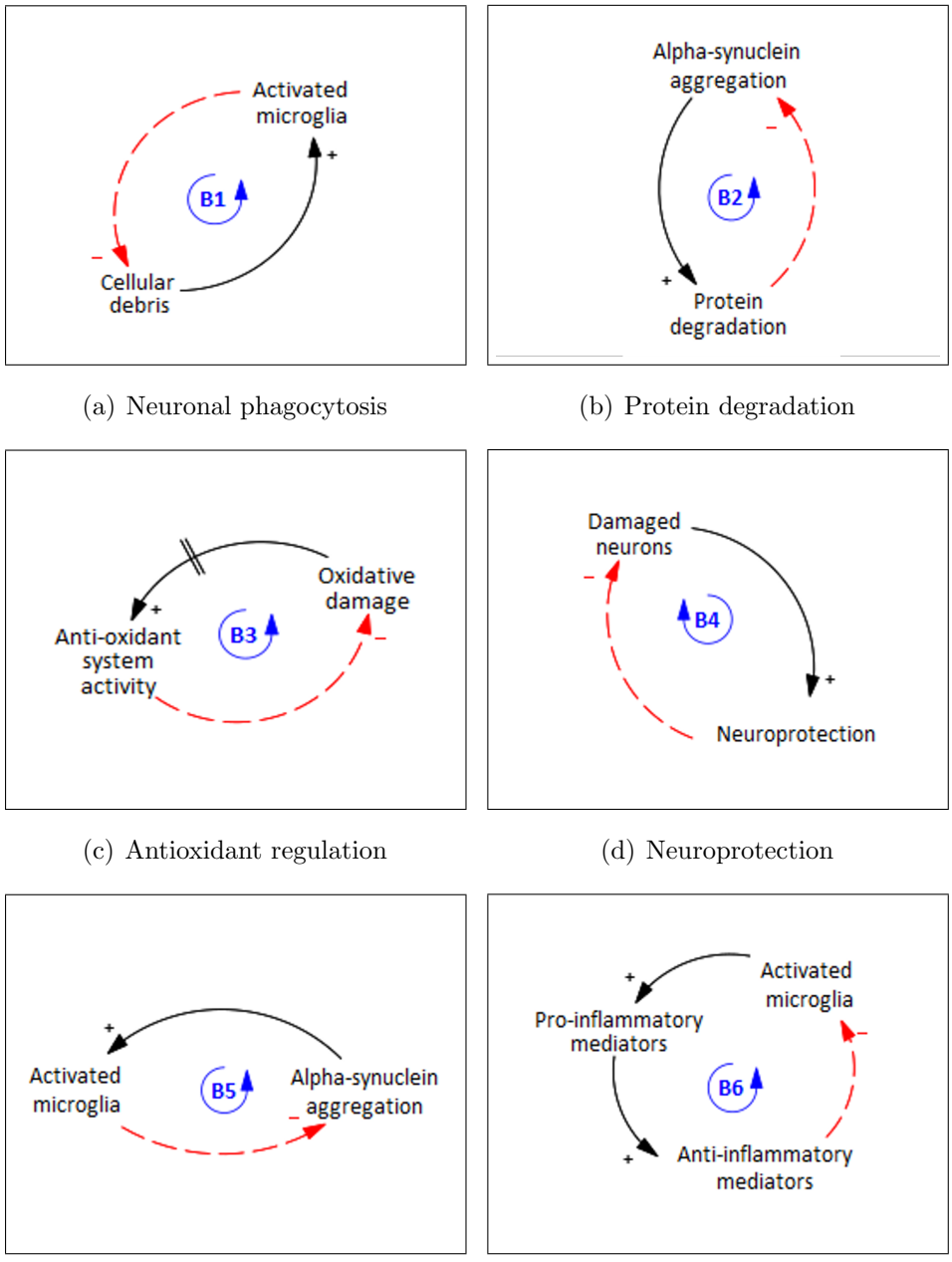


(a) Neuronal phagocytosis

(b) Protein degradation

(c) Antioxidant regulation

(d) Neuroprotection

(e) Alpha-synuclein phagocytosis

(f) Neuroinflammation

Figure 4.3. Negative (balancing) feedback loops of the model.

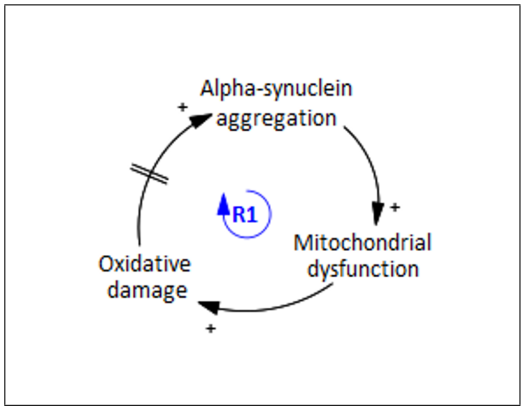


(a) Mitochondrial oxidative damage

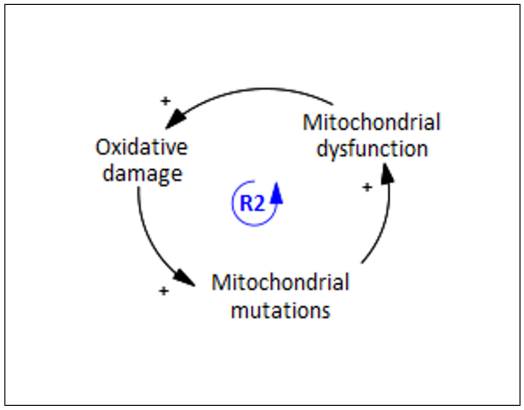


(b) Oxidative damage on mitochondria

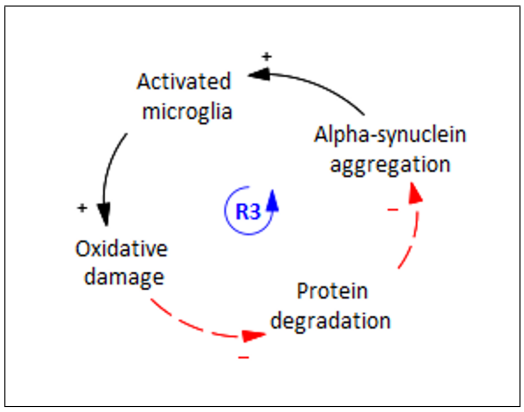


(c) Reduced protein degradation

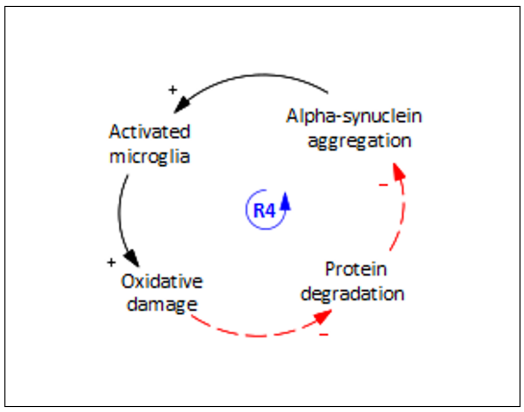


(d) Neuroinflammatory oxidative damage

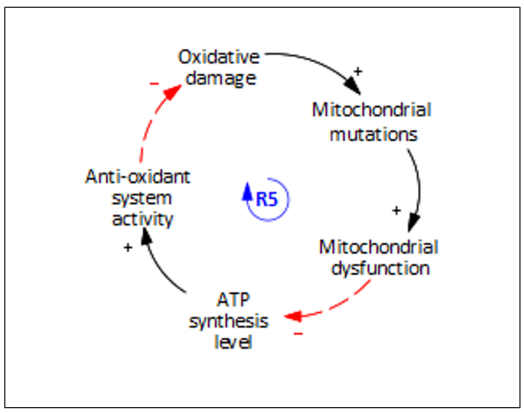


(e) ATP impact on antioxidant capacity

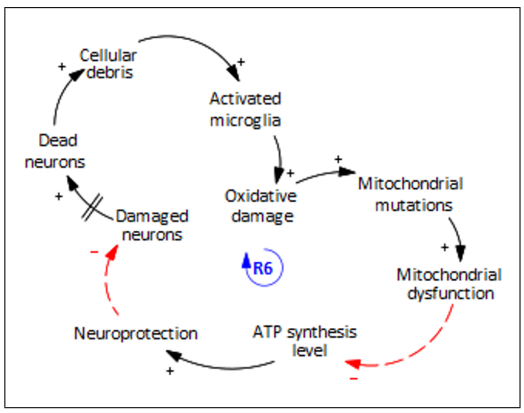


(f) ATP impact on neuroprotection

Figure 4.4. Positive (reinforcing) feedback loops of the model.

By producing pro-inflammatory mediators, activated microglia promote an inflammatory response. To limit the adverse effects of excessive inflammation, neuroinflammation is kept under control by anti-inflammatory mediators stimulated by pro-

inflammatory mediators. Anti-inflammatory mediators trigger a program that actively resolves activated microglia [75]. The interaction between microglia and inflammatory mediators is examined through the neuroinflammation loop (B6) (Figure 4.3f).

Misfolded alpha-synuclein proteins inhibit mitochondrial function and play a pivotal role in mitochondrial dysfunction [76]. Impaired mitochondria produce increased levels of oxidative stress. The alpha-synuclein proteins are then subjected to oxidation, which amplifies their tendency to form insoluble conformations [77]. These interactions create a vicious cycle between alpha-synuclein, mitochondria, and oxidative damage which has been considered central to the pathogenesis of PD in many studies. The reinforcing loop in our model representing this vicious cycle is called the mitochondrial oxidative damage loop (R1) (Figure 4.4a). In addition, oxidative damage also disrupts the protein degradation mechanisms [78], thus, promoting the accumulation of alpha-synuclein through another positive feedback loop. This secondary loop is represented by the reduced protein degradation loop (R3) (Figure 4.4c).

Another positive loop that adversely impacts mitochondrial function is mutations in mitochondrial DNA (mtDNA) driven by oxidative stress. This is shown in the causal loop diagram as the oxidative damage on mitochondria loop (R2) (Figure 4.4b). Because mitochondria are very susceptible to oxidative stress, mtDNA mutations accumulate over time. Resulted mitochondrial dysfunction leads to enhanced production of ROS, which in turn increases the generation of mtDNA mutations [79].

To defend brain health, acute neuroinflammation clears toxic materials by phagocytosis. However, enzymes necessary for these mechanisms produce reactive species and result in oxidative damage [80]. If acute neuroinflammation evolves into chronic neuroinflammation, it indicates a self-perpetuating detrimental response [81]. The neuroinflammatory oxidative damage loop (R4) (Figure 4.4d) depicts this vicious cycle.

Dysfunctional mitochondria are unable to synthesize sufficient levels of Adenosine triphosphate (ATP). This mitochondrial deficiency adversely affects neuroprotection

and antioxidant regulation mechanisms, which provide a balancing impact as described previously. Two reinforcing loops due to ATP shortage: (1) ATP impact on antioxidant capacity loop (R5) (Figure 4.4e), and (2) ATP impact on neuroprotection loop (R6) (Figure 4.4f). The GSH and neuroprotection depletion in PD patients is considered to be caused by ATP depletion [82].

# 5. MODEL DESCRIPTION

The model consists of five sectors: (1) neuroinflammation, (2) protein aggregation, (3) dopaminergic neuron, (4) oxidative damage, and (5) mitochondria. In this section, the mathematical model and effect functions of each sector are explained. In addition, the medical foundations and assumptions behind the model, are summarized to explain the quantitative representation of variables. Since our study aims to examine long-term dynamics, a "month" is used as time unit. The substantia nigra (SN) region in the brain of a healthy 30-year-old healthy individual is simulated up to 80 years of age using a time horizon of "50 years". After monitoring normal aging dynamics in the brain, different scenarios are simulated to gain insights into the potential relationship between Parkinson's disease (PD) and traumatic brain injury (TBI). Finally, the impacts of genetic variations and/or lifestyle variables such as a healthy diet and regular exercise are evaluated on both healthy and PD-prone individuals.

Some real-life parameters and relations change rapidly and their dynamics lose their meaning at a month level. The secretion of inflammatory mediators, for instance, occurs within minutes. Therefore, to have a model structure that serves our month-level purpose, the average values of the variables are adjusted, instead of instantaneous production and degradation values. Similarly, the performances of some biological mechanisms change immediately according to their triggers. However, our model takes into account the average performance of these mechanisms.

As discussed in the previous sections, instant measurement of changes in the brain is not possible. Although blood or cerebrospinal fluid tests provide some insight, we cannot directly determine the alterations in the brain or diagnose a neurodegenerative disease (ND). This is still an emerging area, thus, necessary values to develop our model are gathered or calculated utilizing post-mortem analysis. For cases, when there are no existing autopsy results for younger ages, initial values of stocks are calculated by using the findings from elderly individuals and fold changes during aging.

The maximum values used in the model represent an 80-year-old PD patient. With comprehensive research, firstly, qualitative real reference behaviors of brain aging in both healthy control and PD patients have been established for 50 years. It is assumed that if individuals live long enough, everyone will experience Parkinsonian symptoms. Based on this information, the saturation points of the effect functions are calibrated according to the levels of 80-year-old PD patients. Thus, it is aimed to provide a realistic approach.

## 5.1. Neuroinflammation Sector

### 5.1.1. Background Information

Neuroinflammation sector represents the inflammatory response within the brain. Neuroinflammation has immunological, physiological, biochemical, and psychological effects. Besides, the context, duration, and progression of the initial stimulation or injury determine the degree of neuroinflammation [61]. This mechanism is regulated by the generation of pro- and anti-inflammatory mediators. Microglia cells play a major role in the innate immune system by producing these mediators. They are primarily involved in immune activation in response to a variety of insults, including pathogens, injury, toxic metabolites, or tissue damage to maintain homeostasis. Microglial activation can be triggered by molecules released from dying dopaminergic neurons [83].

An acute neuroinflammatory response is gainful because it defends the central nervous system. However, persistent neuroinflammation may cause microglia to produce neurotoxic substances that amplify the disease state [84]. For instance, reactive species generated by microglia play a significant role in oxidative stress generation [85]. Eventually, all neuroinflammatory activities must be terminated by an effective resolution program to prevent further damage to the brain. Several studies, meanwhile, show that a neuroinflammatory response is ongoing in the Parkinsonian brain [86]. Figure 5.1 depicts the inflammatory response which is a sequence of events highly coordinated by the onset and subsequent resolution phase.

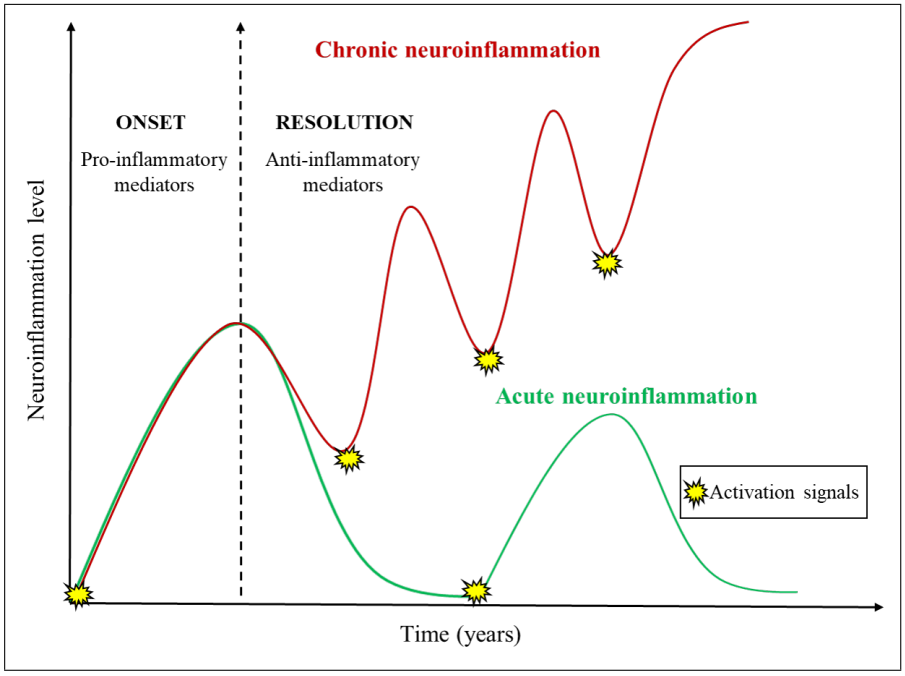


Figure 5.1. Acute and chronic inflammation (based on [87]).

Microglia can have various phenotypes and so perform a variety of activities. These cells retain a resting character under normal conditions and actively monitor the surrounding microenvironment. When brain homeostasis is disturbed, microglia exhibit microglial activation, which is described as quick and substantial alterations in cell shapes and functional activities [88]. As seen in Figure 5.2, upon stimuli, resting microglia become activated by changing their cellular shape and functions. The classical (M1) microglia are responsible for pro-inflammatory response by producing several mediators, whereas alternative (M2) microglia produce anti-inflammatory mediators to control the resolution phase of the neuroinflammation. The activated microglia variable in our model corresponds to the M1 type due to its connection with chronic neuroinflammation. Moreover, research on activated microglia in literature is based on M1 microglia to observe the detrimental impact of excessive microglial activation.

Evidence indicates that pro-inflammatory molecules are involved in the resolution program by triggering the release of anti-inflammatory mediators [75]. Thus, a causal relationship exists between the level of pro-inflammatory mediators and the production

of anti-inflammatory mediators. Anti-inflammatory mediators which are responsible for the resolution of neuroinflammation modulate microglial activation [89]. Tumor necrosis factor alpha (TNF-$\alpha$) and Interleukin 10 (IL-10) cytokines are employed to represent pro- and anti-inflammatory mediators in our model, respectively. IL-10 is released with or after the secretion of pro-inflammatory mediators [90].

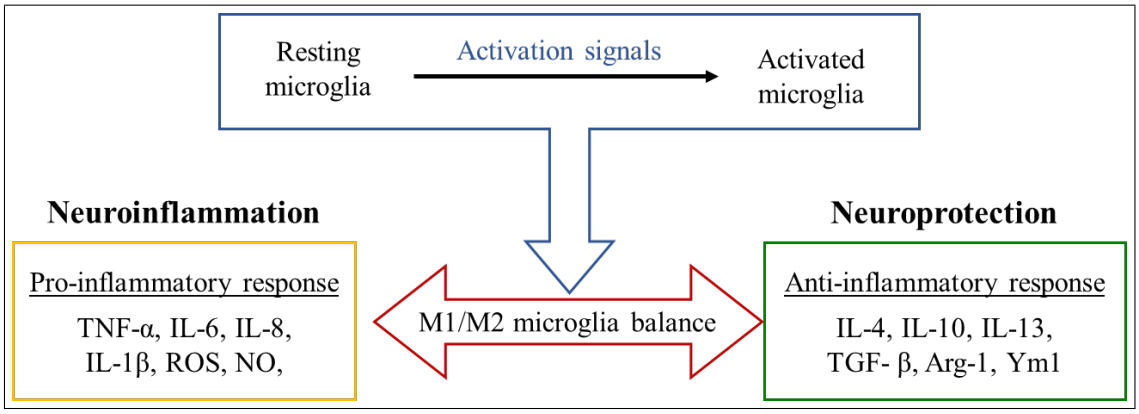


Figure 5.2. Microglia phenotypes (based on [84]).

### 5.1.2. Sector Structure

The stock-flow diagram of the neuroinflammation sector is shown in Figure 5.3. There are four stocks: (1) activated microglia, (2) resting microglia, (3) pro-inflammatory mediators, and (4) anti-inflammatory mediators. Neuroinflammation sector stocks and parameters are listed in Table 5.1 and Table 5.2, respectively.

Table 5.1. Neuroinflammation sector stocks.

| Stock Name | Initial Value | Unit |
|---|---|---|
| Activated microglia | 3,319 | microglia |
| Resting microglia | 162,664 | microglia |
| Pro-inflammatory mediators | 11 | pg/mg |
| Anti-inflammatory mediators | 11 | pg/mg |

It is assumed that the increase fractions of pro- and anti-inflammatory mediators are equivalent since they have the same initial values at the beginning of the simulation for a healthy young adult. Activated microglia stock stands for the M1-type microglia that produce pro-inflammatory mediators and phagocytose dead neurons and toxic protein aggregates. There is no data available for the total microglial population in human substantia nigra (SN), thus, some mathematical calculations have been performed.

Table 5.2. Neuroinflammation sector parameters.

| **Variable Name** | **Value** | **Unit** |
|---|---|---|
| microglial activation per neuron | 0.4 | (microglia/neuron)/month |
| microglial activation per alpha-synuclein | 45 | microglia/(pg/mg)/month |
| microglial resolution fraction | 9 | microglia/(pg/mg)/month |
| anti-inflammatory increase fraction | 0.45 | (pg/mg)/month |
| pro-inflammatory release fraction | 0.45 | (pg/mg)/month |
| anti-inflammatory decrease fraction | 0.48 | (pg/mg)/month |
| pro-inflammatory decrease fraction | 0.3 | (pg/mg)/month |

According to research conducted by VanGuilder and coworkers, there was no difference in the total microglial population between age groups [91]. As young mice age, the ratio of activated microglia increases from 2% to 25%. There is 2.5 fold change between healthy control and PD mice [92]. The (neuron/microglia) ratio in the SN of mice is determined using neuronal and microglial densities. With this ratio, the total microglial population in the human SN and the initial value of activated microglia stock are calculated. To be employed in the validation phase, the number of activated microglia for an 80-year-old individual is calculated. The activated microglia amount of an 80-year-old PD patient is necessary for the calibration of the graphical functions of effects. Table 5.3 presents all the constants utilized in the computation and corresponding references.

Table 5.3. Sources for microglia initial values.

| | **Value** | **Source** |
|---|---|---|
| total neuron (mouse SN) | 65,451 | [93] |
| total microglia (mouse SN) | 13,400 | [94] |
| activated microglia/total microglia (young mouse SN) | 2% | [92] |
| activated microglia/total microglia (old mouse SN) | 25% | [92] |
| total neurons (human SN) | 810,000 | [95] |
| total microglia (human SN) | 165,983 | calculated |
| activated microglia (adult human SN) | 3319 | calculated |
| activated microglia (old human SN) | 41495 | calculated |
| activated microglia (old PD SN) | 103739 | calculated |

Depending on the microenvironment in the brain, microglia can have resting or activated phenotypes. There are two flows -microglial activation and microglial resolution- regulating the values of microglia stocks. Activated microglia and resting microglia stocks are calculated as follows:

$$\frac{dActivated\,microglia}{dt} = microglial\,activation - microglial\,resolution, \tag{5.1}$$

$$\frac{dResting\,microglia}{dt} = microglial\,resolution - microglial\,activation. \tag{5.2}$$

Microglial activation can be triggered by either toxic insoluble protein aggregates or dead neurons. If there are enough microglia in resting microglia stock, this flow is the summation of those two elements as

$$\begin{aligned} microglial\,activation = & MIN(\frac{Resting\,microglia}{adj\,time}, \\ & activation\,by\,dead\,neurons + activation\,by\,alphasyn). \end{aligned} \tag{5.3}$$

MIN() function helps avoid negative flows in microglial activation. The length of the time unit is sufficient enough for the activities of neuroinflammation sector, thus, adjustment times are built to preserve unit consistency and are equal to 1. Activation

by alpha-synuclein is determined by the multiplication of insoluble alpha-synuclein level and activation per alpha-synuclein. Similarly, activation by dead neurons is calculated by multiplying dead neurons and activation per neuron.

Microglial discrepancy, the difference between the actual and the desired activated microglia levels, influences microglial resolution flow. Under normal conditions, some activated microglia are assumed to be present for brain health and safety. Microglial resolution fraction is sensitive to microglial density which is incorporated into the model by the effect of activated microglia on resolution. Responsible materials for the effective resolution, anti-inflammatory mediators, are further multiplied by this fraction. Thus, the microglial resolution flow is calculated as

$$\begin{aligned} microglial\ resolution = & MIN(\frac{microglial\ discrepancy}{adj\ time}, \\ & Antiinflam\ mediators \times microglial\ resolution\ fr \times \\ & Eff\ of\ activated\ microglia\ on\ resolution). \end{aligned} \tag{5.4}$$

The initial value of pro-inflammatory mediators stock is obtained from a study comparing the TNF-$\alpha$ cytokine levels from control and PD brains. As people age, this value triples [96]. The equation for pro-inflammatory mediators is

$$\frac{dProinflammatory\ mediators}{dt} = proinf\ increase - proinf\ decrease. \tag{5.5}$$

Pro-inflammatory increase is regulated by pro-inflammatory release fraction multiplied by activated microglia effect on pro-inflammation as follows:

$$\begin{aligned} proinf\ increase = & proinf\ release\ fr \times \\ & Eff\ of\ activated\ microglia\ on\ proinf. \end{aligned} \tag{5.6}$$

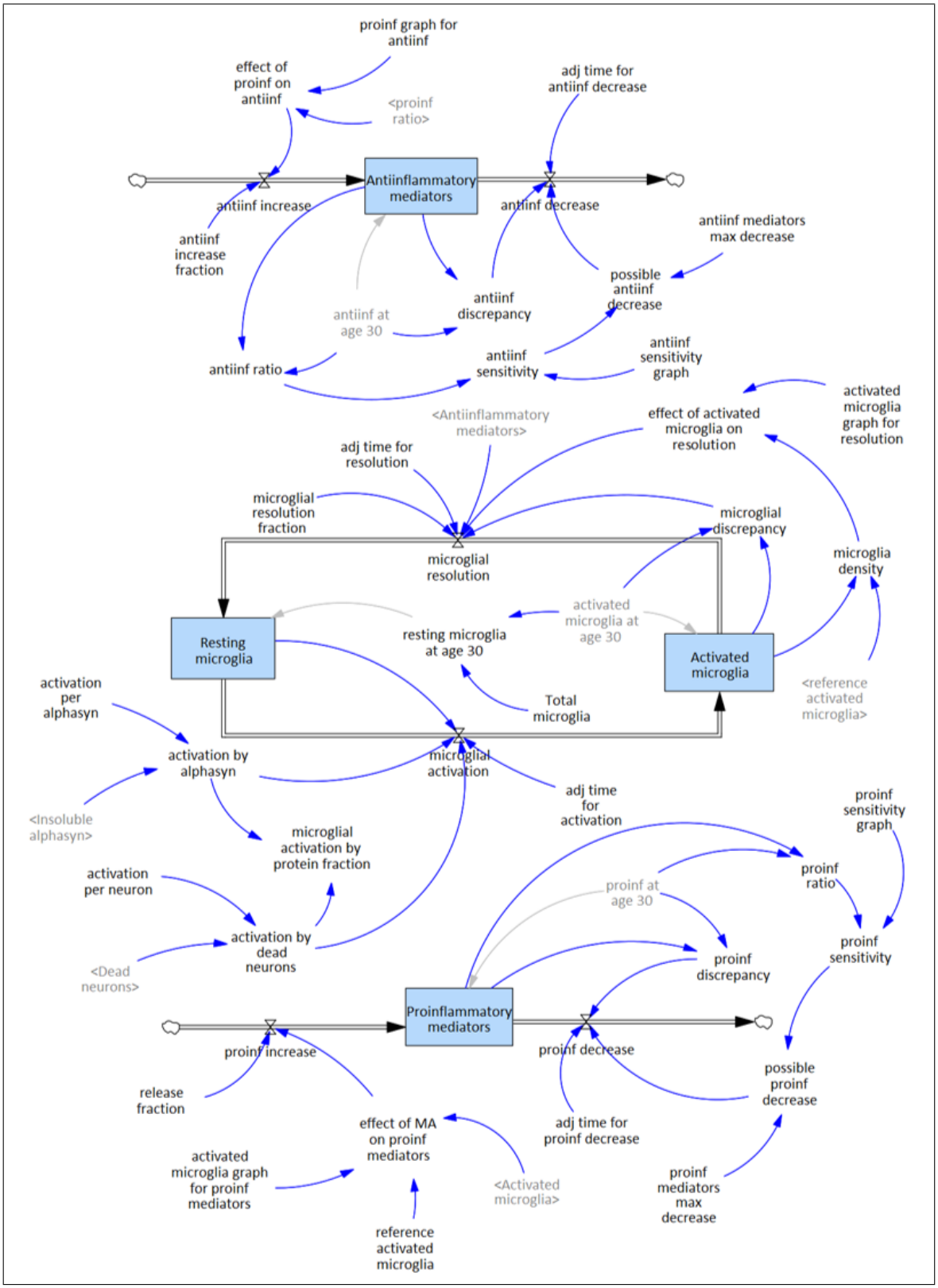


Figure 5.3. Stock-flow diagram of the neuroinflammation sector.

Pro-inflammatory decrease then comes into play in response to an increase in the pro-inflammatory level with the equation of

$$proinf\ decrease = MIN(\frac{proinf\ discrepancy}{adj\ time}, possible\ proinf\ decrease). \quad (5.7)$$

This flow is dependent on pro-inflammatory discrepancy and possible pro-inflammatory decrease. Pro-inflammatory decrease is formulated as

$$\begin{aligned} proinf\ discrepancy = & MAX(0, (Proinflammatory\ mediators - \\ & proinflam\ mediators\ at\ age\ 30)). \end{aligned} \quad (5.8)$$

For cases where the pro-inflammatory mediators stock level is less than the desired, MAX() function is used to prevent a decrease in pro-inflammatory mediators stock. At the beginning, change in this stock is not influential for the pro-inflammatory decrease which is included in the model by pro-inflammatory sensitivity. This variable is used in the calculation of possible pro-inflammatory decrease as

$$possible\ proinf\ decrease = proinf\ sensitivity \times proinf\ decrease\ fr. \quad (5.9)$$

IL-10 cytokine represents anti-inflammatory mediators. The concentration of IL-10 in the brain is not available in the literature. Instead, its initial value is determined based on a study indicating the ratio between TNF-$\alpha$ and IL-10 as approximately 1 for healthy adults. There is a fold change of 2 between young and old healthy individuals [97]. PD people have 20% elevated levels of IL-10, compared to healthy-aged individuals [98]. The equation for anti-inflammatory mediators is

$$\frac{dAntiinflammatory\ mediators}{dt} = antiinf\ increase - antiinf\ decrease. \quad (5.10)$$

The anti-inflammatory increase depends on amount of pro-inflammatory mediators, thus, formulated by using an effect function of proinflammation. The anti-inflammatory

decrease follows a similar procedure to the previously explained pro-inflammatory decrease and its formulation is

$$antiinf\ decrease = MIN(\frac{antiinf\ descrepancy}{adj\ time}, possible\ antiinf\ decrease). \quad (5.11)$$

Anti-inflammatory discrepancy is the gap between the desired and the actual levels. This gap is tried to be minimized by anti-inflammatory decrease flow depending on the possible decrease as follows:

$$\begin{aligned} antiinf\ discrepancy = & MAX(0, (Antiinflammatory\ mediators - \\ & antiinflam\ mediators\ at\ age\ 30)). \end{aligned} \quad (5.12)$$

Possible anti-inflammatory decrease is dependent on the anti-inflammatory sensitivity, and the corresponding equation is

$$possible\ antiinf\ decrease = antiinf\ sensitivity \times antiinf\ decrease\ fr. \quad (5.13)$$

Reference activated microglia corresponds to the amount of activated microglia an elderly individual at the age of 80 has. In advanced PD cases, this number can rise up to threefold. Thus, the microglia effects on resolution and pro-inflammation saturate around y=1 because it is calibrated according to the maximum values of the resolution and release fractions. For lower levels than the desired microglia (until x=0.08), these functions are zero elements (Figure 5.4).

Inflammatory sensitivity effects are standardized according to the desired value, which is equal to the initial levels of pro- and anti-inflammatory mediators. Until x=1, the inflammatory mediators are lower than the desired, thus, there is no impact on pro- and anti-inflammatory decrease flows. The saturation points are determined according to elderly PD patients (Figure 5.5).

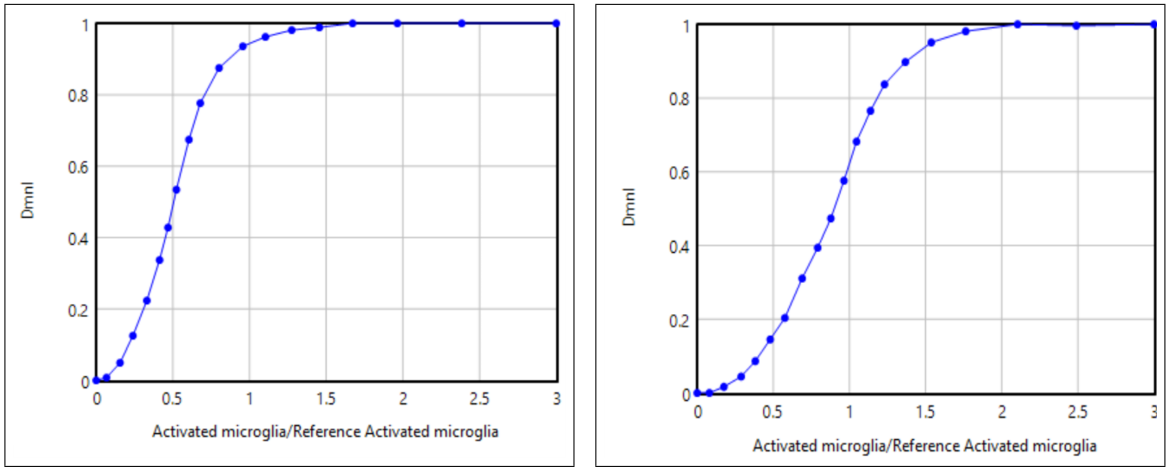


(a) Microglia effect on resolution (b) Microglia effect on pro-inflammation

Figure 5.4. Graphical functions of microglia effects.

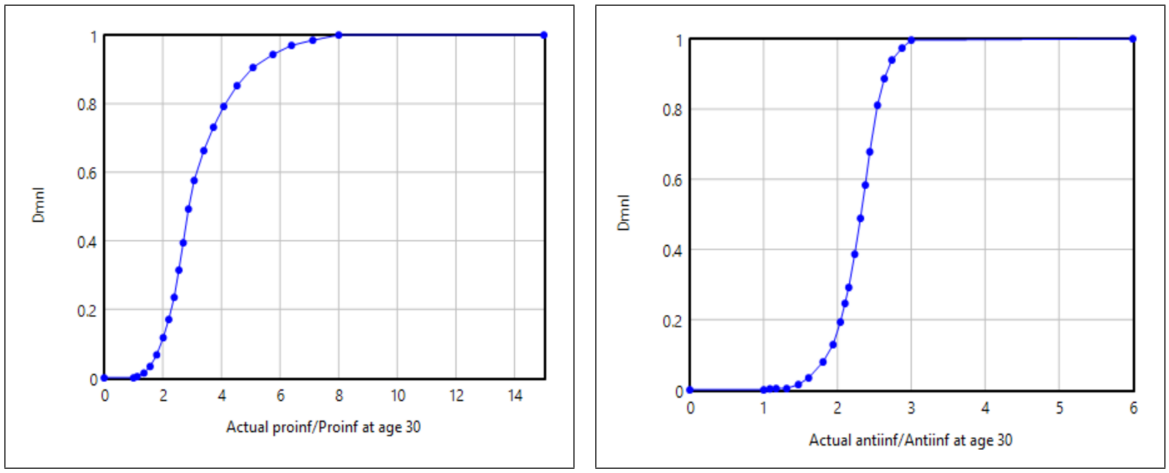


(a) Pro-inflammatory sensitivity (b) Anti-inflammatory sensitivity

Figure 5.5. Graphical functions of inflammatory sensitivity effects.

Depending on the activated microglia level, pro-inflammatory mediators level can rise up to 10-fold. Thus, the pro-inflammation effect on anti-inflammation saturates around y=1 because it is calibrated according to the maximum value of the anti-inflammatory increase fraction. For lower levels than the desired (until x=1), pro-inflammation does not affect anti-inflammation (Figure 5.6).

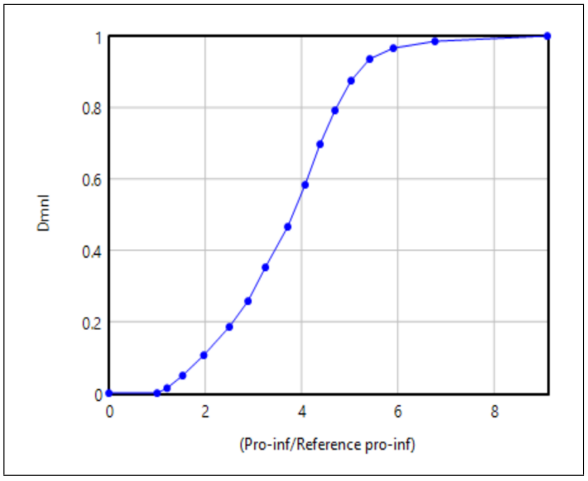


Figure 5.6. Graphical function of pro-inflammation effect on anti-inflammation.

## 5.2. Protein Aggregation Sector

### 5.2.1. Background Information

Protein aggregation sector represents the accumulation of toxic forms of alpha-synuclein protein. These forms are regulated by the production, degradation, and phagocytosis mechanisms. Protein degradation by proteasomal system and phagocytosis by activated microglia attempt to protect neurons by removing this toxicity, while, oxidative damage plays a significant role in its formation. In its natural state, alpha-synuclein is a small and unfolded protein, which is highly soluble. This protein can self-assemble and generate insoluble aggregates, depending on the environment [99]. Uncertainty exists regarding the precise function of alpha-synuclein. Scientists believe it has physiological functions that assist control of dopamine synthesis and release [100].

Oxidative stress induces the formation of alpha-synuclein aggregates in both in vitro and in vivo observations [101]. Soluble oligomeric forms, which are fibrillization intermediates, are generated when two or more monomers aggregate [102]. The ubiquitin–proteasome system (UPS) is one of the endogenous cellular mechanisms that can reduce oligomers [103]. Yet, the effectiveness of UPS activity is known to deteriorate with age [104]. The aforementioned causes increase the alpha-synuclein levels in the

human brain during aging [105]. Unfolded alpha-synuclein proteins, arising from the combined effects of oxidative stress and/or genetic mutations, become unfolded. in the presence of impaired protein degradation processes, those unfolded conformations form oligomeric species with increased molecular complexity. Subsequently, these alpha-synuclein oligomers aggregate and evolve into inclusions termed Lewy bodies (LBs) in PD patients [106]. Figure 5.7 depicts the protein aggregation process.

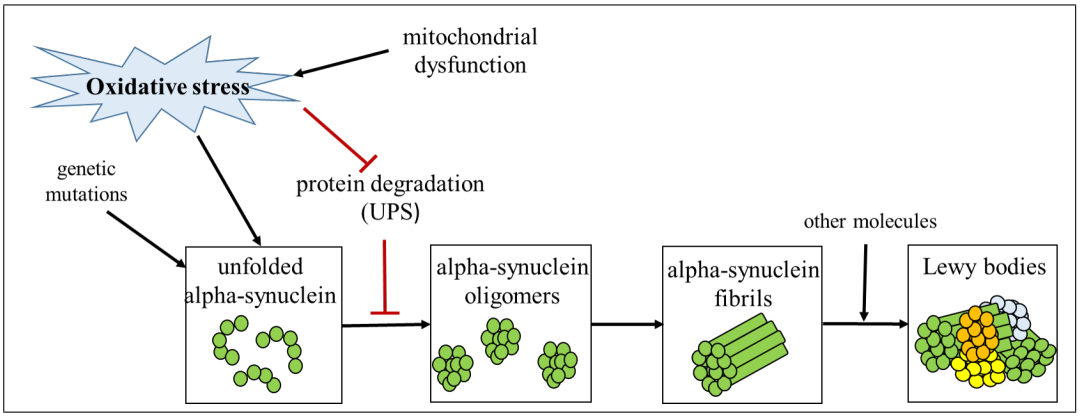


Figure 5.7. Aggregation of alpha-synuclein protein (based on [106]).

Lewy pathology presence is one of the neuropathological hallmarks for post-mortem confirmation of PD, for more than a century [107]. Its principal component is toxic alpha-synuclein aggregates. LBs protect neurons by isolating toxic protein aggregations from the cytoplasm, thus, it is a defense mechanism developed by the cells [108]. As a result, the primary cause of toxicity, alpha-synuclein aggregation, is the focus of our model. Similarly, the majority of research in the literature has emphasized the negative effects and aggregation mechanisms of alpha-synuclein, rather than LB dynamics.

There are several disorders characterized by protein misfolding and aggregation. Particularly for neurodegenerative ones, three generic hypotheses have been suggested. The illustration for those hypotheses with the corresponding disorders and aggregated proteins can be seen in Figure 5.8. According to the loss-of-function hypothesis, the

loss of a protein's normal activity results in neuronal death. The gain-of-toxic claims that protein misfolding and protein aggregation lead to neurotoxic impact. Protein aggregates, based on the inflammation hypothesis, generate a prolonged inflammatory response [109]. The gain-of-toxic and inflammation hypotheses form the foundation of our modeling concept. The loss-of-function hypothesis is not included in the scope of the study since the exact role of the alpha-synuclein protein and the associated cellular problems are not well explained in the literature.

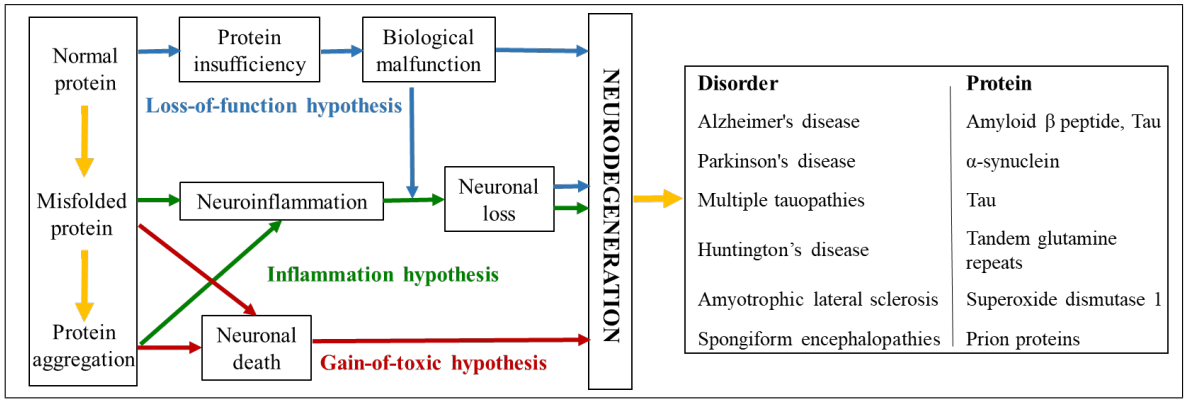


Figure 5.8. Protein aggregation hypotheses (based on [109, 110]).

### 5.2.2. Sector Structure

The stock-flow diagram of the protein aggregation sector is shown in Figure 5.9. There are three stocks: (1) soluble alpha-synuclein, (2) insoluble alpha-synuclein, and (3) protein degradation activity. Alpha-synuclein sector stocks and parameters are listed in Table 5.4 and Table 5.5, respectively.

Table 5.4. Protein aggregation sector stocks.

| Stock Name | Initial Value | Unit |
|---|---|---|
| Soluble alpha-synuclein | 0 | $\mu$g/mg protein |
| Insoluble alpha-synuclein | 0 | $\mu$g/mg protein |
| Protein degradation activity | 39 | FU/(min*$\mu$g protein) |

Table 5.5. Protein aggregation sector parameters.

| **Variable Name** | **Value** | **Unit** |
|---|---|---|
| phagocytosis capacity | 0.0000009 | $\mu$g/(month*mg protein)/microglia |
| oligomerization fraction | 0.045 | $\mu$g/mg protein/month |
| degradation decrease fraction | 0.45 | Fu/(min*$\mu$g protein)/month |
| fibrillization delay | 2.5 | month |

Soluble alpha-synuclein stock represents the oligomers generated by the aggregation of two or more monomeric forms, whereas insoluble alpha-synuclein stands for a more advanced stage of aggregation. Soluble alpha-synuclein oligomers are cleaned by UPS, whereas insoluble fibrils are phagocytized by activated microglia. Since activated microglia stock is explained in the neuroinflammation sector, protein clearance by UPS is highlighted in this sector. In animal experimental studies, the amounts of alpha-synuclein are measured as microgram ($\mu$g) alpha-synuclein per milligram (mg) protein. Misfolded alpha-synuclein is not present in the adult human brain, however, it starts to aggregate around the age of 60 and rises over time exponentially [105].

The UPS is subjected to oxidative stress as individuals age, which causes a decline in its degradation activity. Because of this, protein degradation activity is incorporated into the model as a stock. Peptidyl glutamyl-peptide hydrolytic (PGPH), the most consistently impacted activity of UPS [111], serves as the representation of this activity. In general terms, PGPH activity takes part in the destruction of bonds in proteins. Fluorescence unit (FU)/min/$\mu$g protein is selected for the unit of this stock, in line with the measurements of McNaught and coworkers [112]. The initial value for protein degradation activity is gathered from the same study.

Protein aggregation is regulated by oligomerization, degradation, fibrillization, and phagocytosis. Thus, alpha-synuclein stock variables are formulated as

$$\frac{dSoluble\ alphasyn}{dt} = oligomerization - degradation - fibrillization, \qquad (5.14)$$

$$\frac{dInsoluble\,alphasyn}{dt} = fibrillization - phagocytosis. \tag{5.15}$$

Since the model's time unit is a month, which is a sufficient amount for most mechanisms in our study, adjustment time variables for degradation and phagocytosis are equal to 1. The oligomerization is formulated by including the effect of oxidative damage degree as

$$oligomerization = oligomerization\,fr \times Eff\,of\,OD\,on\,oligomerization. \tag{5.16}$$

The degradation flow is dependent on degradation efficiency as

$$degradation = \frac{(Soluble\,alphasyn \times degradation\,efficiency)}{adj\,time}. \tag{5.17}$$

The initial value of protein degradation activity is chosen as the reference activity. In the presence of alpha-synuclein oligomers, the protein degradation mechanism attempts to remove these intermediates. This mechanism operates at 100% efficiency for young adults, however, declines as a result of oxidative damage during aging. The accumulated soluble alpha-synuclein forms fibrils after some fibrillization delay [113], and the equation for fibrillization is

$$fibrillization = \frac{Soluble\,alphasyn}{fibrillization\,delay}. \tag{5.18}$$

When insoluble alpha-synuclein exists, activated microglia seek to clear this toxicity and create phagocytosis flow. Given that there are two sources of microglial activation, the assigned microglia numbers for phagocytosis of both alpha-synuclein and dead neurons must be determined. To address this, we identified an auxiliary called microglial activation by protein with the following equation:

$$microglial\,act\,by\,protein = ZIDZ(act\,by\,alphasyn, total\,act). \tag{5.19}$$

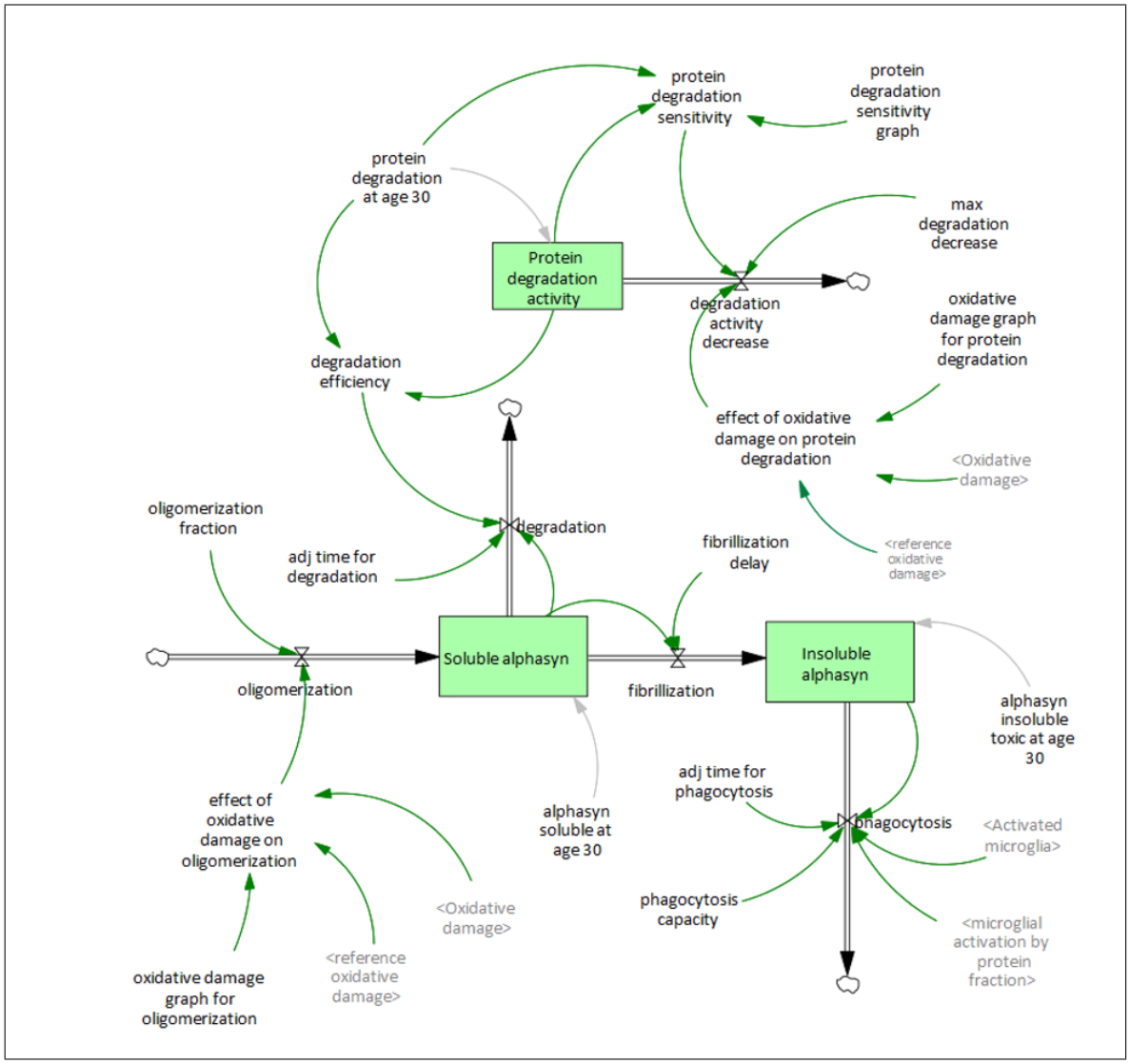


Figure 5.9. Stock-flow diagram of the protein aggregation sector.

ZIDZ() function is utilized in the formula to eliminate floating time error. This variable is further employed in the calculation of phagocytosis flow as

$$phagocytosis = MIN(\frac{Insoluble\ alphasyn}{adj\ time}, Activated\ microglia \times phagocytosis\ capacity \times microglial\ act\ by\ protein). \quad (5.20)$$

Since there is no substantial inflow within the scope of our research, protein degradation activity is solely controlled by an outflow that is governed by oxidative

damage. The corresponding formula is

$$\frac{dProtein\ degradation\ activity}{dt} = -degradation\ activity\ decrease. \tag{5.21}$$

Degradation activity decrease is formulated by considering the effect of oxidative damage on protein degradation and protein degradation compensation as

$$\begin{aligned} degradation\ activity\ decrease = & Eff\ of\ OD\ on\ protein\ degradation \times \\ & Protein\ degradation\ compensation \times \\ & degradation\ decrease\ fr. \end{aligned} \tag{5.22}$$

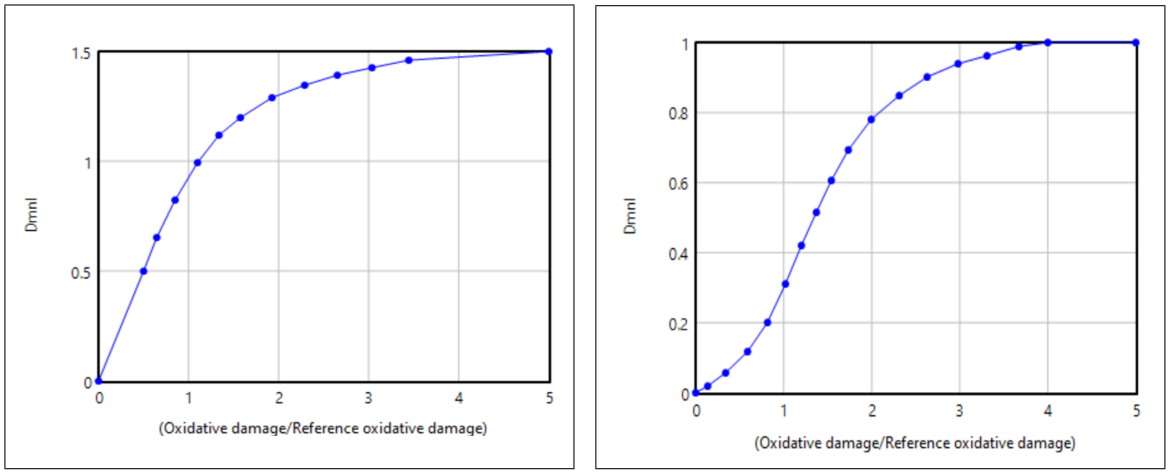


(a) Oxidative damage effect on oligomerization (b) Oxidative damage effect on degradation

Figure 5.10. Graphical functions of oxidative damage effects.

Reference oxidative damage refers to the amount of oxidative damage an elderly person at the age of 80 has. In PD patients, this value can be up to 4 times the normal value. Until some point, oxidative damage effect on oligomerization is linear, later, the graph saturates. The oligomerization fraction is equal to the elderly individual at the age of 80. For PD cases, this can show a 50% increase and saturates around y=1.5 (Figure 5.10a). Oxidative damage effect on degradation is S-shaped. Until the reference value, there is no substantial change, but then, the nonlinear graph saturates

around y=1 because of the calibration procedure according to the maximum value for degradation decrease (Figure 5.10b).

Protein degradation compensation effect is standardized according to the desired value, which is equal to the initial level of the protein degradation activity stock. For input values higher than 1, this function does not affect the oxidative damage impact on degradation. For lower ratios, neurons try to decrease the oxidative damage impact by functioning more. The output of this S-shaped function changes between 0 and 100 (Figure 5.11).

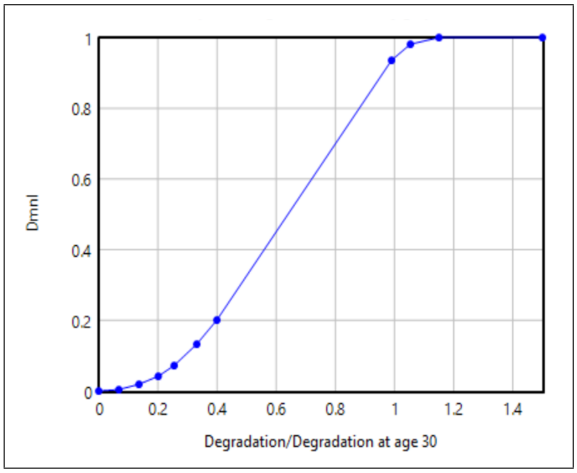


Figure 5.11. Graphical function of protein degradation compensation.

## 5.3. Dopaminergic Neuron Sector

### 5.3.1. Background Information

This sector represents the population of dopaminergic neurons in human brain substantia nigra (SN). These neurons account for fewer than 1% of all brain neurons, yet they play an essential role in controlling various fundamental functions [114]. Since dopaminergic neurons are post-mitotic cells, they cannot be replaced when they are destroyed. Consequently, the density of neurons diminishes during aging. This poses a great threat to the elderly demographic. There is an ongoing flow between healthy,

damaged, and dead neuron populations in the human brain, regulated by neuronal protection, neuronal damage, and neuronal death.

Dopamine is one of the main neurotransmitters in the nervous system that is involved in numerous centrally regulated activities, ranging from motor control to cognition. It is produced and released by dopaminergic neurons, which are found in several brain areas but are particularly abundant in the SN [115]. Due to their high rate of oxygen metabolism and poor antioxidant levels, they are particularly vulnerable to oxidative stress. In terms of dopaminergic neuronal loss, an age-related decrease is mainly noticeable in pigmented ones, starting around the age of forty [116, 117].

Loss of neuromelanin pigment-containing dopaminergic neurons is the primary pathogenic feature of PD. Dopaminergic cell loss, resulting in a reduced concentration of dopamine in the human body, is associated with the presence of Lewy bodies (LBs) [118]. Classical Parkinsonian symptoms appear when dopamine levels are lowered by 80%, however, this decline corresponds to 50% dopaminergic neuron loss. This suggests that a subset of dopaminergic neurons form a damaged population, which produces insufficient dopamine, before dying [119].

In animal models, brain-derived neurotrophic factors (BDNF) upregulate neurotransmission and support neuroprotection. Since lower amounts of BDNF are discovered in the nigrostriatal pathway in both human and animal PD models, it is proposed that BDNF acts as a therapeutic agent [120]. Regular and systematic moderate-intensity physical activity may consistently increase BDNF levels in the brain [121].

### 5.3.2. Sector Structure

There are three stocks: (1) healthy neurons, (2) damaged neurons, and (3) dead neurons in the dopaminergic neuron sector. Table 5.6 represents the sector stocks, whereas in Table 5.7 parameters are listed.

Table 5.6. Dopaminergic neuron sector stocks.

| **Stock Name** | **Initial Value** | **Unit** |
|---|---|---|
| Healthy neurons | 450,000 | neuron |
| Damaged neurons | 170 | neuron |
| Dead neurons | 28 | neuron |

Table 5.7. Dopaminergic neuron sector parameters.

| **Variable Name** | **Value** | **Unit** |
|---|---|---|
| BDNF production capacity | 0.00044 | 1/month |
| BDNF production reduction | 0.2 | dmnl |
| microglial phagocytosis capacity | 0.2 | neuron/microglia/month |
| neuronal death delay | 6 | month |
| minimum neuronal damage | 200 | neuron/month |

Healthy neurons represent the neurons that effectively perform their functions. Damaged neurons are generated when cells experience elevated oxidative damage from a variety of sources, which oxidizes the DNAs and materials of neurons. According to the neuroprotection capacity of neurons, some of those damaged neurons are repaired and rejoin the stock of healthy neurons. Insufficient neuroprotection, on the other hand, results in neuronal death and causes a flow from damaged neurons to dead neurons.

According to a post-mortem analysis, the amount of pigmented dopaminergic neurons in human SN for young adults is around 450,000 [116]. At the beginning of the simulation, some amount of damaged and dead neurons are also expected. We determined the initial values for those stocks as a result of trial runs. The flows of neuronal protection, neuronal damage, neuronal death, and neuronal phagocytosis regulate the levels of sector stocks as follows:

$$\frac{dHealthy\,neurons}{dt} = neuronal\,protection - neuronal\,damage, \tag{5.23}$$

$$\frac{dDamaged\,neurons}{dt} = neuronal\,damage - neuronal\,protection - neuronal\,death, \tag{5.24}$$

$$\frac{dDead\,neurons}{dt} = neuronal\,death - neuronal\,phagocytosis. \tag{5.25}$$

Neuronal damage is affected by oxidative damage intensity. In addition, the availability of healthy neurons is a determinant factor for this flow. The probability of neuronal damage to healthy neurons increases with the environment's healthy neuron abundance. As it is not significant to the model, damage that occurs to cells that are already damaged or dead is not of concern. Brain injury-induced neuronal damage formulation is explained in the scenario analysis section. Neuronal damage equation is

$$neuronal\,damage = (min\,neuronal\,damage \times Eff\,of\,OD\,on\,neuronal\,damage \times neuronal\,damage\,availability) + brain\,injury \tag{5.26}$$

where neuronal damage availability is

$$neuronal\,damage\,availability = \frac{Healthy\,neurons}{Total\,neurons}. \tag{5.27}$$

BDNF, one of the prominent neuroprotective factors expressed by dopaminergic neurons, represents the neuroprotection capacity in our model. Neurons with the lowest BDNF levels are more vulnerable to damage [122]. Depending on the literature, neuronal protection is calculated as

$$neuronal\,protection = MIN(BDNF\,neuroprotection\,capacity, \frac{Damaged\,neurons}{adj\,time}). \tag{5.28}$$

In contrast to their healthy counterparts, damaged neurons produce 20% reduced levels of BDNF [123]. In addition, neuroprotection is highly dependent on ATP efficiency, which is formulated as the actual ATP synthesis level divided by the desired

ATP synthesis level. Altogether, we build the following equation for BDNF neuroprotection capacity as

$$\begin{aligned} BDNF\ neuroprotection\ capacity = & BDNF\ production\ capacity \times \\ & (Healthy\ neuron + Damaged\ neurons \times \\ & (1 - BDNF\ production\ reduction)) \times \\ & ATP\ efficiency. \end{aligned} \tag{5.29}$$

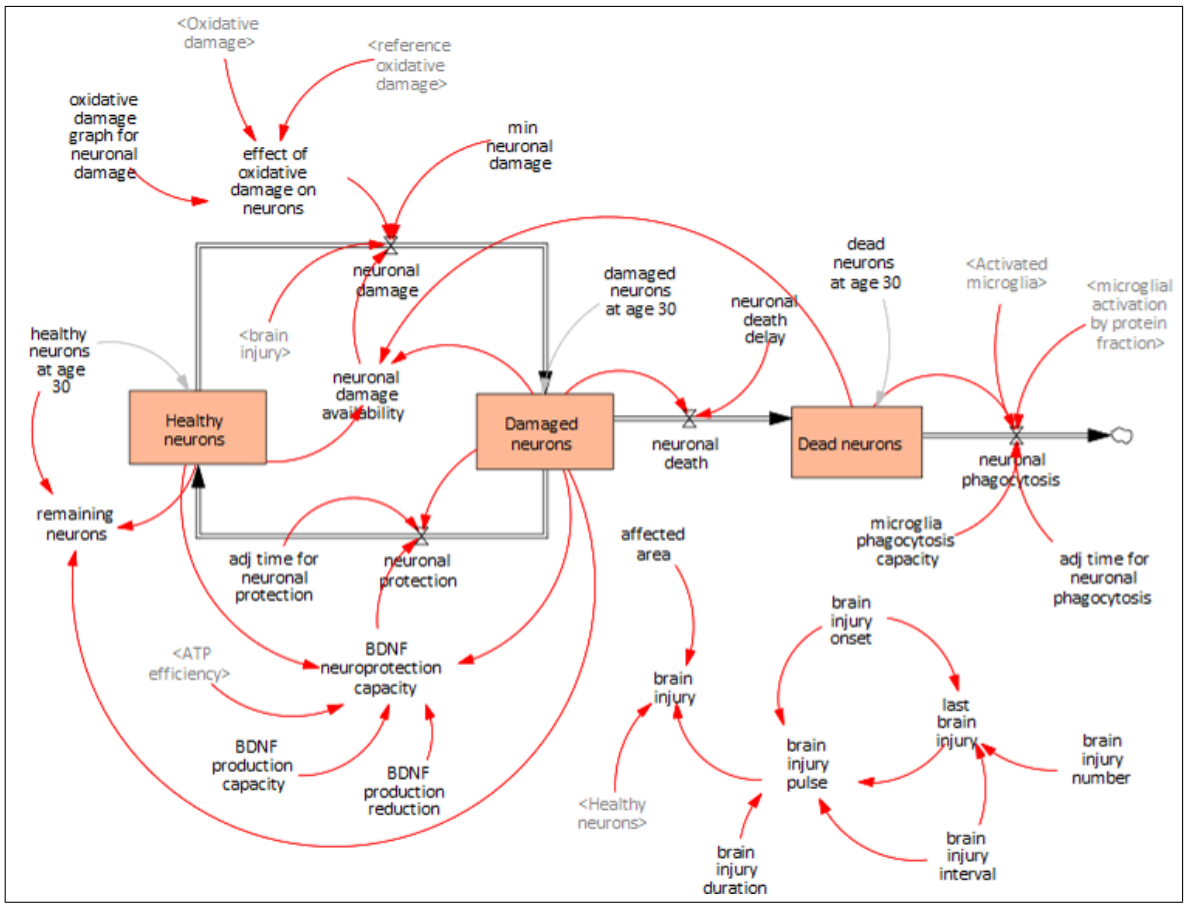


Figure 5.12. Stock-flow diagram of the dopaminergic neuron sector.

Based on existing literature findings, damaged neurons die after some amount of time. According to Greffard and others, Lewy body-containing neurons have a 6-month lifespan [124]. Thus, we assumed a neuronal death delay of 6 months while formulating

the neuronal death flow as

$$neuronal\ death = \frac{Damaged\ neurons}{neuronal\ death\ delay}. \tag{5.30}$$

The last flow, neuronal phagocytosis, is controlled by the level of activated microglia. As previously mentioned, to determine the amount of activated microglia responsible for neuronal phagocytosis, we have multiplied the microglia level by (1-microglial activation by protein). The equation for neuronal phagocytosis is

$$\begin{aligned} neuronal\ phagocytosis = & MIN(\frac{Dead\ neurons}{adj\ time}, Activated\ microglia \times \\ & (1 - microglial\ activation\ by\ protein) \times \\ & microglial\ phagocytosis\ capacity). \end{aligned} \tag{5.31}$$

Reference oxidative damage refers to the amount of oxidative damage an elderly individual at the age of 80 has. Under normal circumstances, there is no oxidative damage in neurons. Therefore, initiation of oxidative damage results in a minimum amount of damage in neurons. The graph starts at y=1, and saturates at y=4, meaning maximum neuronal damage depending on oxidative damage density is approximately four times the minimum value (Figure 5.13).

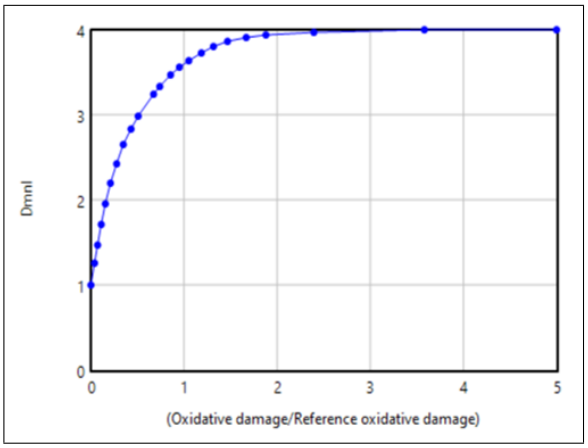


Figure 5.13. Graphical function of oxidative damage effect on neuronal damage.

## 5.4. Oxidative Damage Sector

### 5.4.1. Background Information

This sector explores the oxidative damage accumulated in the brain over time and the anti-oxidant mechanism efforts to mitigate this damage. About 20% of the body's oxygen supply is consumed by the brain, and a substantial fraction of that oxygen is turned to reactive oxygen species (ROS) [125]. These metabolites adjust the normal functions of neurons, yet an uncontrolled rise in ROS levels harms neurons [126]. An impairment in the physiological generation of reactive species and the body's capacity to combat them via antioxidant activities leads to oxidative damage [127].

The free radical theory of aging, also known as the oxidative stress theory of aging, is predicated on the notion that age-related functional declines are caused by the accumulation of oxidative damage by reactive species [128]. Many studies consider aging as an external risk factor in their research. However, based on this hypothesis, we attempt to scientifically reflect the aging impact in our study using oxidative damage.

Among many sources of ROS in the brain, mitochondrial failure- and activated microglia-related pathways are directly connected to our scope of the study. Further research leads us to the conclusion that toxic alpha-synuclein aggregations are involved in ROS generation via mitochondrial pathways [129]. On the other hand, antioxidant systems try to minimize intracellular redox balance to prevent cellular damage [130]. Oxidative damage directly harms the materials of protein degradation system, which results in improper degradation activity and propagates protein misfolding [64]. Since mitochondrial DNA is quite susceptible to oxidative stress, mutations accumulate over time [79]. Most importantly, excessive amounts of ROS oxidize the necessary materials for neurons, which leads to cellular damage and death [131]. 4-hydroxy-2-nonenal (HNE) is employed in many studies as a biomarker for oxidative stress-induced damage since oxidative damage cannot be directly assessed. In terms of weighing neuronal oxidative damage, the proportion of positively stained neurons is measured [132].

Over time, antioxidant levels and function are reduced in the aged brain due to the progressively increasing ROS [133]. The most prominent antioxidant in the brain, glutathione (GSH), protects neurons against oxidative stress-induced damage by reducing reactive species. GSH deficiency is one of the initial signs of oxidative damage during aging and PD in the substantia nigra (SN), which is accompanied by a rise in ROS levels [72]. Data gathered from PD patients in the early stages reveal that high oxidative stress is a prominent characteristic of the early stages of the disease, appearing before substantial neuron loss [134]. This suggests that unregulated ROS formation, rather than being a subsequent reaction to increasing neurodegeneration, is a possible cause of dopaminergic cell death [135].

### 5.4.2. Sector Structure

The stock-flow diagram of the oxidative damage sector is shown in Figure 5.14. There are two stocks: (1) oxidative damage, and (2) GSH level. Table 5.8 shows the oxidative damage sector stocks, and parameters are given in Table 5.9. The procedure for assigning initial values is given in the descriptions of the stocks.

Table 5.8. Oxidative damage sector stocks.

| **Stock Name** | **Initial Value** | **Unit** |
|---|---|---|
| Oxidative damage | 0 | level |
| GSH level | 56.8 | $\mu$g/g |

Table 5.9. Oxidative damage sector parameters.

| **Variable Name** | **Value** | **Unit** |
|---|---|---|
| microglial OD production | 0.000001 | (level/microglia)/month |
| mitochondrial OD production | 0.19 | level/month |
| GSH increase delay | 3 | month |
| GSH decrease fraction | 4.7 | ($\mu$g/g)/month |
| GSH capacity for OD reduction | 0.004 | ($\mu$g/g)/month |

A biomarker is used to identify the proportion of positively stained neurons that are oxidatively damaged to quantify oxidative damage. The stock's unit is thus determined to be level. Yoritaka et al. evaluated oxidative damage in PD and control brains. Healthy people had oxidative damage ranging from 0% to 15%, increasing with age. However, in those with PD, it could go up to 50% [132]. It is essential to underline that oxidative damage of 0, does not imply that the individual is not experiencing any oxidative stress. All people are subjected to oxidative stress regularly, which is mitigated by antioxidant mechanisms. On the other hand, oxidative damage in this study refers to the harm resulting from oxidative stress over time on cells and their functions. GSH level depicts the antioxidant capacity in our model. The unit and initial value of this stock are obtained from an autopsy report [72].

Oxidative damage changes with its increase and decrease flows and the related formulation is

$$\frac{dOxidative\ damage}{dt} = OD\ increase - OD\ decrease. \tag{5.32}$$

Oxidative damage (OD) increase is caused by dysfunctional mitochondria and activated microglia, and the related equation is

$$OD\ increase = \ mitochondrial\ OD + microglial\ OD. \tag{5.33}$$

Mitochondrial complex I activity (MCIA) is chosen as the mitochondrial function representation in our model. Mitochondrial oxidative damage (OD) formulates reactive generation via mitochondria-related pathways. Under normal conditions, mitochondrial activity does not affect oxidative damage because its function is tightly regulated. However, in case of mitochondrial dysfunction, electrons are leaked to the neurons, exacerbating oxidative damage. The formulation for mitochondrial OD production is

$$\begin{aligned} mitochondrial\ OD =& MIN(1, (1 - MCIA\ efficiency)) \times \\ & mitochondrial\ OD\ production. \end{aligned} \tag{5.34}$$

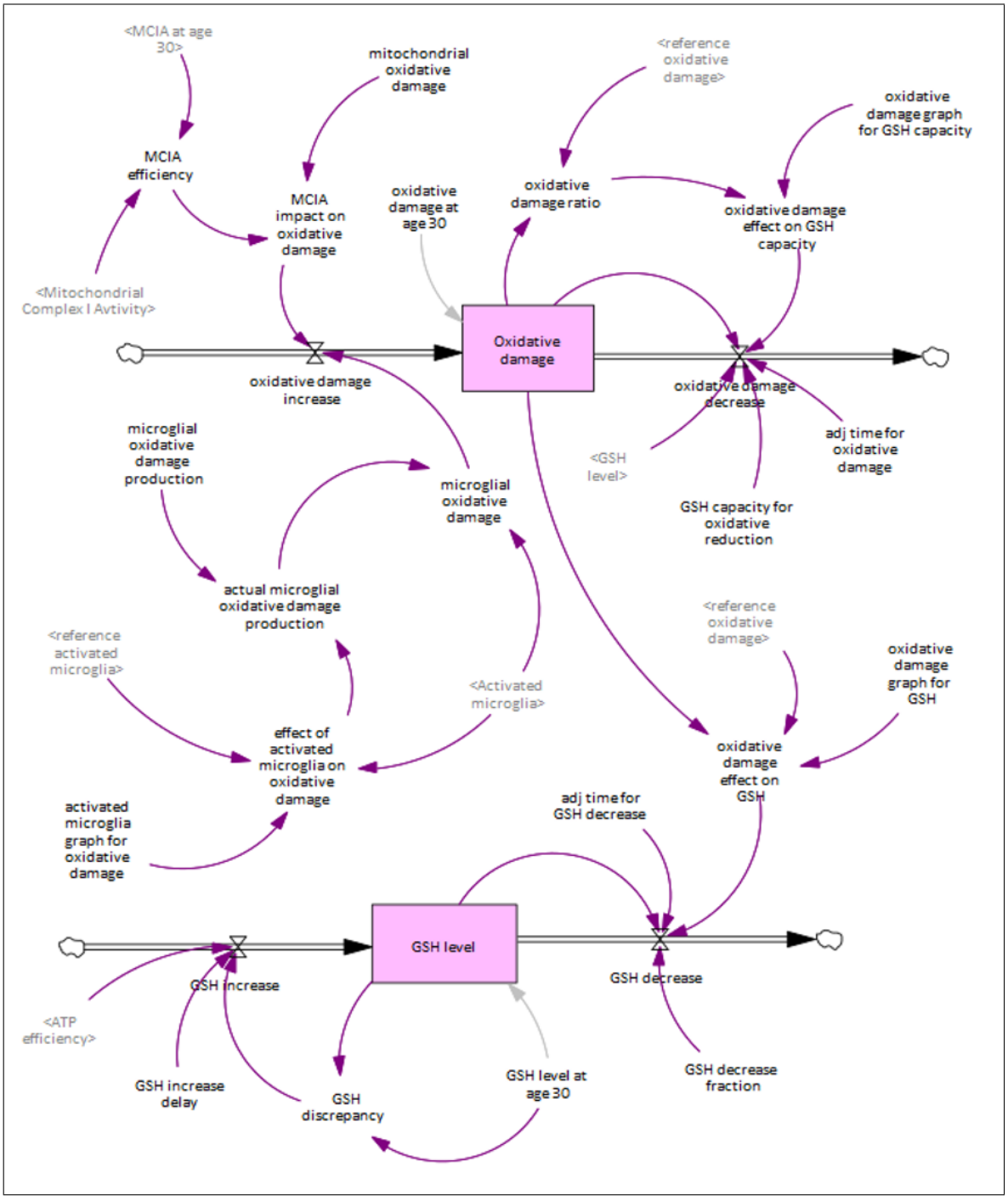


Figure 5.14. Stock-flow diagram of the oxidative damage sector.

Activated microglia are the other source of oxidative damage. As the amount of activated microglia grows, cells that stimulate each other produce more enzymes, leading to an uncontrolled increase in oxidative damage. This affects the microglial

oxidative damage production per activated microglia. To obtain actual microglial oxidative damage production, we include the effect of microglia on oxidative damage in the following formula

$$\begin{aligned} actual\ microglial\ OD\ production =& microglial\ OD\ production \times \\ & Eff\ of\ microglia\ on\ OD. \end{aligned} \tag{5.35}$$

Oxidative damage decrease is regulated via GSH level. The multiplication of GSH level and GSH capacity give the possible decrease. Existing oxidative damage also reduces capacity negatively. To employ this, we included the effect of oxidative damage on GSH capacity to determine the actual capacity in the following formulation:

$$\begin{aligned} OD\ decrease =& MIN(\frac{Oxidative\ damage}{adj\ time}, GSH\ level \times \\ & GSH\ capacity \times Eff\ of\ OD\ on\ GSH\ capacity). \end{aligned} \tag{5.36}$$

In our model, GSH level is calculated as

$$\frac{GSH\ level}{dt} = GSH\ increase - GSH\ decrease. \tag{5.37}$$

The presence of oxidative damage causes a decrease in GSH levels due to the reaction between oxidant and anti-oxidant materials. Thus, GSH decrease is formulated by including the effect of oxidative damage on GSH as

$$\begin{aligned} GSH\ decrease =& MIN(\frac{GSH\ level}{adj\ time}, Eff\ of\ OD\ on\ GSH\ decrease \times \\ & GSH\ decrease\ fr). \end{aligned} \tag{5.38}$$

We then proposed that cells should try to bring their GSH level to desired levels as a balancing act. Therefore, the GSH discrepancy between the desired and the actual value triggers the GSH increase flow. GSH production is highly dependent on ATP. In a follow-up study, scientists find out that GSH supplementation increases GSH levels

after approximately 3 months [136]. Thus, GSH increase flow is

$$GSH\ increase = \frac{ATP\ efficiency \times GSH\ discrepancy}{GSH\ delay}. \tag{5.39}$$

Reference oxidative damage refers to the amount of oxidative damage an elderly individual at the age of 80 has. In PD patients, this value can be up to 4 times the normal value. Oxidative damage effect on GSH capacity is S-shaped. A rapid rise starts around x=0.5. Graph saturates at x=3 with an output value of around 1 because of the calibration procedure according to the maximum value of GSH capacity (Figure 5.15a). Oxidative damage effect on GSH decrease shows a sharp and linear increase at first and then saturates at oxidative densities of PD patients. This graph is calibrated according to the maximum value of GSH decrease fraction (Figure 5.15b).

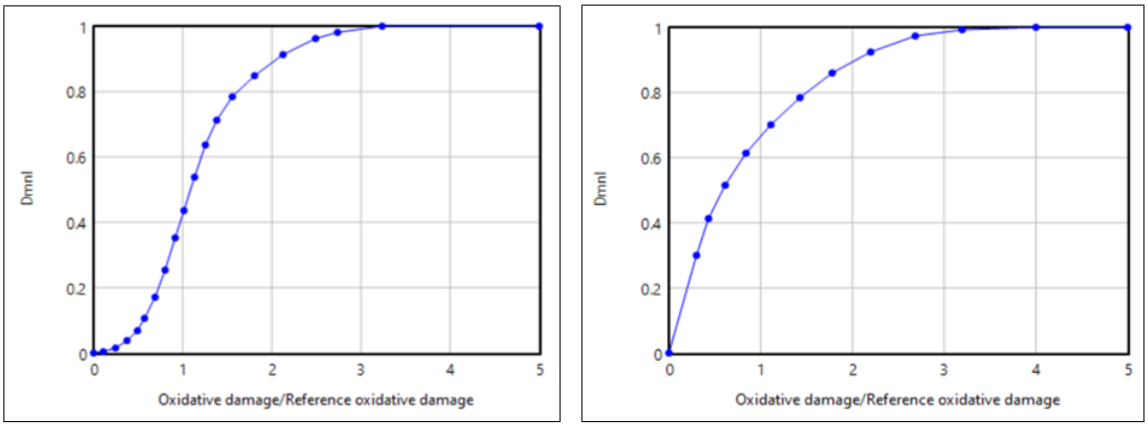


(a) Oxidative damage effect on GSH capacity (b) Oxidative damage effect on GSH decrease

Figure 5.15. Graphical functions of oxidative damage effects on GSH.

Reference activated microglia corresponds to the amount of activated microglia an elderly individual at the age of 80 has. In advanced PD cases, this number can rise up to threefold. The microglia effect on oxidative damage saturates around y=1 because it is calibrated according to the maximum value of microglial OD production. For lower microglia levels than the desired (until x=0.08), microglia do not affect oxidative damage (Figure 5.16).

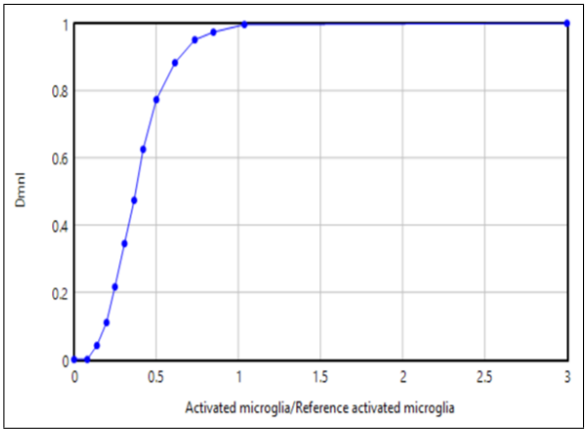


Figure 5.16. Graphical function of microglia effect on oxidative damage.

## 5.5. Mitochondria Sector

### 5.5.1. Background Information

The central nervous system is vulnerable to mitochondrial activity because its function is highly dependent on energy production. Mitochondrial dysfunction initially detected as a deficiency in mitochondrial complex I activity (MCIA), is found within the neurons of the substantia nigra (SN). This deterioration is caused by mitochondrial DNA (mtDNA) deletions and alpha-synuclein oligomers. Both normal aging and neurodegeneration are associated with mtDNA deletions [137]. These deletions accumulate progressively during life and are directly responsible for a measurable deficiency in mitochondrial functions. In turn, increased reactive species result in further mtDNA damage [79]. In summary, there is a continuous vicious cycle between mitochondrial variables and oxidative damage.

### 5.5.2. Sector Structure

The stock-flow diagram of the mitochondria sector is shown in Figure 5.17. There are three stocks: (1) accumulated mtDNA deletions, (2) mitochondrial complex I activity, and (3) ATP synthesis level. Table 5.10 shows the mitochondria sector stocks and the parameters are given in Table 5.11.

Table 5.10. Mitochondria sector stocks.

| **Stock Name** | **Initial Value** | **Unit** |
|---|---|---|
| Accumulated mtDNA deletions | 20 | level |
| Mitochondrial complex I activity | 24.7 | nmol/(min*mg) |
| ATP synthesis level | 100 | level |

Table 5.11. Mitochondria sector parameters.

| **Variable Name** | **Value** | **Unit** |
|---|---|---|
| mtDNA deletion fraction | 0.055 | level/month |
| other sources of deletions | 0.012 | level/month |
| ATP decrease fraction | 0.125 | level/month |
| MCIA reduction fraction | 0.14 | nmol/(month*min*mg) |

Accumulated mtDNA is regulated by a net flow called mtDNA deletions which stands for the deletion mutations in the DNA of mitochondria during aging. Thus, the formulation for the corresponding stock is

$$\frac{dAccumulated\,mtDNA\,deletions}{dt} = mtDNA\,deletions. \tag{5.40}$$

This stock's unit is determined to be level. Because studies investigating this variable use the deletion level in terms of percentage. According to the study of Dolle and friends, 20% of mtDNA deletions were observed even in individuals aged 20 years [138]. Therefore, an inflow other than oxidative damage-related reasons should increase mtDNA deletions. Depending on this, mtDNA deletions flow is formulated as

$$\begin{aligned} mtDNA\,deletions =& other\ sources\ of\ deletions + (mtDNA\,deletion\ fr\times \\ & Eff\ of\ OD\ on\ mtDNA \times mtDNA\,deletion\,possibility). \end{aligned} \tag{5.41}$$

Higher densities of oxidative damage result in more devastating impacts. Thus, we include the effect of oxidative damage on mtDNA in our formula. mtDNA deletion possibility is formulated to ensure that accumulated mtDNA deletions cannot surpass

100. The probability of deletion increases with the environment's healthy mtDNA abundance. As it is not significant to the model, deletions that occur to mtDNA that have already had deletions are not of concern.

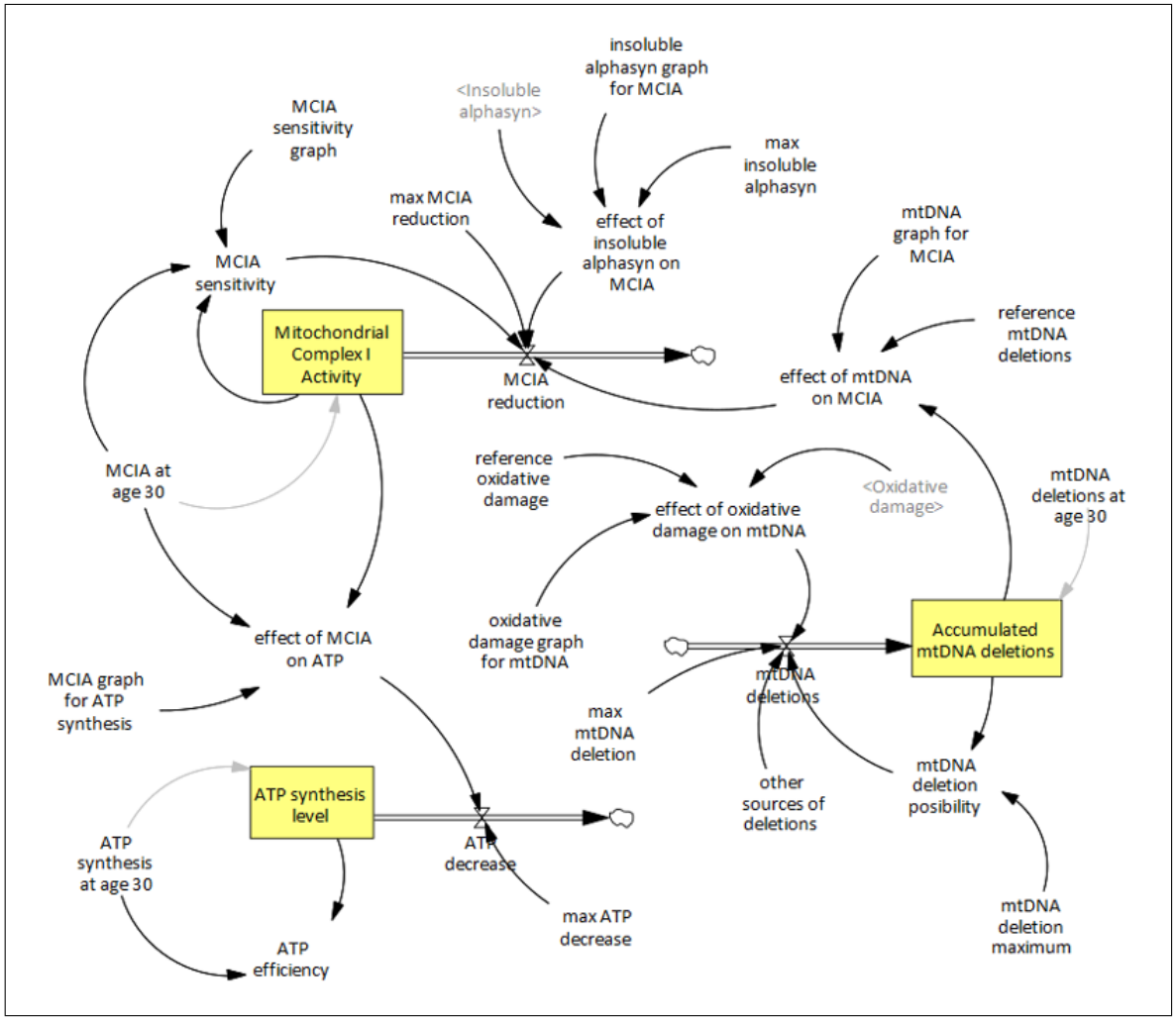


Figure 5.17. Stock-flow diagram of the mitochondria sector.

Mitochondrial complex I activity is the largest enzyme complex of the mitochondrial functions, therefore, it is implemented to reflect mitochondrial function [139]. The equation for mitochondrial complex I activity (MCIA) is

$$\frac{Mitochondrial\ complex\ 1\ activity}{dt} = -MCIA\ reduction. \tag{5.42}$$

Insoluble alpha-synuclein and mtDNA deletions both contribute to MCIA reduction flow, thus, the formulation includes those elements as

$$\begin{aligned} MCIA\,reduction =& MCIA\,reduction\,fr \times (Eff\,of\,mtDNA\,on\,MCIA+ \\ & Eff\,of\,insoluble\,alphasyn\,on\,MCIA)\times \\ & MCIA\,compensation. \end{aligned} \tag{5.43}$$

The unit of the last stock in our model, ATP synthesis level, is level. This stock is approximately 100% while a person is young, but it gradually declines during aging due to mitochondrial dysfunction. Thus, we only include an outflow to conceptualize this stock variable as

$$\frac{dATP\,synthesis\,level}{dt} = -ATP\,decrease. \tag{5.44}$$

The effect of MCIA on ATP regulates this outflow as follows:

$$ATP\,decrease = ATP\,decrease\,fr \times Eff\,of\,MCIA\,on\,ATP. \tag{5.45}$$

Reference oxidative damage refers to the amount of oxidative damage an elderly individual at the age of 80 has. In PD patients, this value can be up to 4 times the normal value. The graphical function is S-shaped. A rapid rise starts around x=0.5. Graph saturates at x=2 with an output value around 1 because of the calibration procedure according to the maximum value of mtDNA deletion fraction (Figure 5.18a).

Reference MCIA presents the desired level for mitochondrial function which is equal to the initial level of the MCIA stock. For young and healthy individuals, the input for this graphical function is around 1, which gives an output of 0. Thus, there will be no MCIA-induced ATP synthesis decrease. If this ratio gets closer to 0, the ATP decrease flow reaches its maximum value (Figure 5.18b).

The quantity of insoluble alpha-synuclein in an advanced PD is referred to as the reference insoluble protein. This number is expected to increase up to 1.5 times during the aging process. Because of the calibration method based on the maximum MCIA reduction fraction, the S-shaped graphical function saturates at y=1. In young and healthy people, the input for this function is close to zero, resulting in zero or very low amounts of reduction in mitochondrial function (Figure 5.18c).

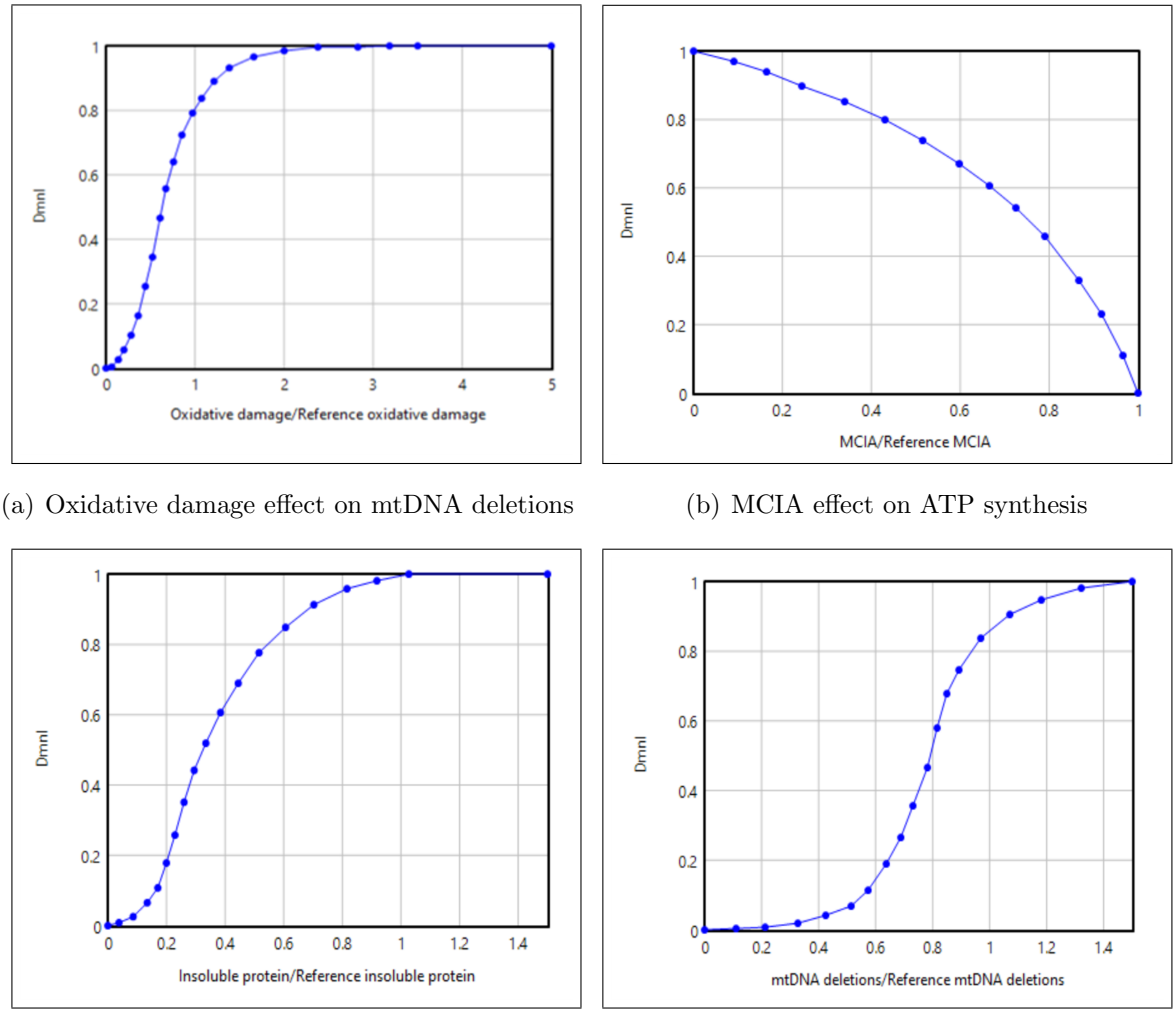


(a) Oxidative damage effect on mtDNA deletions

(b) MCIA effect on ATP synthesis

(c) Insoluble alpha-synuclein effect on MCIA

(d) mtDNA effect on MCIA

Figure 5.18. Graphical functions of mitochondria sector effects.

Reference mtDNA deletion amount is set to the level of advanced PD patients. This amount is assumed to rise up to 1.5 times as people age. The graphical function

is S-shaped. For input values lower than 0.5, which is equal to the amounts healthy and young individuals have, there is not much impact on mitochondrial activity by mtDNA deletions. Then, a sharp increase happens and the function saturates at y=1 (Figure 5.18d).

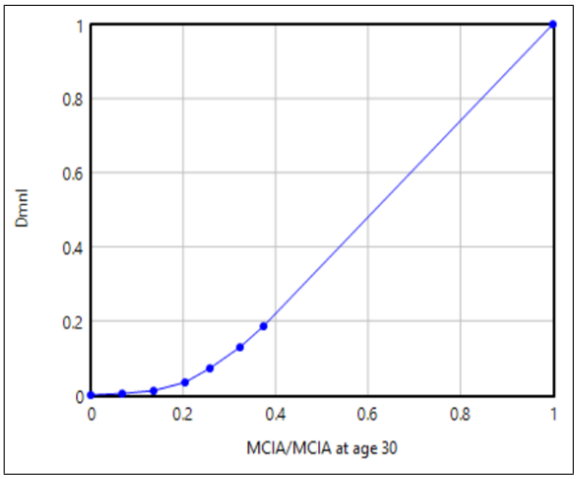


Figure 5.19. Graphical function of MCIA compensation.

MCIA compensation effect is standardized according to the desired value, which is equal to the initial level of the MCIA stock. In our model, mitochondrial activity is modeled as the average activity which declines during aging. Thus, there is only MCIA reduction outflow. The input values of the graphical function can change between 0 and 100. For low ratios, mitochondria try to compensate for the MCIA reduction by functioning more (Figure 5.19). Each equation is given in Appendix A.

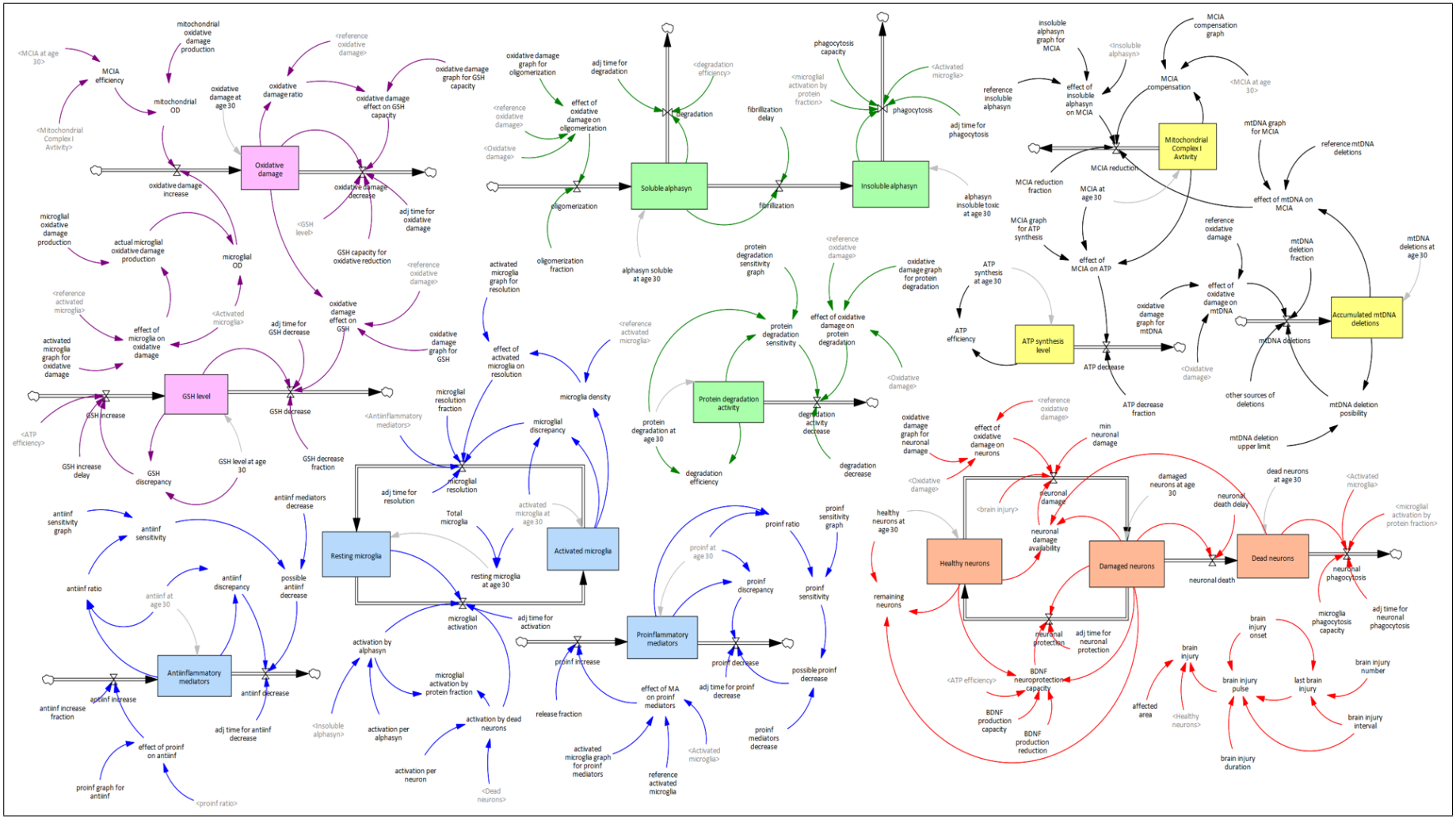


Figure 5.20. Stock-flow diagram of the whole model.

# 6. MODEL VALIDATION AND BASE RUN

This chapter aims to further demonstrate and analyze the model's validity. Our model is simulated by Vensim DSS software, version 9.3.0. This software provides an interface for developing and analyzing dynamic feedback models by solving differential equations. The simulation time unit and time step are chosen as one month, and 0.0625 months, respectively. The time horizon is 600 months, which stands for a 50-year period for a 30-year-old healthy individual up to the age of 80. The validation roadmap, inspired by the literature, is given in Figure 6.1.

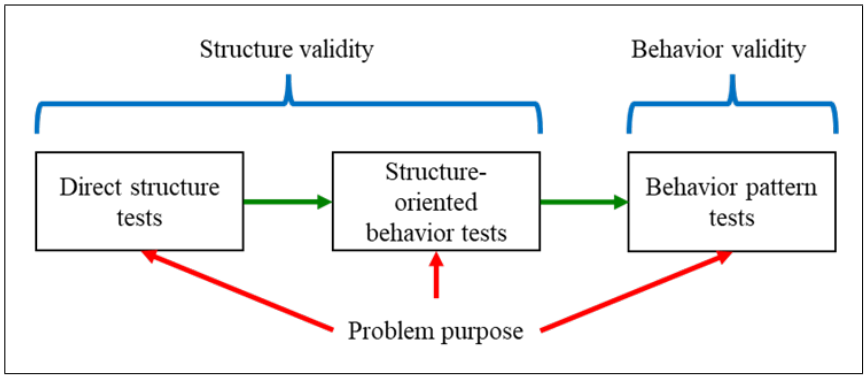


Figure 6.1. Formal model validation procedure (based on [140]).

The validation of system dynamics models consists of two fundamental concepts: (1) structure validity and (2) behavior validity. Model validation tests all depend on the objective, which is specified in the problem identification step. Behavior validity tests are only meaningful when there is sufficient confidence in the model structure. Hence, a formal procedure of validation requires testing the structure validity first and then the behavior adequacy. Structural validity tests verify if the model structure properly reflects the existing relationships in the real system. These tests can be further divided into two groups, direct structure, and structure-oriented behavior tests. The former directly compare the structure with available knowledge about real systems, whereas, the latter evaluates the structure indirectly by performing behavior tests on model

output. To assess whether the dynamic behaviors generated by the model can adequately capture the underlying real patterns, behavior validity tests are implemented. The focus of behavior validity testing is on pattern prediction rather than point estimation [140].

## 6.1. Direct Structural Tests

Structure confirmation tests try to compare the mathematical equations of the model, directly with the nature of the existing relationships between variables in the real system. Since the knowledge currently available in the literature is largely qualitative, they are challenging to define and quantify. In this study, the direct structure tests are simultaneously accomplished through the entire model construction phase. Because it is not possible to complete these tests in isolation. Since there are still many unanswered questions regarding PD and human brain aging, the missing information in the literature has been derived from the insights gained from rodent experimental studies.

The preceding chapter provides a comprehensive explanation of the parameterization of the base run (normal aging). The brain activities and materials are measured through post-mortem analyses, which makes instant detection of changes practically impossible. Thus, the numerical values of many parameters are not accessible in the literature. To overcome this, the quantities of these factors are chosen based on insights gathered from available papers. Predicted approximate real reference behaviors for a normal aging individual is prepared. Missing parameter values and effect functions are defined accordingly. More details are addressed while explaining the base run.

When compared to normal settings, it is relatively simple to estimate what values the real system's variables would acquire. Therefore, a direct extreme condition test for each equation is performed in isolation. Finally, dimensional consistency is satisfied in all equations. All variables in the model have real-life meanings and units.

## 6.2. Structure-Oriented Behavior Tests

To conduct an indirect extreme condition test, extreme values are assigned to the specified parameters, and the model's behavior is compared to the expected behavior of the real system. This aims to ensure that the simulation model would produce valid behaviors under extreme conditions as the real system would produce. The system examined in this study has no natural equilibrium, since the brain and related subsystems change with aging, resulting in disequilibrium (dynamics). However, just to test the structure of the model, it can be simulated under some hypothetical (extreme) conditions. Some examples of such conditions in our model are having no initial activated microglia, no external increase in mitochondrial DNA deletions, and no initial damaged neurons. In selected hypothetical conditions, brain variables would remain at equilibrium. We observe constant equilibrium values for the important variables demonstrated in Figure 6.2. Behavior graphs are colored to visualize different sectors.

When all microglia are in resting phenotype, there will be no activated microglia. Thus, microglia-induced oxidative stress does not exist in the system. Pro- and anti-inflammatory mediators remain constant at their initial values. Mitochondrial dysfunction does not develop, and mitochondrial complex I activity remains unchanged. Accordingly, ATP synthesis performance is 100%, which maintains a steady GSH level. Because neither mitochondria nor microglia generates oxidative stress, oxidative damage level in substantia nigra (SN) is zero throughout the simulation. Thus, insoluble alpha-synuclein does not accumulate and protein degradation activity stays unchanged. Most importantly, all neurons are healthy.

Modified-behavior prediction is another approach adopted in structure-oriented behavior tests. In this method, available modified situations are analyzed to increase the credibility of the model. However, in the context of human brain aging, there are no such potential behaviors. The tests conducted so far within the current knowledge are considered to have ensured the validity of the model structure. The following stage in the validation phase is to apply a behavior pattern test to examine behavior validity.

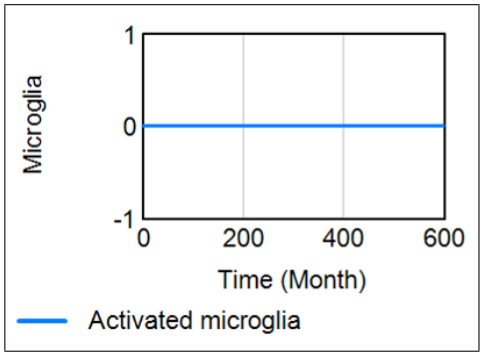


(a) Activated microglia

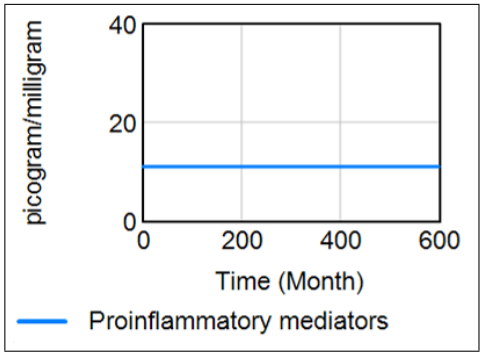


(b) Pro-inflammatory mediators

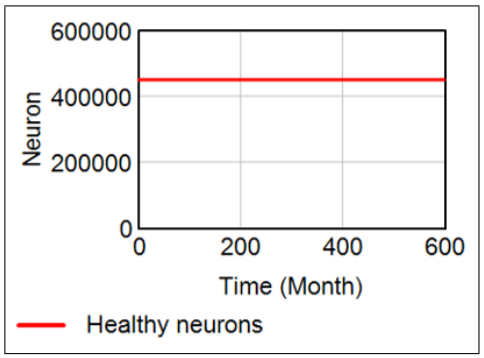


(c) Healthy neurons

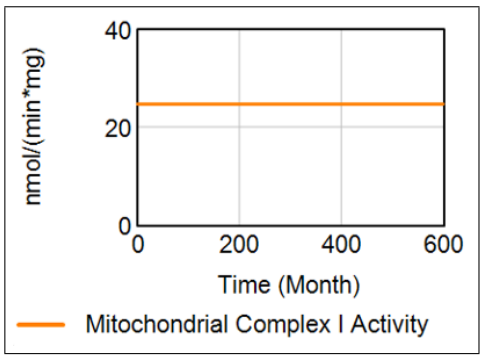


(d) Mitochondrial complex I activity

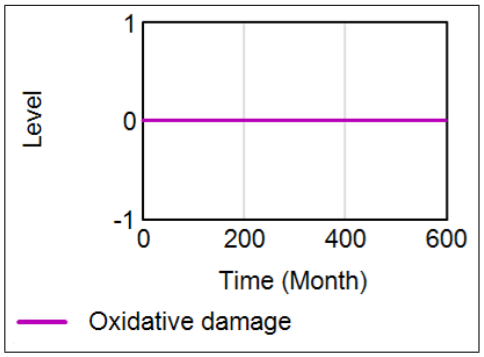


(e) Oxidative damage

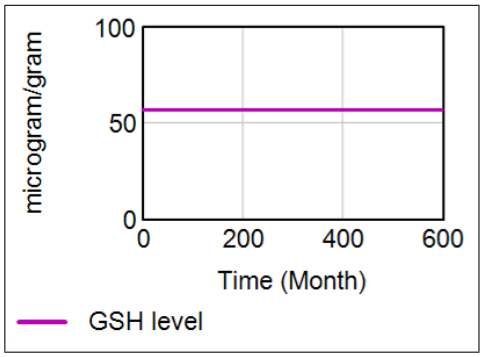


(f) GSH level

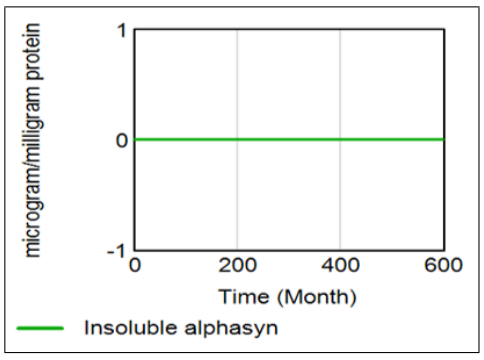


(g) Insoluble alpha-synuclein

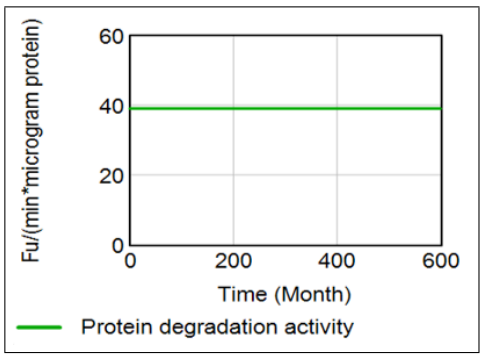


(h) Protein degradation activity

Figure 6.2. Hypothetical equilibrium run.

## 6.3. Behavior Pattern Tests

Comparing graphical or visual measurements of the most common behavior patterns with simulation output is the key approach in testing the validity of the model. No graph or measurement exists in the literature that can be utilized to assess directly the model behavior for several stocks. To create such visual patterns, post-mortem analyses of normal individuals of various ages are investigated. In cases where autopsy reports are insufficient, the proportional changes specified during aging in the animal experiments are used. Thus, the initial and final values of the stocks are determined or calculated. Between-point behaviors are predicted by exhaustive literature research.

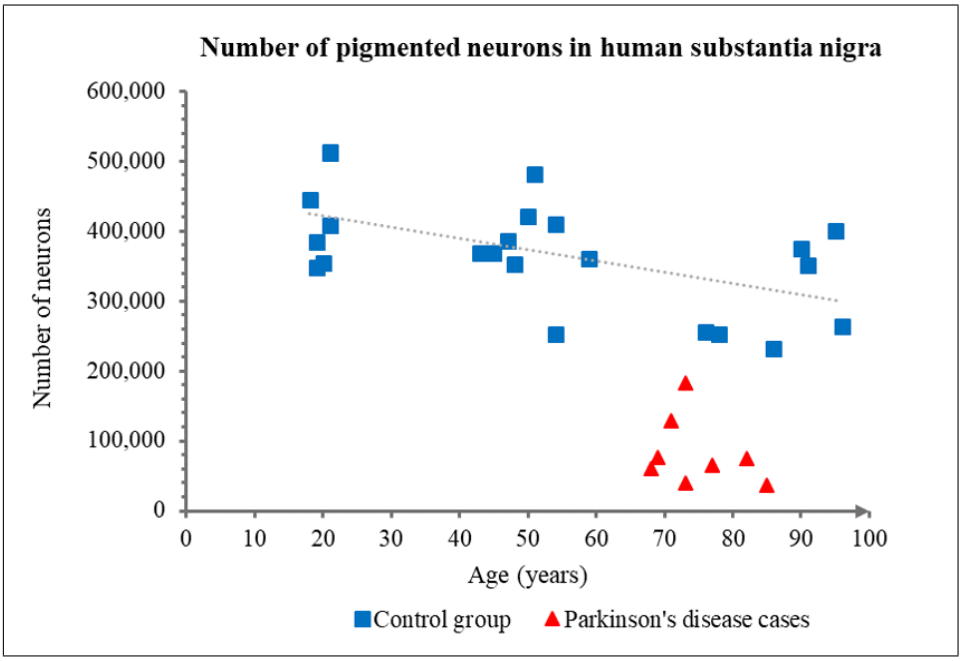


Figure 6.3. Real reference behavior of dopaminergic neurons (data from [116]).

Figure 6.3 demonstrates the real reference behavior for pigmented dopaminergic neuron population in the human substantia nigra (SN). For other variables, qualitative approximate real reference behaviors are predicted from partial data in the literature to employ in the model calibration for the base run (normal aging). Relevant references and explanations are provided.

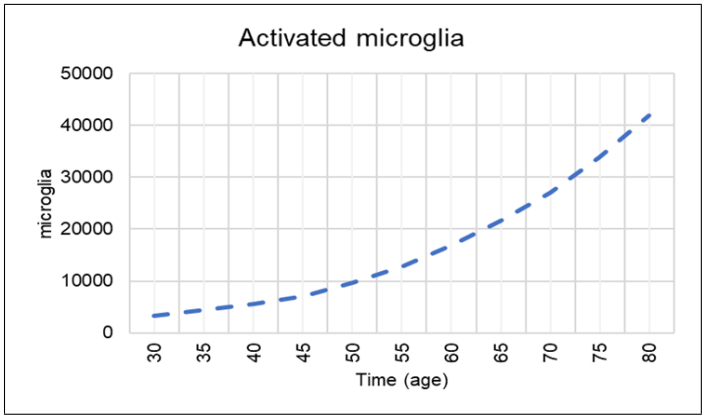


(a) Activated microglia

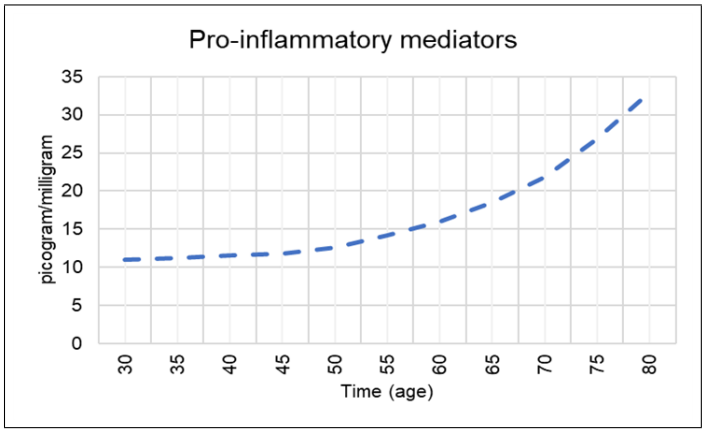


(b) Pro-inflammatory mediators

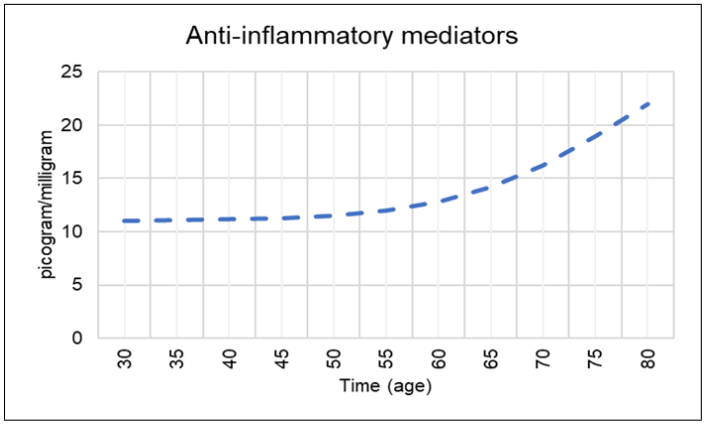


(c) Anti-inflammatory mediators

Figure 6.4. Neuroinflammation sector approximate real reference behaviors.

There was no difference in total microglial population between age groups [91]. However, microglia undergo increasing activation as individuals advance in age. [141].

The number of activated microglia in aged mice is approximately 12.5 times the number in adult mice. The fold change between healthy mice and PD mice is 2.5 [92]. Age-related dystrophy in microglia cells increases linearly in adulthood while exponentially in old age according to neuroimaging graphs [142] (Figure 6.4a).

Pro-inflammatory mediators are secreted by activated microglia, thus, their dynamics are dependent on microglia level. While a linear increase with a lower slope is expected in adulthood, this becomes self-perpetuating as individuals get older. Aging triggers the upregulation of inflammatory mediators in the rodent brain regions. The level of TNF-$\alpha$ triples as individuals age [97]. PD patients have roughly three times higher TNF-$\alpha$ levels than controls [96](Figure 6.4b).

The levels of anti-inflammatory mediators are regulated in response to the amount of pro-inflammatory mediators. They are released with or after the secretion of pro-inflammatory mediators [90], thus, their dynamics are dependent on pro-inflammatory mediators. IL-10 level doubles as individuals age [97]. The fold change between elderly PD and control is 1.2 [98]. Pro-inflammatory mediators can grow much more than anti-inflammatory mediators (Figure 6.4c).

Insoluble alpha-synuclein is equal to 0 under normal conditions since it is a toxic protein form which is harmful to neurons. The value in the brain SN at old ages for both PD and control are calculated using the soluble alpha-synuclein amount [143], the ratio between the toxic and healthy forms of soluble alpha-synuclein [144], and the insoluble/soluble alpha-synuclein ratio [145] from post-mortem analyses in the literature. The alpha-synuclein number in human SN shows an exponential increase during the aging process [105] (Figure 6.5a).

Aged cells experience a 1.5–2 fold decrease in proteasomal activities [111]. The post-mortem analysis of an elderly control reveals the protein degradation value for the brain. The level of protein degradation for PD is 45% reduced compared to healthy controls [112]. With those papers, initial and final values of protein degradation activity

are determined. There is not much change until the sixties in protein degradation activity, however, after that point, a nonlinear decrease occurs [146] (Figure 6.5b).

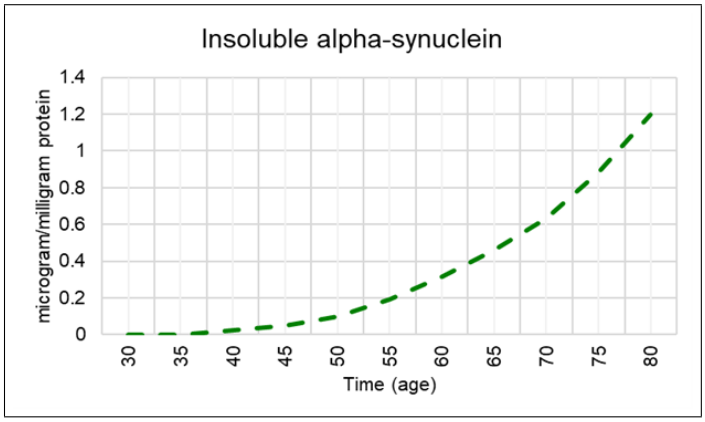


(a) Insoluble alpha-synuclein

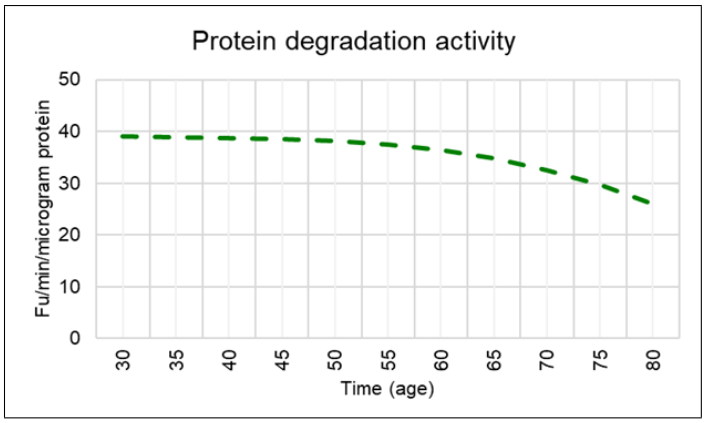


(b) Protein degradation activity

Figure 6.5. Protein aggregation sector approximate real reference behaviors.

The number of pigmented dopaminergic neurons in the SN of human brain for healthy adults is approximately 450,000. There is a linear decrease during aging which amplifies after the age of sixties. The remaining neurons are roughly equal to 300,000 for those elderly controls which means a 33% neuronal loss during aging (Figure 6.3 and Figure 6.6) [116]. PD patients are believed to lose 50% of dopaminergic neurons before the diagnosis [23], and the pigmented ones are typically lost [147].

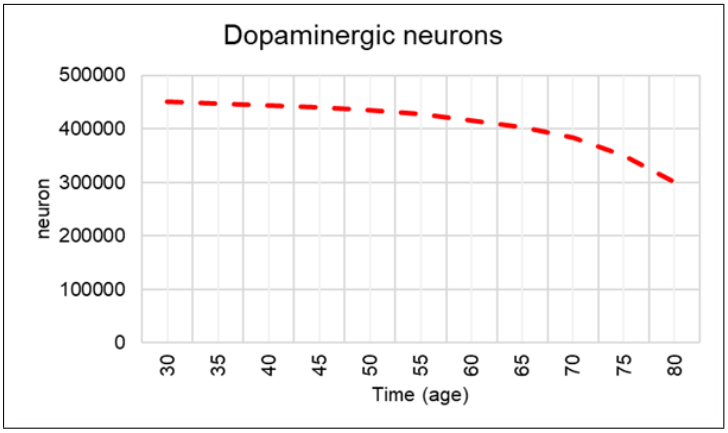


Figure 6.6. Dopaminergic neuron sector approximate real reference behavior.

There is no possible assessment of ROS in the brain. Instead, studies investigate oxidative stress-induced damage by immunostaining by post-mortem analysis. We obtain the positively stained nigral neurons for oxidative damage for healthy control and PD from an analysis [132]. According to this study, the oxidative damage (%) was ranging between 0 and 15 for controls with different age groups, whereas for PD cases this value reach up to 55. The behavior of oxidative damage during aging is believed to be exponential by several experts [79] (Figure 6.7a).

Riederer and colleagues analyzed the brains of controls and PD patients to observe the Glutathione (GSH) levels [72]. According to varying age groups the initial and final values are defined in our model. The human brain tries to raise the GSH level to the desired level since it declines as a consequence of its reaction to ROS. However, it was assumed that GSH production, which is mainly dependent on mitochondrial energy [82], exhibits similar behavior to ATP synthesis level (Figure 6.7b).

During the course of life, there is a gradual accumulation of mitochondrial DNA (mtDNA) deletions in response to oxidative damage [79]. The percentage of mtDNA deletions demonstrates a statistically significant positive correlation with age. Also, the SN neurons of individuals with PD have higher levels of mtDNA deletions, compared with age-matched controls [138]. Starting from young adulthood ages, it is assumed

from the same paper that there is a linear increase in mtDNA deletions which amplifies after the age of sixties (Figure 6.8a).

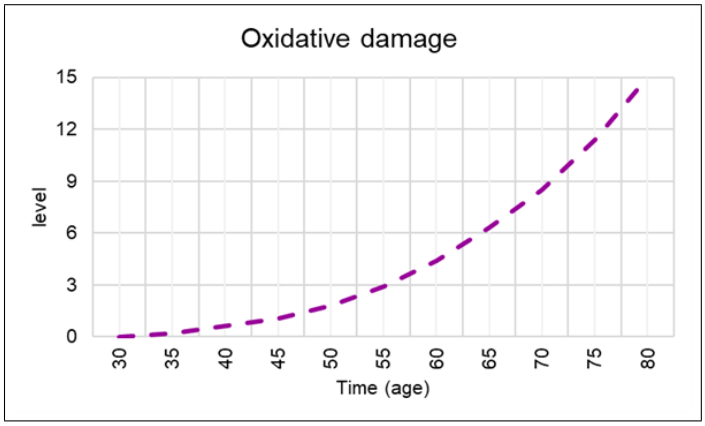


(a) Oxidative damage

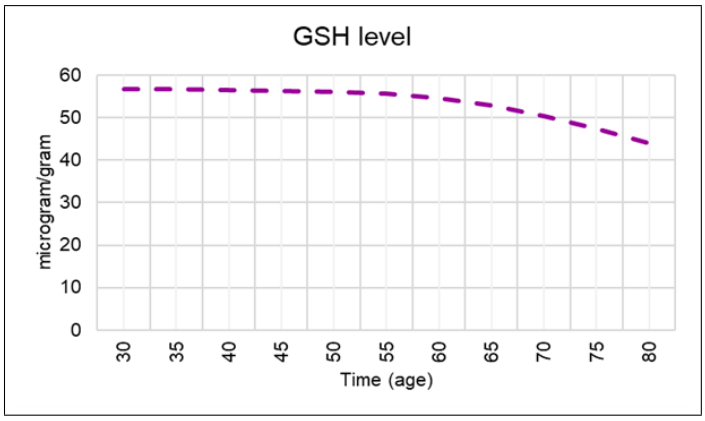


(b) GSH level

Figure 6.7. Oxidative damage sector approximate real reference behaviors.

In a post-mortem analysis, the mitochondrial complex I activity (MCIA) changed between 24.7 and 13.5 nmol/(min*mg) for controls with varying ages. PD individuals have the mitochondrial activity capacity as roughly 50% of age-matched controls [148]. The MCIA decrease is dependent on oxidative damage and protein aggregation which are increasing exponentially. Thus, an exponential decrease in MCIA during aging is expected (Figure 6.8b).

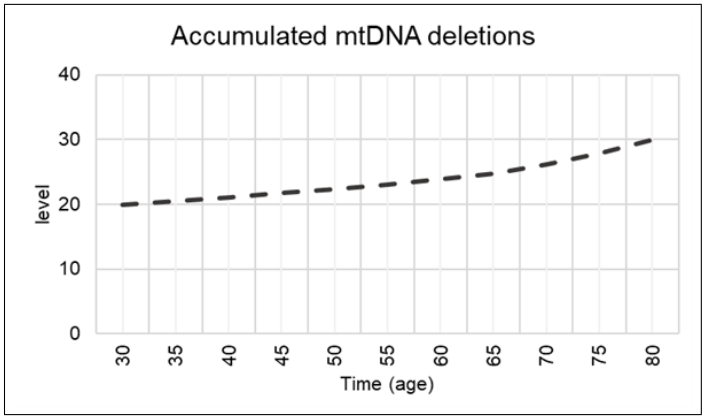


(a) Accumulated DNA deletions

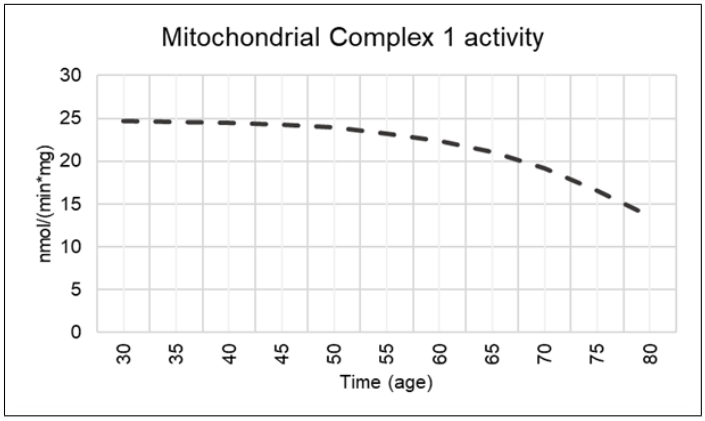


(b) Mitochondrial complex I activity

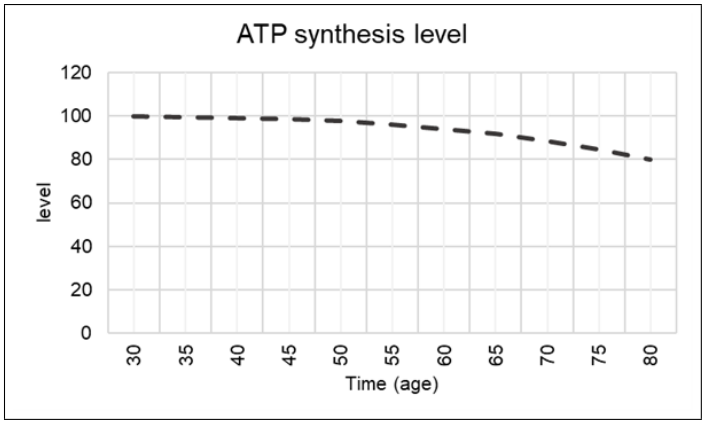


(c) ATP synthesis level

Figure 6.8. Mitochondria sector approximate real reference behaviors.

Research examining ATP levels across various age groups has unveiled a notable decline of approximately 20% during aging. [149]. This decrease displays an increasing decrease after some age. ATP synthesis levels of PD individuals are almost half of the

age-matched controls [150]. In our model, we assume that the ATP synthesis level is initially set at 100% for young adults. However, this level exhibits a significant decline, particularly after the sixties and shows an exponential decrease (Figure 6.8c).

## 6.4. Base Run

Base run aims to simulate normal aging dynamics for a healthy individual. Qualitative approximate real reference behaviors are included in Vensim via GRAPH() functions to compare with the model outputs of the base run (normal aging). The model behavior reflects the expected approximate real reference behaviors gathered from literature and experimental animal studies.

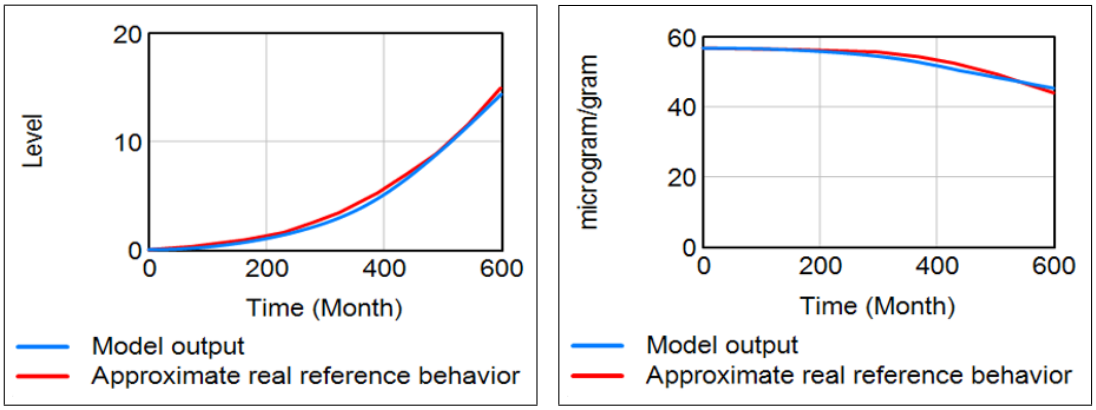


(a) Oxidative damage (b) GSH level

Figure 6.9. Comparison of model behavior and approximate real reference behavior for oxidative damage sector.

The free radical theory of aging posits that oxidative damage follows an exponential growth pattern, serving as a fundamental concept in understanding the aging process. Once a certain burden of oxidative damage is reached, irreversible changes commence within the brain. Various factors, including protein degradation activity, levels of glutathione (GSH), and the formation of alpha-synuclein aggregates, experience exponential declines as they are influenced by oxidative damage. These observations highlight the link between oxidative damage and age-related physiological changes.

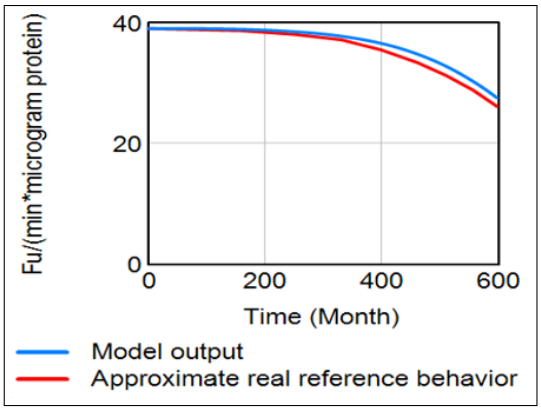


(a) Protein degradation

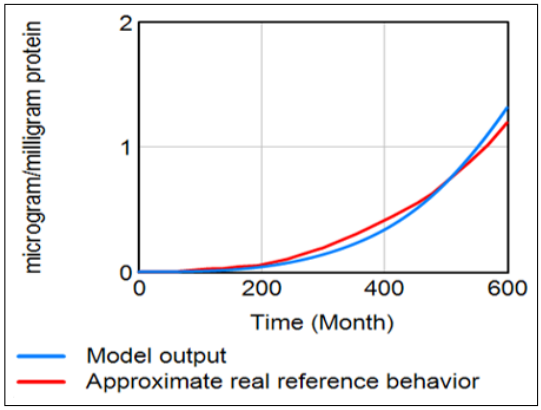


(b) Insoluble alpha-synuclein

Figure 6.10. Comparison of model behavior and approximate real reference behavior for protein aggregation sector.

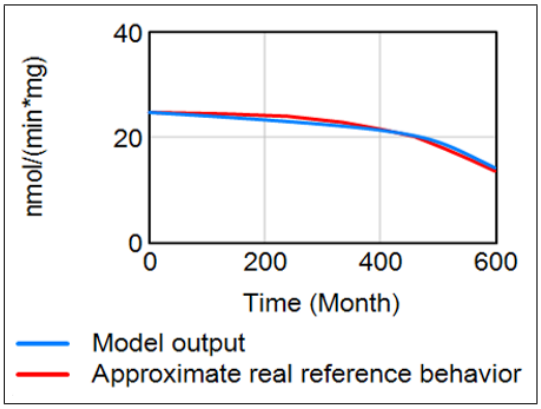


(a) Mitochondrial complex I activity

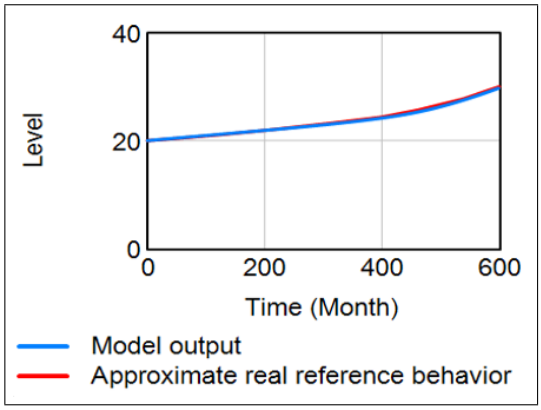


(b) Accumulated mtDNA deletions

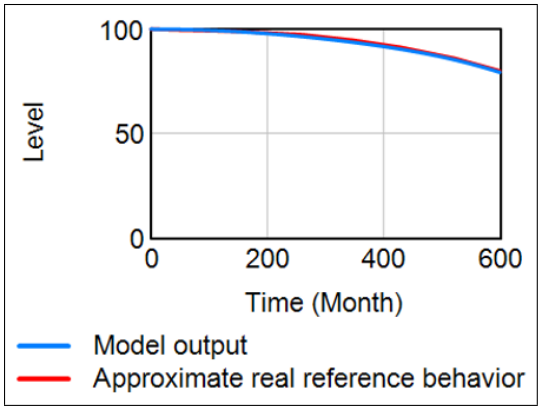


(c) ATP synthesis level

Figure 6.11. Comparison of model behavior and approximate real reference behavior for mitochondria sector.

Multiple studies provide compelling evidence supporting a close association between the accumulation of mitochondrial DNA (mtDNA) deletions and the aging process. Furthermore, mitochondrial activity is adversely affected by oxidative damage and mtDNA deletions during the aging process. With advancing age, mitochondrial activity decline accelerates.

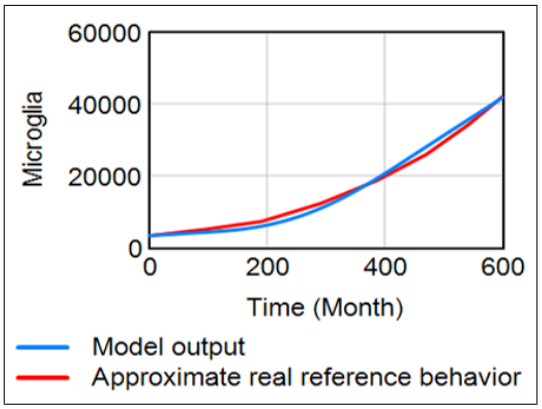


(a) Activated microglia

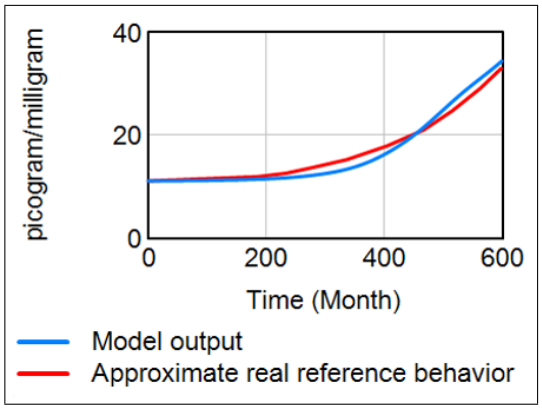


(b) Pro-inflammatory mediators

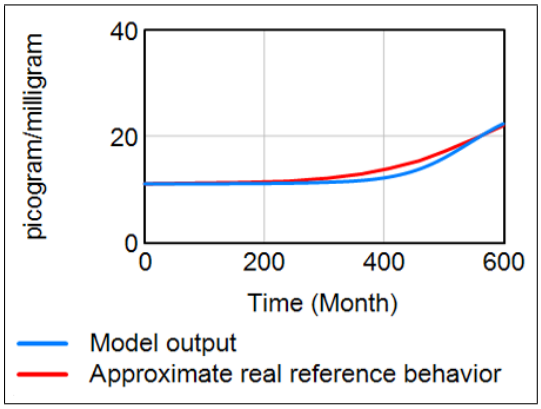


(c) Anti-inflammatory mediators

Figure 6.12. Comparison of model behavior and approximate real reference behavior for neuroinflammation sector.

During adulthood, the population of activated microglia exhibits linear growth. Beyond a certain age, this increase becomes more pronounced and leads to exponential growth in the brains of older individuals. The expansion of activated microglia has a direct impact on the production and release of inflammatory mediators.

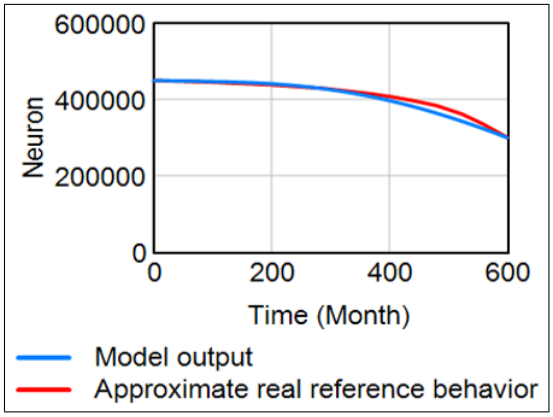


Figure 6.13. Comparison of model behavior and approximate real reference behavior for dopaminergic neuron sector.

There is a gradual and continuous loss of dopaminergic neurons while aging, however, it amplifies after some age. At some point, the neuroprotective mechanisms that exist in the brain become insufficient to adequately repair or replace damaged neurons, which results in an increase in the stock of dead neurons.

# 7. SENSITIVITY ANALYSIS

The sensitivity of a model to changes in its parameter values and structural properties is evaluated via sensitivity analysis. This analysis is often conducted as a series of experiments in which alternative values are set to observe how a change in the parameter value or initial quantity affects the dynamic behavior of the system. With this approach, model confidence is improved by exploring uncertainties. In real life, several parameters are exceptionally hard, if not impossible, to measure. Sensitivity tests help uncover parameters that the model is indifferent to. In such cases, the use of an estimation rather than a precise value saves time for the modeler. Also, sensitivity analysis can reveal important parameters, whose change identifies a leverage point.

In this section, sensitivity analysis with several experiments is conducted. To avoid combinatorial complexity, the analysis is performed one change at a time. We examined the impact of different initial values of some stocks, and then different parameter values. Overall, the model shows consistent behavior in terms of model assumptions and real-life expectations. As a result of sensitivity analysis, some effect functions have been revised to include greater input values. Thus, sensitivity analysis is also a critical tool for ensuring model robustness. While comparing sensitivity runs, two outcomes of interest are defined: (1) remaining healthy neurons, and (2) insoluble alpha-synuclein. Because Parkinson's disease (PD) is characterized by these two indicators. Scientists focus on the neurons expressed as a percentage, rather than the absolute number [151], thus, we provide the remaining percentage for neurons.

## 7.1. Model Sensitivity to Changes in Initial Values

The model is simulated for 600 months, like in the base run, by modifying the initial values of five stocks. These stocks include; (1) oxidative damage, (2) activated microglia, (3) mitochondrial complex I activity (MCIA), (4) accumulated mtDNA deletions, and (5) insoluble alpha-synuclein due to their substantial causal links.

Table 7.1. Initial values for base and test runs.

| Stock | Base run | Run 1 | Run 2 | Run 3 | Run 4 |
|---|---|---|---|---|---|
| Oxidative damage | 0 | 0.5 | 1 | 1.5 | 2 |
| Activated microglia | 3,319 | 0 | 10,000 | 20,000 | 30,000 |
| Mitochondrial complex I activity | 24.7 | 20 | 22 | 23 | 26 |
| Healthy neurons | 450,000 | 300,000 | 350,000 | 500,000 | 600,000 |
| Accumulated mtDNA deletions | 20 | 5 | 10 | 15 | 25 |
| Insoluble alpha-synuclein | 0 | 0.1 | 0.2 | 0.3 | 0.4 |

As expected, the model is highly sensitive to oxidative damage, both in terms of toxic protein aggregation and neuronal loss. Because it is at the center of intersectoral relationships of the model by affecting many variables from different sectors. This indicates that oxidative damage-induced PD vulnerability is a possible pathological condition (Figure 7.1).

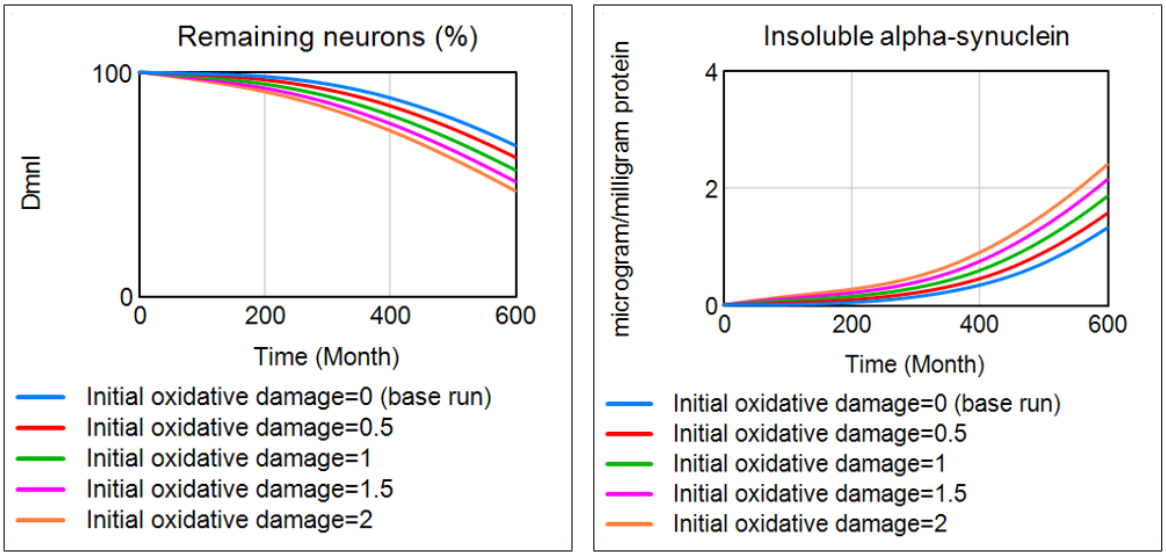


(a) Remaining neurons (%)

(b) Insoluble alpha-synuclein

Figure 7.1. Model sensitivity to different initial values of oxidative damage.

With different runs, several initial values of activated microglia levels, both greater and lower than the base run, are explored. Neuronal death and alpha-synuclein

accumulation increase dramatically when the initial activated microglia is ten times the base value. Activated microglia are responsible for some of the oxidative damage in neurons by producing more of these toxic forms during functioning (Figure 7.2).

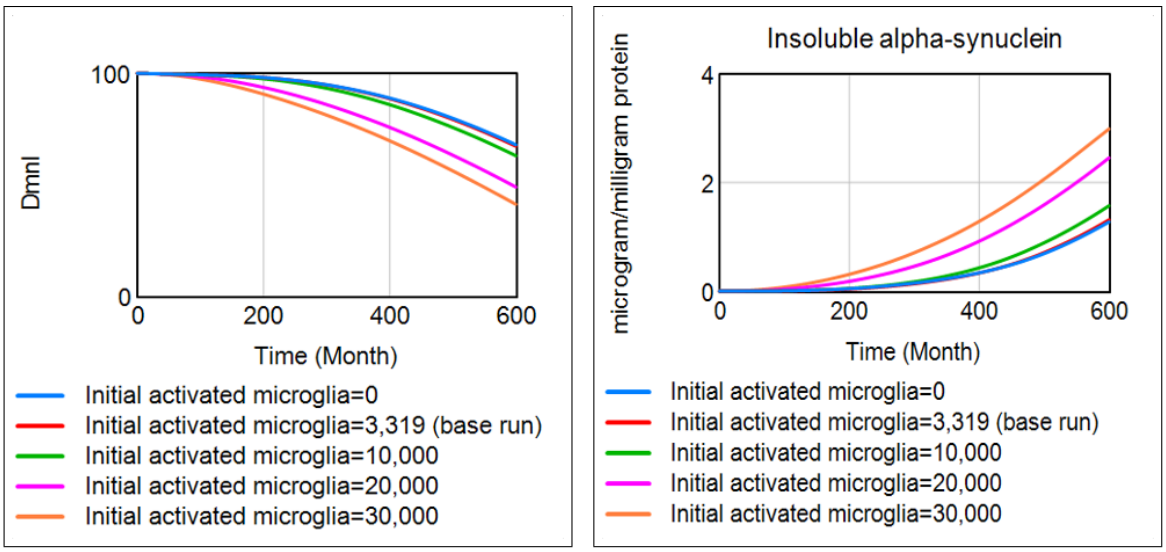


(a) Remaining neurons (%)

(b) Insoluble alpha-synuclein

Figure 7.2. Model sensitivity to different initial values of activated microglia.

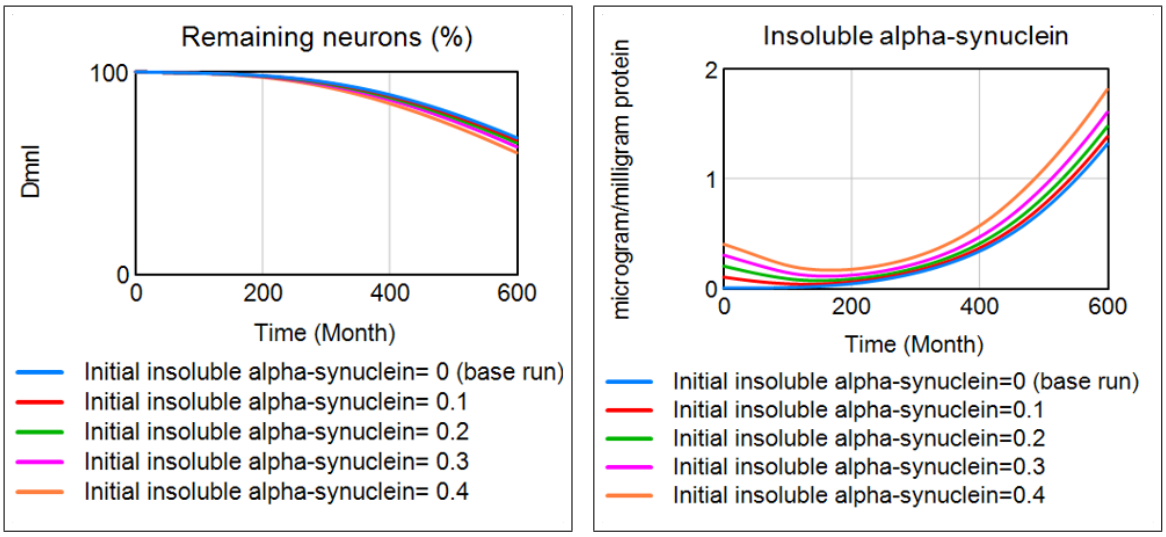


(a) Remaining neurons (%)

(b) Insoluble alpha-synuclein

Figure 7.3. Model sensitivity to different initial values of insoluble alpha-synuclein.

There are no insoluble protein aggregations at the beginning of the simulation in the base run. To further explore the effects of introducing initial amounts of toxic protein, the model was run with different test values. The findings from these simulations indicate that the presence of initial alpha-synuclein protein does not have a significant impact on the overall behavior of the system. This observation can be attributed to the effective degradation systems present in healthy adults. These systems play a crucial role in maintaining protein homeostasis and preventing the accumulation of insoluble protein aggregates (Figure 7.3).

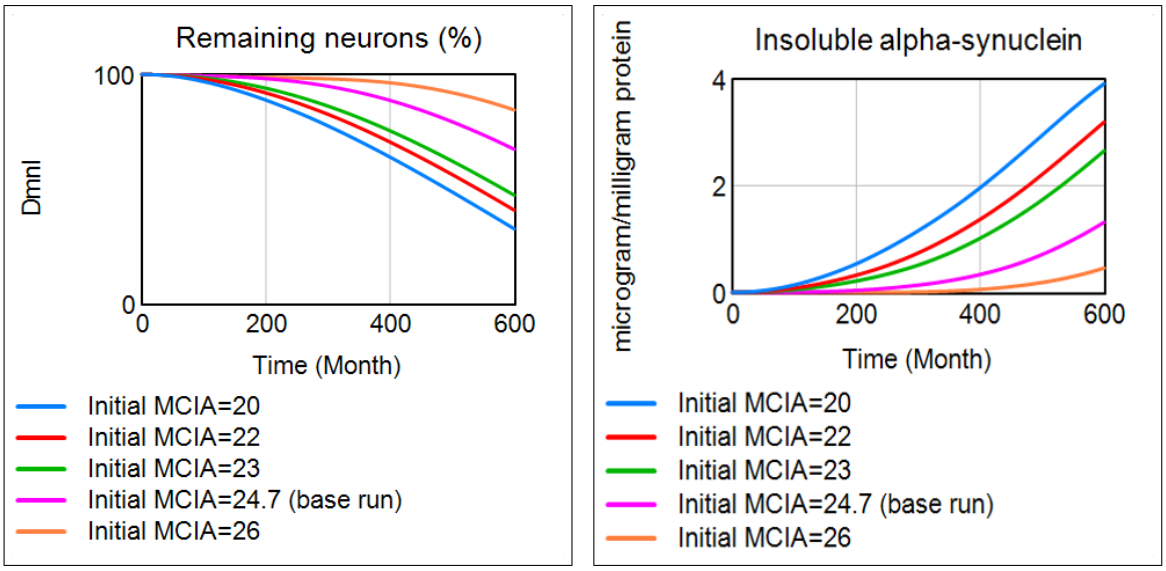


(a) Remaining neurons (%)

(b) Insoluble alpha-synuclein

Figure 7.4. Model sensitivity to different initial values of MCIA.

Mitochondrial function is represented by mitochondrial complex 1 activity (MCIA) in our model. Mitochondria provide the necessary energy for balancing activities in the brain such as antioxidant and neuroprotection mechanisms. Thus, its initial level for a healthy young adult is an important indicator. Another element of the mitochondria sector, mtDNA deletions, affects the same balancing mechanisms via MCIA-related pathways. Our model is sensitive to both mitochondrial function and mtDNA deletions in terms of neuronal death and protein aggregation (Figure 7.4 and Figure 7.5).

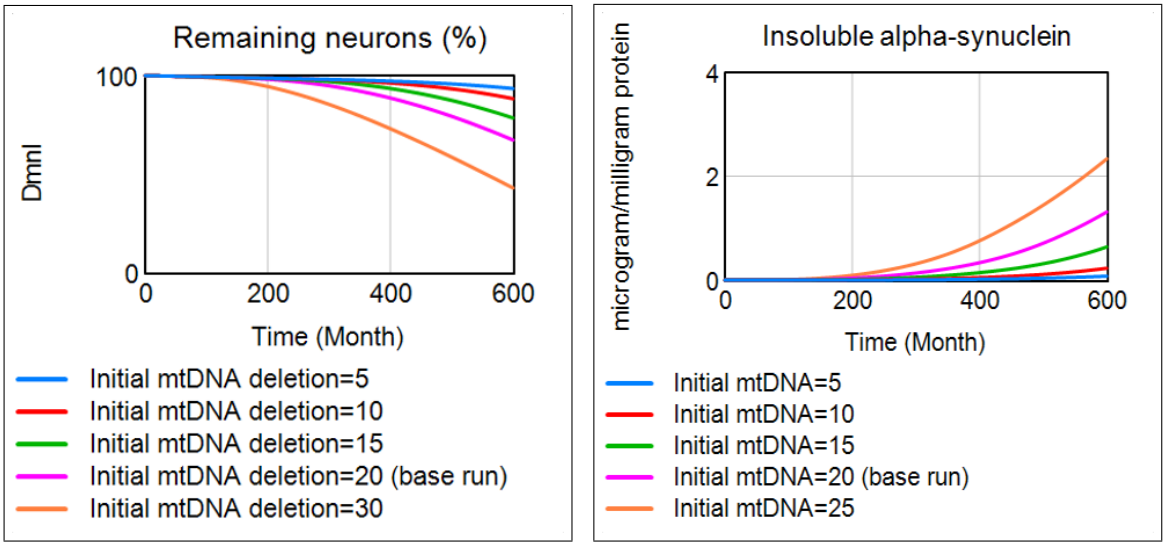


(a) Remaining neurons (%) (b) Insoluble alpha-synuclein

Figure 7.5. Model sensitivity to different initial values of accumulated mtDNA deletions.

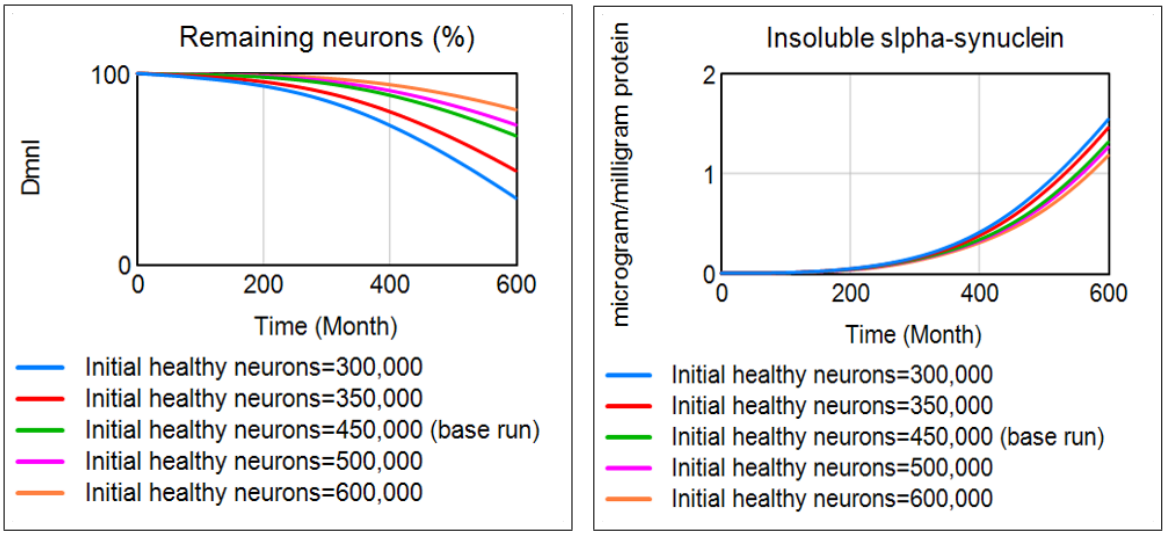


(a) Remaining neurons (%) (b) Insoluble alpha-synuclein

Figure 7.6. Model sensitivity to different initial values of healthy neurons.

The initial value of the healthy dopaminergic neuron population is of interest because a recent article discusses whether people with lower-than-normal dopaminergic neurons due to genetic variance are at more risk. A decline in the neuronal population has no clear causal association with Parkinson's pathology, however, such people may

be more susceptible to triggers [151]. Although experiments show lower levels of initial healthy neuron population increase neuronal death, the toxic protein accumulation, another characteristic of PD, does not change significantly (Figure 7.6).

## 7.2. Model Sensitivity to Changes in Parameter Values

The selected parameters are; (1) MCIA reduction, (2) oligomerization fraction, (3) BDNF production capacity, and (4) microglial oxidative damage (OD) production. The test values of those parameters are determined by multiplying the base value by 0.2, 0.5, 1.5, and 2, respectively. The chosen delays for sensitivity runs are; (1) neuronal death, and (2) fibrillization delay. Table 7.2 presents the values for base and sensitivity runs. All experiments are simulated for 600 months to observe long-term dynamics.

Table 7.2. Parameter values for base and test runs.

| **Parameter** | **Base run** | **Run 1** | **Run 2** | **Run 3** | **Run 4** |
|---|---|---|---|---|---|
| MCIA reduction | 0.14 | 0.028 | 0.07 | 0.21 | 0.28 |
| Oligomerization fraction | 0.045 | 0.009 | 0.0225 | 0.0675 | 0.09 |
| BDNF production capacity | 0.00044 | 0.000088 | 0.00022 | 0.00066 | 0.00088 |
| Microglial OD production | 0.000001 | 0.0000002 | 0.0000005 | 0.0000015 | 0.000002 |
| Neuronal death delay | 6 | 1 | 3 | 12 | 18 |
| Fibrillization delay | 2.5 | 1 | 3 | 6 | 12 |

As previously explained, mitochondria sector-related parameters are involved in the mechanisms affecting both insoluble alpha-synuclein aggregation and neuronal death. Thus, the model is sensitive to MCIA reduction fraction (Figure 7.7). By examining the sensitivity of the model to MCIA reduction fraction, researchers can gain insights into the critical role of mitochondrial function in the pathological processes associated with neurodegenerative diseases.

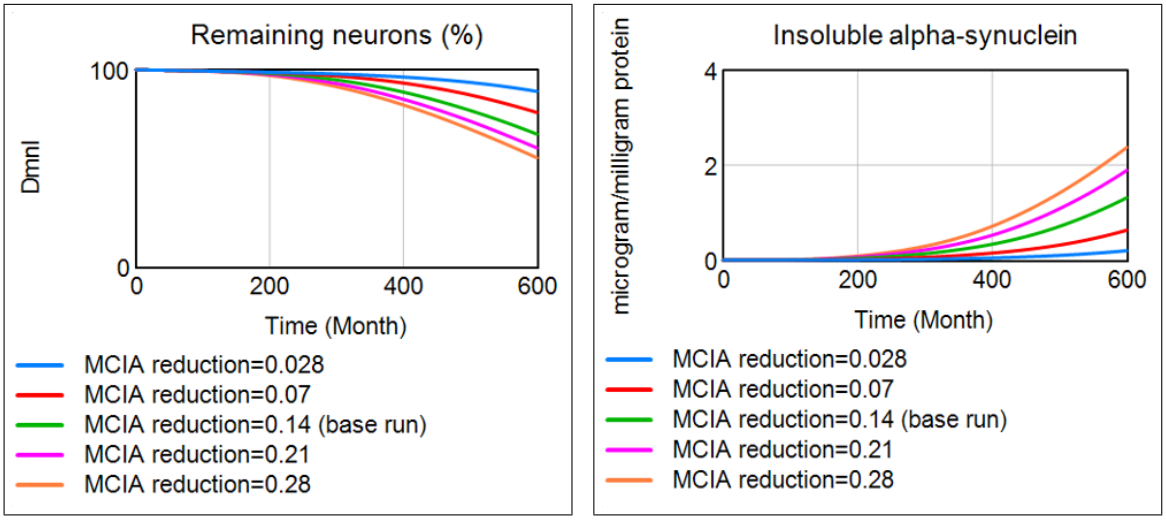


(a) Remaining neurons (%) (b) Insoluble alpha-synuclein

Figure 7.7. Model sensitivity to different MCIA reduction values.

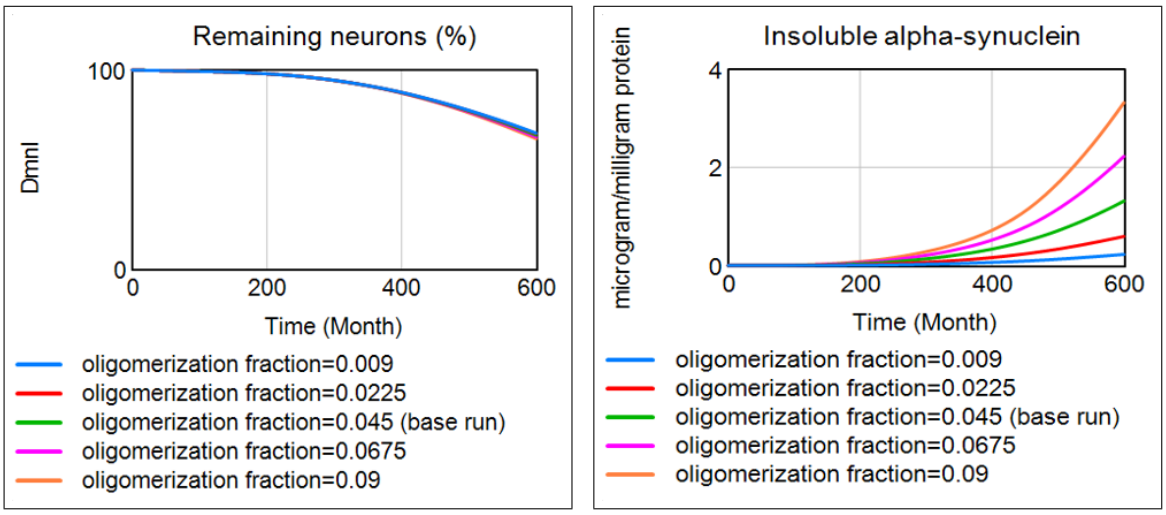


(a) Remaining neurons (%) (b) Insoluble alpha-synuclein

Figure 7.8. Model sensitivity to different oligomerization fraction values.

In our model, the oligomerization fraction plays a crucial role in determining the flow into the soluble alpha-synuclein stock. This process is dependent on oxidative damage and is significant for the subsequent formation of insoluble toxic protein aggregates. The model demonstrates that changes in the oligomerization fraction have a relatively higher sensitivity in terms of protein aggregation (Figure 7.8).

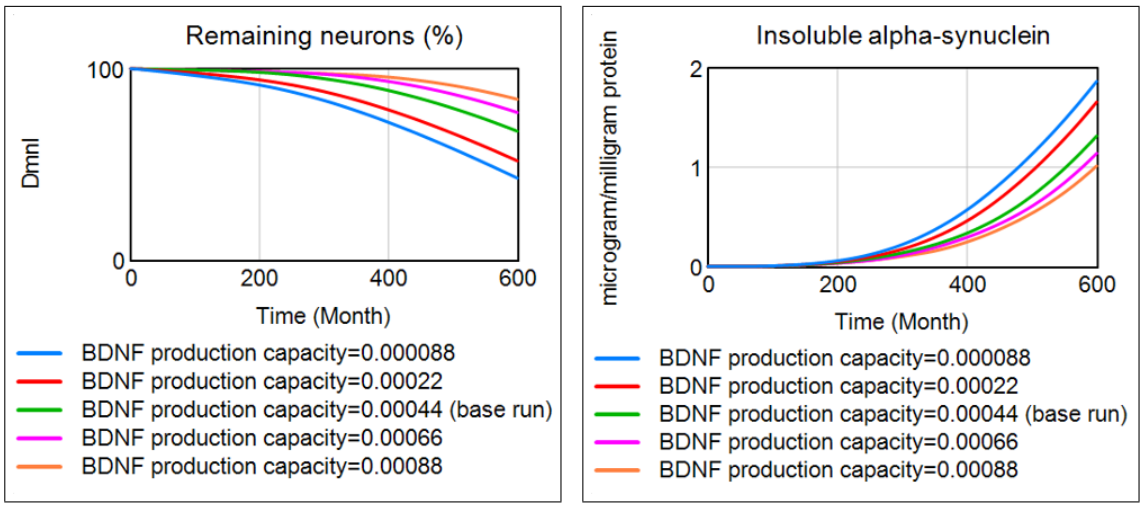


(a) Remaining neurons (%) (b) Insoluble alpha-synuclein

Figure 7.9. Model sensitivity to different BDNF production capacity values.

Brain-derived neurotrophic factor (BDNF) is a key molecule which is released by neurons in the brain for neuronal survival and protection. Thus, BDNF production of neurons directly affects the number of damaged neurons. In addition, sensitivity runs show that although this molecule has an indirect relationship with alpha-synuclein aggregation, the model is still sensitive to the neuroprotection level in terms of toxic protein aggregation (Figure 7.9).

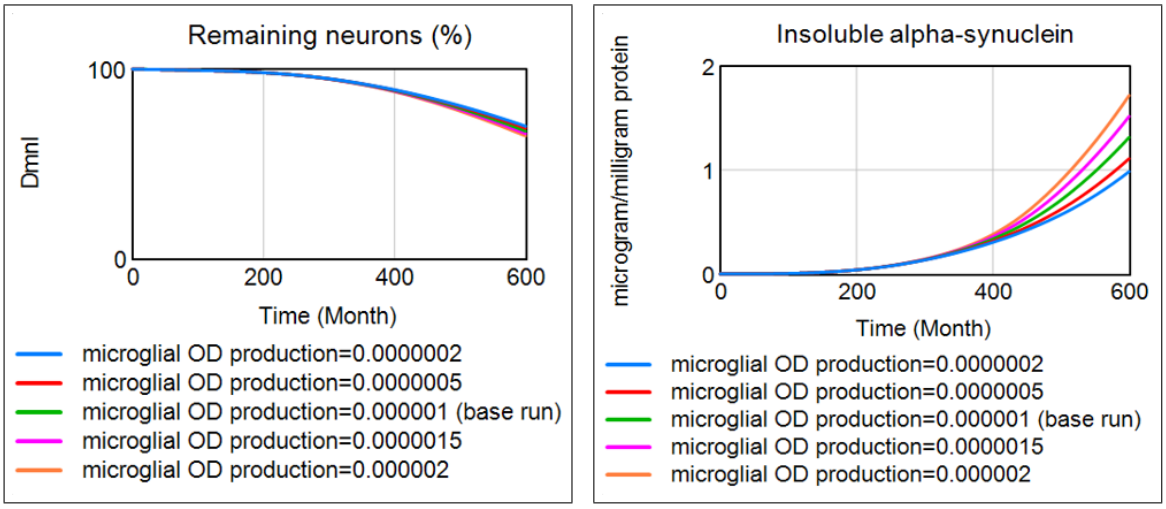


(a) Remaining neurons (%) (b) Insoluble alpha-synuclein

Figure 7.10. Model sensitivity to different microglial OD production values.

Activated microglia are one of the main sources generating oxidative damage in neurons. This oxidative damage further affects protein aggregation and neuronal damage. Sensitivity runs show that the microglial OD production impact on neuronal death is relatively smaller compared to protein aggregation (Figure 7.10).

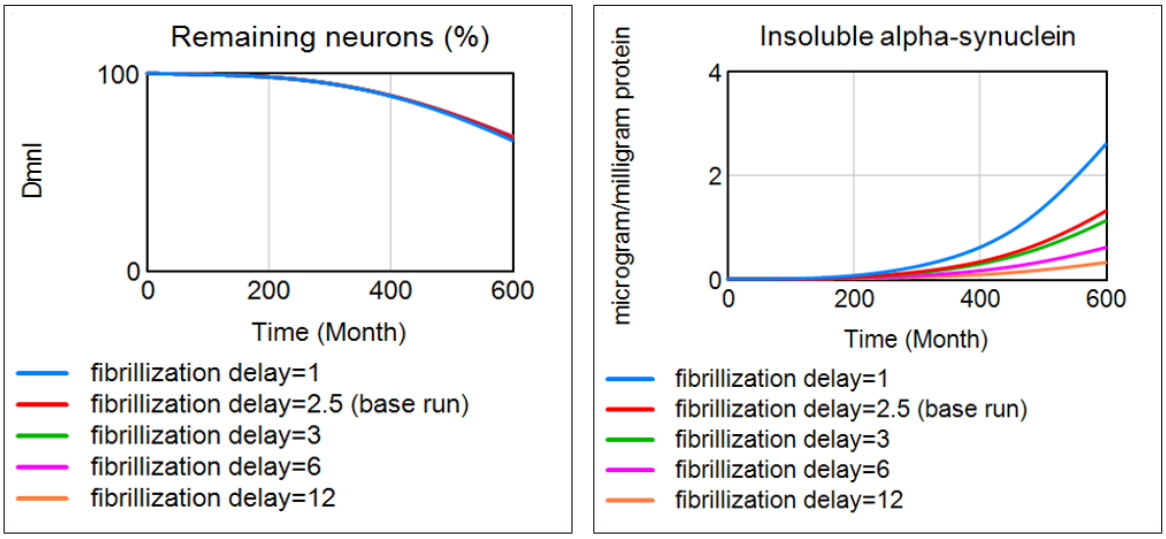


(a) Remaining neurons (%) (b) Insoluble alpha-synuclein

Figure 7.11. Model sensitivity to different fibrillization delay values.

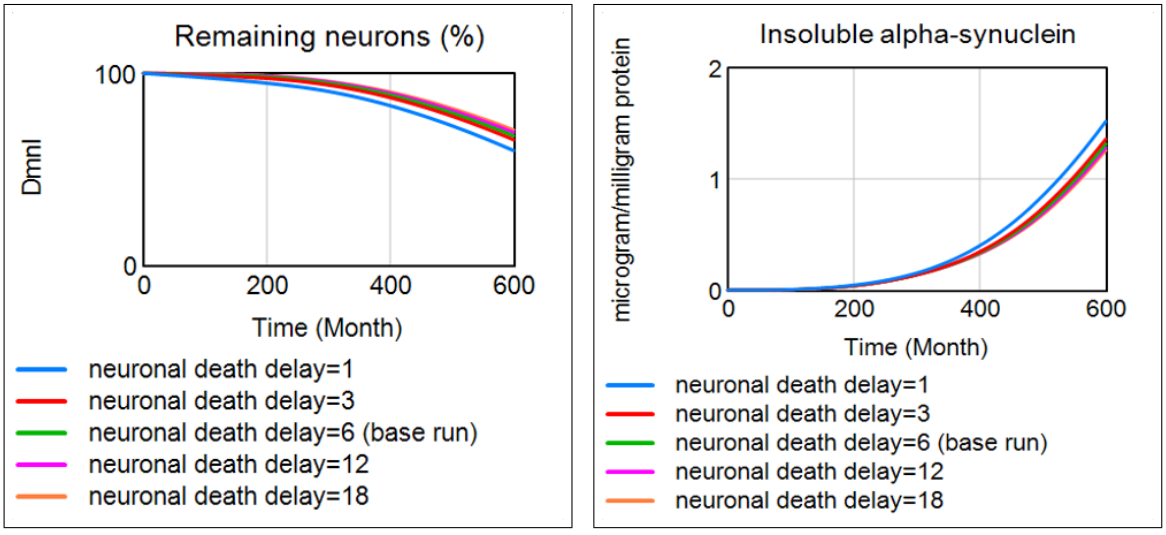


(a) Remaining neurons (%) (b) Insoluble alpha-synuclein

Figure 7.12. Model sensitivity to different neuronal death delay values.

Fibrillization flow between soluble and insoluble alpha-synuclein stocks is dependent on the fibrillization delay in our model. This delay significantly affects protein aggregation, whereas its impact on neuronal death is relatively small. The involvement of fibrillization delay in neuronal death is through indirect pathways (Figure 7.11).

In contrast to fibrillization delay, neuronal death delay does not have a significant impact on the outcomes of interest in our model. In case of insufficient neuroprotection and consistent neuronal damage, delaying neuronal death does not have an adequate impact to reduce protein degradation and neuronal death (Figure 7.12). The final values of key outputs at age 80 for all sensitivity runs are provided in Appendix B.

# 8. SCENARIO ANALYSIS

So far, the model structure and its validity are discussed and the base behavior of the model along with sensitivity analysis have been analyzed. In this section, we aim to expand our study by investigating what-if scenarios and analyzing changes in the outcomes of interests for those scenarios. In the first part, we aim to explore whether external administration of brain injuries would create PD-like outcomes in aging human brains with different injury characteristics. Later, we investigate the impacts of some daily activities and potential treatment strategies for both PD-prone and healthy individuals.

## 8.1. Traumatic Brain Injuries

Several neurodegenerative diseases have been related to brain injury as a risk factor, but the greatest evidence points to the progression of Parkinson's disease (PD) [30]. According to Brain Injury Association of America, there are several types of brain injuries. Congenital brain injury refers to an injury that is present from birth, whereas the term acquired brain injury stands for an injury that occurs after birth. Acquired brain injury can be further divided into two: (1) non-traumatic and (2) traumatic brain injuries. Traumatic brain injury (TBI) is a disturbance in brain function caused by an external force such as falls, accidents, or sports-related injuries. Concussions are the most prevalent kind of TBIs. On the other hand, non-traumatic brain injuries are those that occur as a result of internal conditions such as stroke, heart attack, or meningitis [152]. Figure 8.1 summarizes the forms of brain injuries. In our study, the focus is on repetitive TBIs affecting the substantia nigra (SN) of the human brain.

According to severity, TBIs are classified as mild, moderate, or severe. A scoring system based on an individual's state of consciousness after an injury is used to assess severity. The majority of brain injuries are repetitive and mild, thus, neuroimaging is incapable of detection [33]. A study revealed that the risk of having PD in later life is

56% greater for veterans with a history of mild TBI [30]. Men account for the majority of TBIs, and they are also twice as likely as women to be diagnosed with PD [34, 35]. It is generally recognized that athletes participating in contact sports are frequently at risk of brain injuries and suffering cognitive impairment [36].

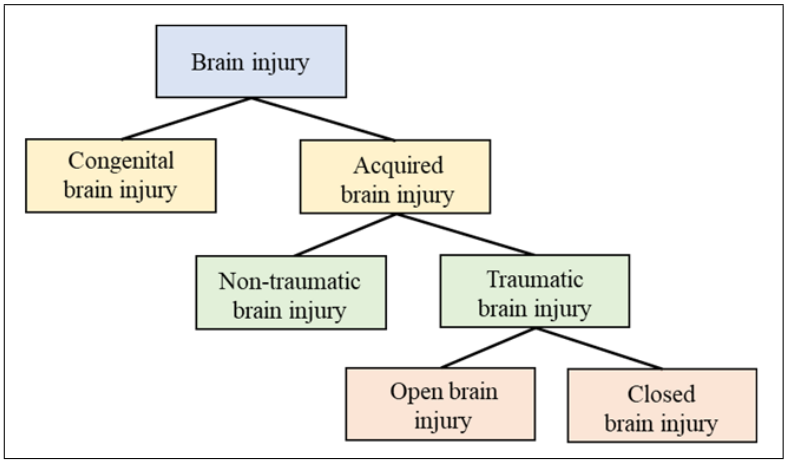


Figure 8.1. Types of brain injuries.

Trauma-induced neuroinflammation is the most reasonable explanation for the connection between brain injury and an increased risk of PD. Damage-associated molecular patterns (DAMPs), which are produced by injured neurons after brain injury, activate microglia and induce them to produce pro-inflammatory mediators [153]. Following the initial TBI, neuroinflammation might last for years in the damaged regions [32]. In a follow-up study, up to 17 years following a TBI event, an increase in activated microglia was observed in brains evaluated by positron emission tomography [154].

Future research on successful therapies and preventative measures will be influenced by an understanding of the potential link between PD and TBI. In addition to pre-existing medical conditions, heterogeneity of polytrauma and severity contribute to differences in the course and outcome of TBIs [155]. To develop new therapeutic approaches, animal models of TBI are used to investigate the biomechanical, cellular, molecular, and behavioral elements of human TBI.

The following research questions are intended to be addressed:

- Could repetitive TBIs result in PD progression in the long-term?
- Are there any links between various injury characteristics—including onset age, frequency, quantity, and severity—and PD vulnerability?
- Are there any age thresholds at which people begin to be more vulnerable to TBI-induced Parkinsonian behavior?

Four age groups are taken into consideration to examine the significance of the age at which the first brain trauma happened. Each age group is exposed to repetitive traumas varying between 1 and 70 times. In our study, the affected area by an injury is employed to express the severity of the trauma. In scenarios, the affected area ranges between 1% and 8%. Since the time elapsed between traumas is also a factor to be examined, intervals of 1 month, 3 months, 6 months, and 1 year are investigated. A total of 1152 simulation runs are observed.

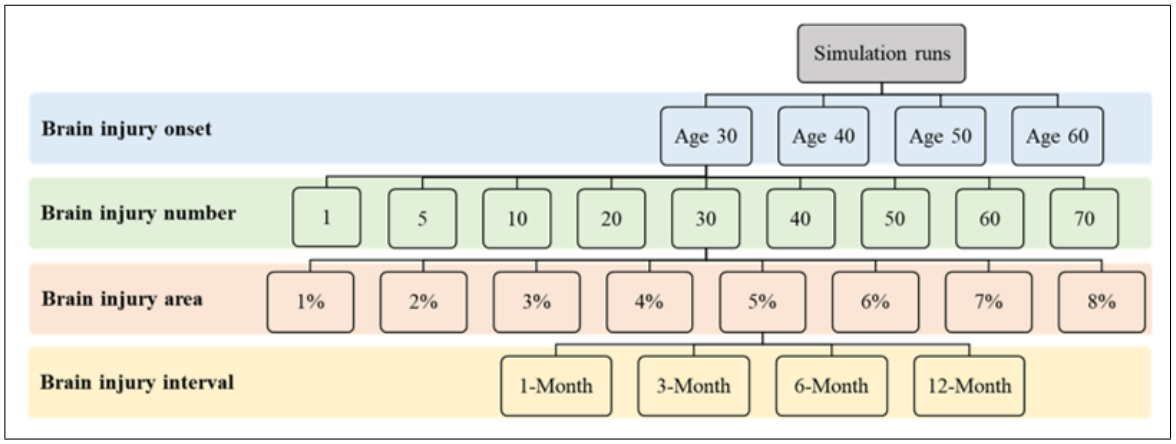


Figure 8.2. Scenario runs with varying injury properties.

PD is characterized by both alpha-synuclein accumulation and loss of dopaminergic neurons, therefore, we need to examine these two variables together. From the literature, the dopaminergic neuronal loss at motor symptom onset [22] and diagnosis [23] are determined as 30% and 50%, respectively. All individuals experience some

symptoms during aging due to neuronal loss, however, it is not appropriate to define all those normal aging abnormalities as PD. During aging, alpha-synuclein aggregation grows to about 1 $\mu$g/mg protein, but in PD patients, it rises to two to three times that amount. We assumed those with an alpha-synuclein accumulation level of more than 2 microgram/mg protein are in poor health. Individuals who have both protein and neuronal unhealthy conditions are believed to have PD.

The model is given pulses with a binary variable called brain injury pulse to indicate when there are injuries. Since these pulses are immediate, PULSE TRAIN() function's duration is set to 0. The formulation for brain injury pulse is

$$\begin{aligned} brain\ injury\ pulse =& PULSE\ TRAIN(brain\ injury\ onset, brain\ injury\ duration, \\ & brain\ injury\ interval, last\ brain\ injury). \end{aligned} \tag{8.1}$$

The last brain injury is calculated according to the total number of brain injuries as

$$\begin{aligned} last\ brain\ injury =& brain\ injury\ onset + \\ & (brain\ injury\ number - 1) \times \\ & brain\ injury\ interval. \end{aligned} \tag{8.2}$$

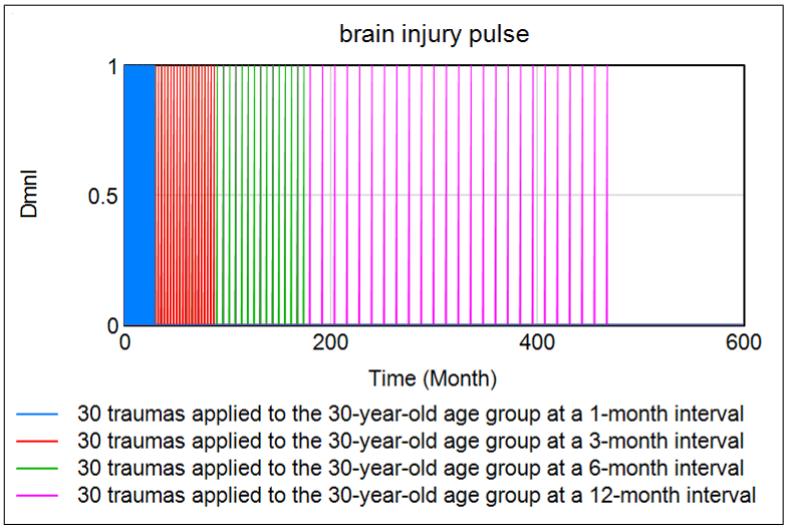


Figure 8.3. Brain injury pulses for different intervals.

The quantity of neurons that are damaged and/or died as a consequence of a TBI in the human brain has not been studied in the literature. Neuroimaging cannot detect many minor traumas. We integrate the severity of the traumas by including the damaged area proportion in SN. Neurons in the affected area flow into the damaged neurons stock after an injury. Thus, the equation for brain injury is

$$brain\ injury = brain\ injury\ pulse \times Healthy\ neurons \times affected\ area. \tag{8.3}$$

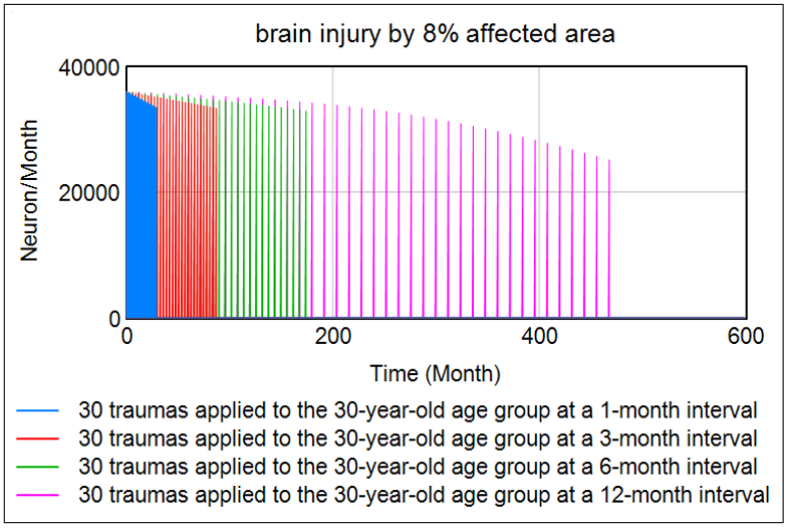


Figure 8.4. Brain injuries for different intervals.

TBI pulses and TBI-induced brain injury flows are illustrated in Figure 8.3, and Figure 8.4, respectively. Younger people have more neurons damaged as a consequence of trauma to the same affected area than elderly people. Because they have higher neuronal density. They also have higher neuroprotection capacity since protective materials are mainly produced by healthy neurons. Trauma-induced neuronal death, as expected, increases microglial activation. This further affects the oxidative damage and mitochondria sectors which in turn limit the protective mechanisms and exacerbate the neuronal damage and protein aggregation.

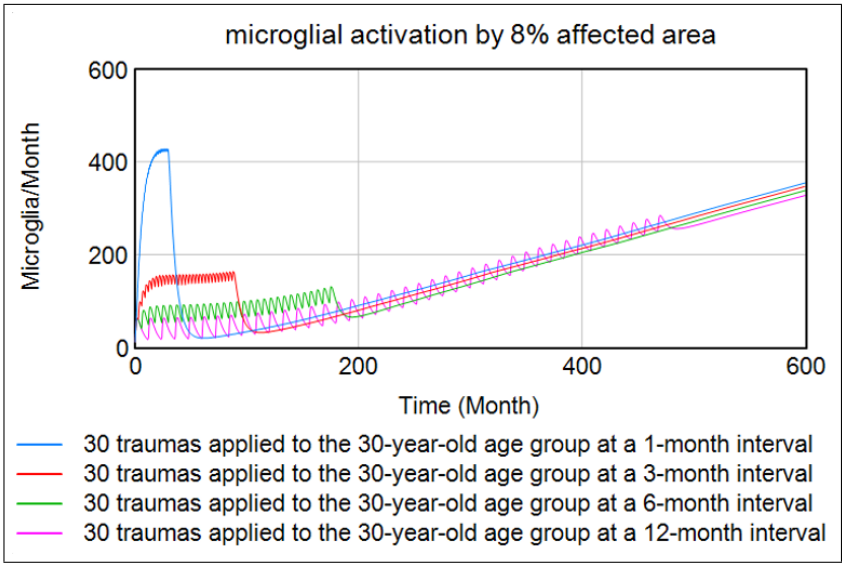


Figure 8.5. Microglial activation by brain injuries for different intervals.

TBI impact on microglial activation from the simulation model is shown in Figure 8.5. The final values of key outputs at age 80 for brain injury scenarios of the 30-year-old onset group are provided in Appendix C.

### 8.1.1. Severity of Repetitive Traumatic Brain Injuries

This scenario aims to examine whether repetitive TBIs can impact PD-like behavior in the long-term. A total amount of 30 brain traumas with different severities are applied monthly to a healthy 30-year-old individual. In model output graphs, We also include the diagnostic threshold values explained previously as 50% and 2 $\mu$g/mg protein for remaining neurons (%) and insoluble alpha-synuclein, respectively.

Trauma-induced dopaminergic neuronal loss at all levels is examined compared to normal aging. However, the results indicate that the loss of neurons does not fall below the diagnostic threshold for areas affected by 1%, 2%, and 3%. For those runs, the remaining dopaminergic neurons are above the diagnostic threshold and insoluble alpha-synuclein protein accumulations are not at an unsafe level. Although lower-than-normal neuronal density can result in cognitive issues, these cognitive impairments

alone are not sufficient for the diagnosis of PD. Therefore, in cases where the affected areas constitute 1%, 2%, or 3% of the total substantia nigra (SN), the observed results do not meet the criteria for a PD diagnosis. On the other hand, when the affected areas reach 4% or more, PD characteristics become more prominent. This suggests that a significant loss of dopaminergic neurons combined with the accumulation of insoluble alpha-synuclein protein may lead to the manifestation of PD symptoms.

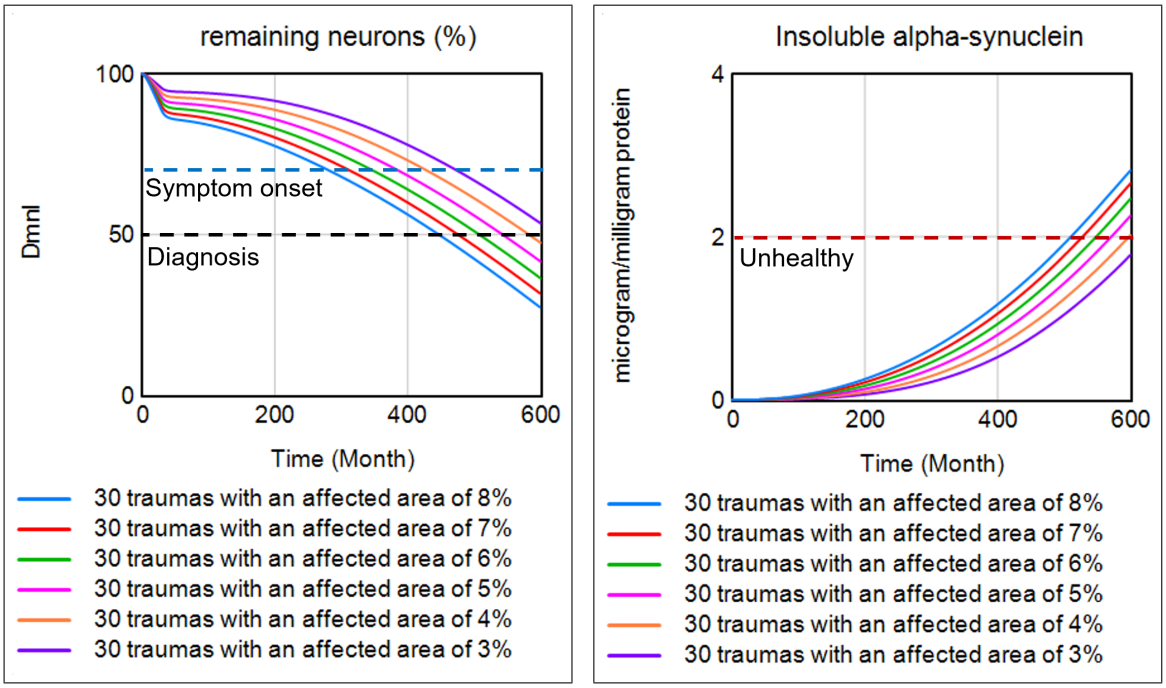


(a) Remaining neurons (%)

(b) Insoluble alpha-synuclein

Figure 8.6. Comparative plots of Scenario 1.

Table 8.1 displays the detailed results of the first scenario runs. Bold outputs indicate the values below the diagnostic threshold (for neurons) and above the unhealthy accumulation level (for insoluble alpha-synuclein). Depending on the impact area of the trauma, a healthy 30-year-old individual may show PD-like behavior in long-term as a result of repetitive TBIs. In other words, if the impact area of the trauma reaches a certain threshold, it can lead to neuronal damage that falls below the diagnostic threshold for PD and trigger an accumulation of insoluble alpha-synuclein protein above unhealthy levels.

Table 8.1. Model outputs of Scenario 1.

| **Brain injury Characteristics** | | | | **Final value** | |
|---|---|---|---|---|---|
| **Onset (age)** | **Total number** | **Interval (month)** | **Affected area (%)** | **Protein aggregation** | **Remaining neuron (%)** |
| 30 | 30 | 1 | 8% | **2.81** | **27.24** |
| | | | 7% | **2.65** | **31.57** |
| | | | 6% | **2.47** | **36.38** |
| | | | 5% | **2.26** | **41.60** |
| | | | 4% | **2.02** | **47.43** |
| | | | 3% | 1.78 | 53.50 |
| | | | 2% | 1.56 | 59.30 |
| | | | 1% | 1.40 | 64.07 |

We also monitor the effect of trauma-induced neuroinflammation on other sectors for runs generating PD-like output in terms of neuronal loss and protein aggregation before proceeding to other scenarios. As seen in Figure 8.7, dynamic interactions between subsystems affect the model behavior. Different colors: blue, red, and green correspond to affected areas of 8%, 7%, and 6%, respectively. We also include the base run (normal aging) with a pink line. While the direct impact of neuroinflammation on oxidative damage sector can be observed easily, the indirect effect on mitochondria sector occurs after some time.

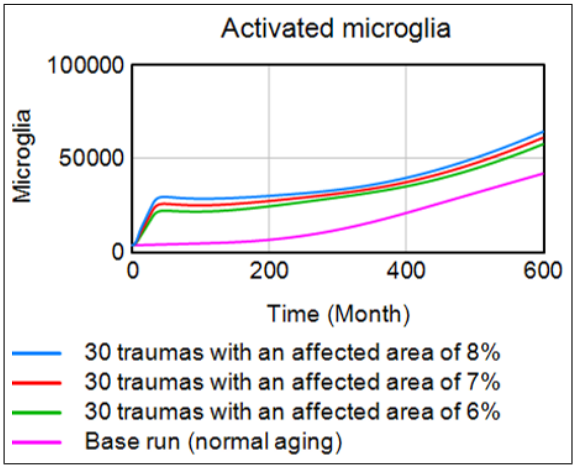


(a) Activated microglia

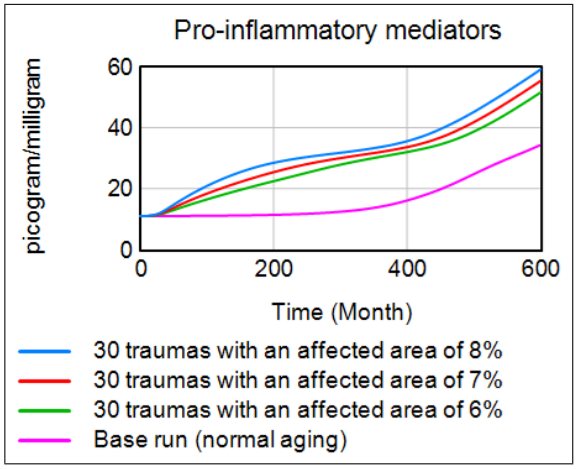


(b) Pro-inflammatory mediators

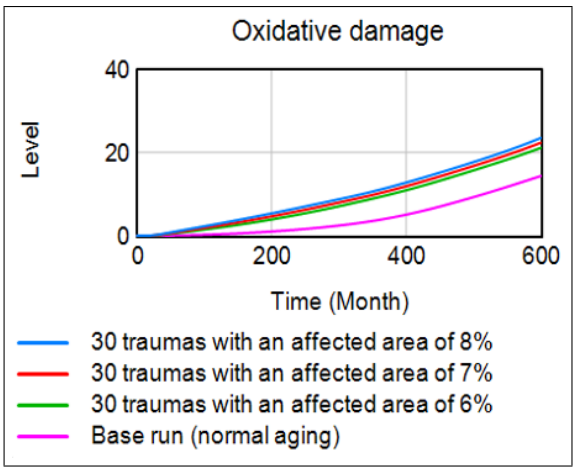


(c) Oxidative damage

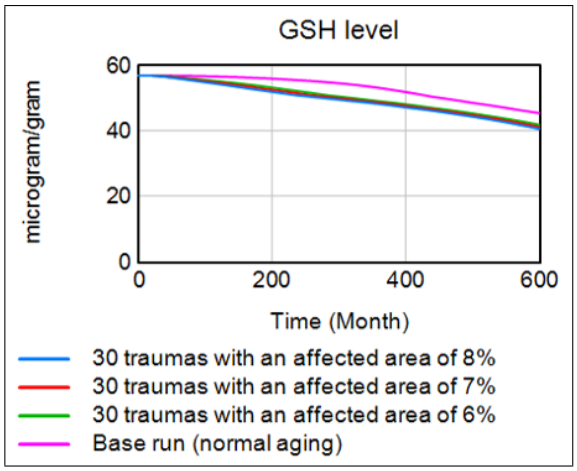


(d) GSH level

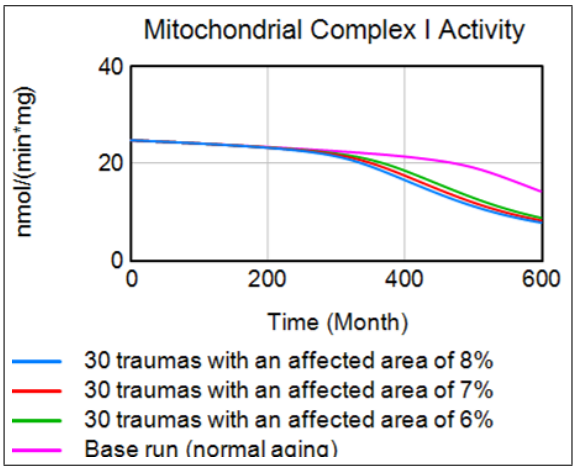


(e) OMitochondrial complex I activity

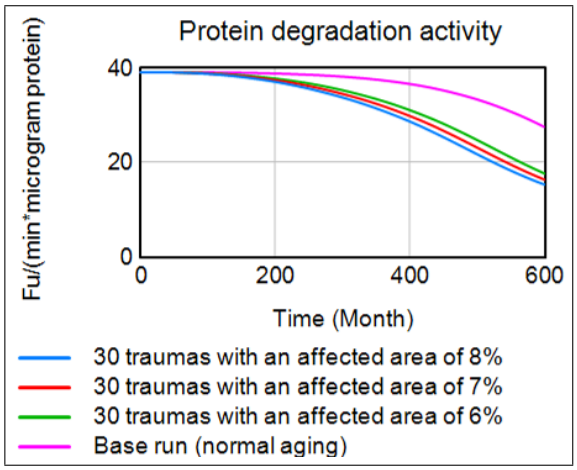


(f) Protein degradation activity

Figure 8.7. Final values of other stocks for Scenario 1.

### 8.1.2. Number of Repetitive Traumatic Brain Injuries

This scenario is aimed to investigate the impact of the number of repetitive TBIs. First, we reduce the number of monthly injuries for 8% affected area which resulted in PD-like behavior in the previous scenario for a 30-year-old age group. Later, we increase the number of injuries for 3% injury area.

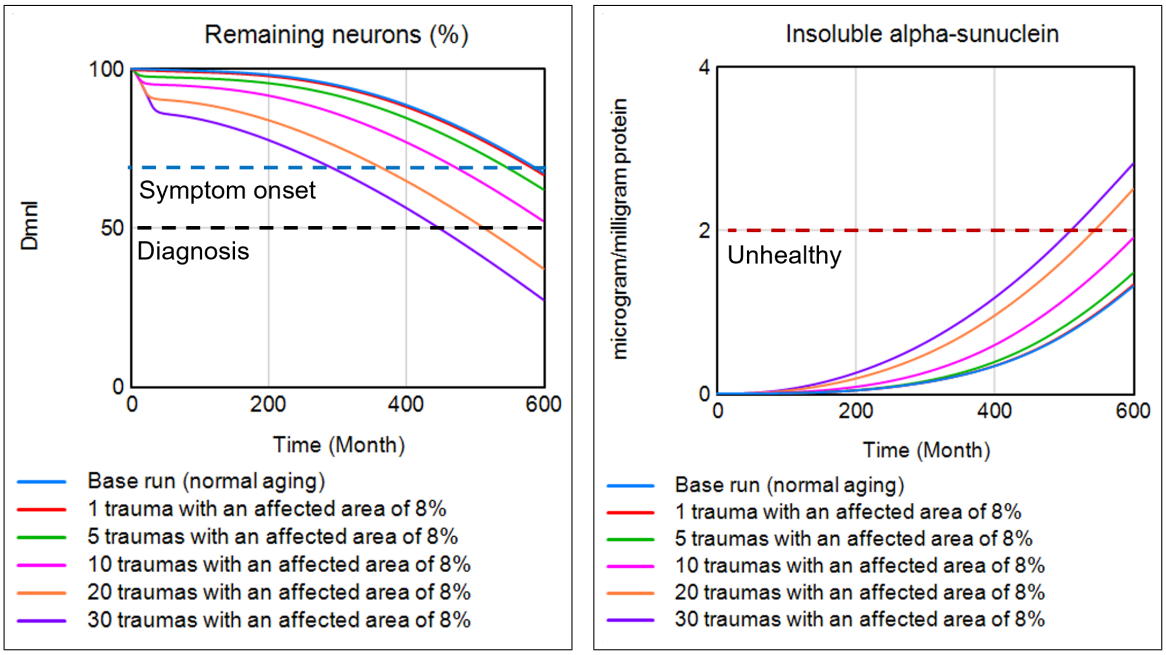


(a) Remaining neurons (%) (b) Insoluble alpha-synuclein

Figure 8.8. Comparative plots of Scenario 2-1.

The quantity of head traumas is significant for both higher and lower severities. While we observe 20 TBIs at 8% severity (affected area) produce PD-like output, similar results could not be obtained for 10 or fewer traumas. On the other hand, while we could not observe PD-like output for 30 traumas at 3% severity, for greater sets of traumas PD-like outputs are possible. Less severe injuries can produce PD when more repetitions occur. Similarly, more severe injuries may not produce PD with fewer repetitions. It should be noted that in these theoretical scenarios, it is assumed that all traumas are affecting a proportional area in the substantia nigra (SN) of the brain.

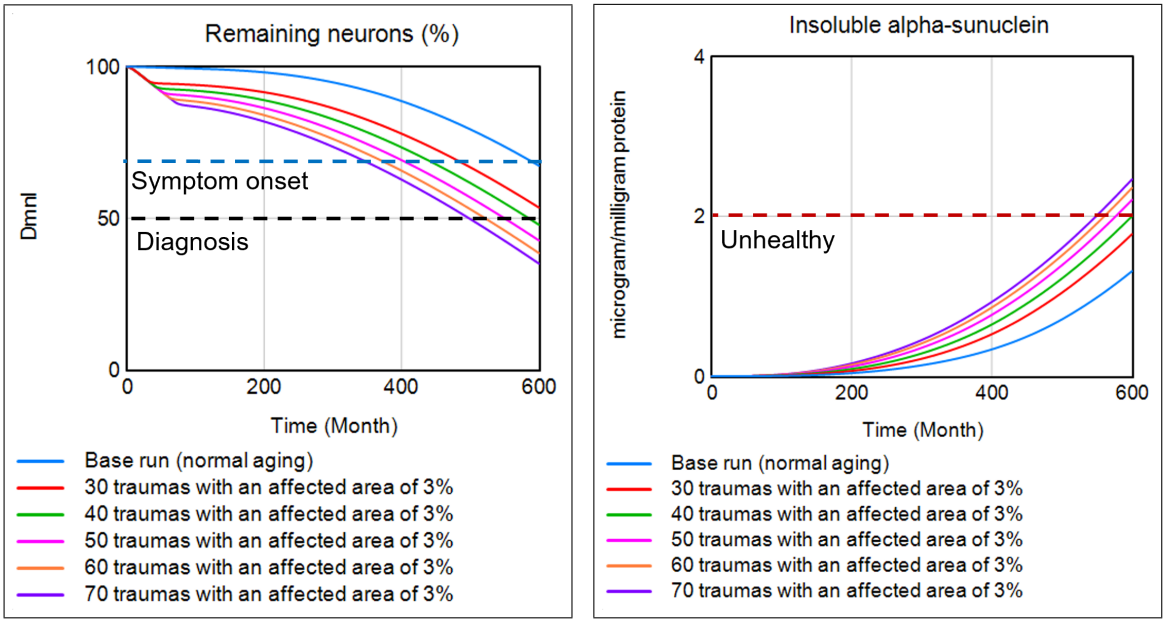


(a) Remaining neurons (%) (b) Insoluble alpha-synuclein

Figure 8.9. Comparative plots of Scenario 2-2.

Table 8.2. Model outputs of Scenario 2.

| **Brain injury characteristics** | | | | **Final value** | |
|---|---|---|---|---|---|
| **Onset (age)** | **Affected area (%)** | **Interval (month)** | **Total number** | **Protein aggregation** | **Remaining neuron (%)** |
| 30 | 8% | 1 | 1 | 1.33 | 66.58 |
| | | | 5 | 1.48 | 61.97 |
| | | | 10 | 1.90 | 51.98 |
| | | | 20 | **2.50** | **37.04** |
| | | | 30 | **2.81** | **27.24** |
| | 3% | | 30 | 1.78 | 53.50 |
| | | | 40 | 2.00 | **47.82** |
| | | | 50 | **2.21** | **42.64** |
| | | | 60 | **2.36** | **38.47** |
| | | | 70 | **2.46** | **35.01** |

Table 8.2 provides detailed results of simulation runs, focusing on neuronal death and protein aggregation. By considering both neuronal death and protein aggregation, the table highlights the importance of both the quantity and severity of injuries in influencing the progression and severity of neurodegenerative conditions.

### 8.1.3. Interval of Repetitive Traumatic Brain Injuries

The purpose of this scenario is to examine how the frequency of repetitive TBIs affects Parkinsonian-like behavior. We change the interval of a total amount of 30 traumas with an affected area of 4% for the 30-year-old onset group. As shown in Table 8.3, there is reduced alpha-synuclein accumulation in response to larger time intervals between injuries. More protein accumulation as a result of frequent injuries can be explained by the fact that the mechanisms of the neurons trying to control toxic accumulations are overwhelmed. Similarly, the remaining dopaminergic neuron percentage is higher when we apply traumas with extended intervals.

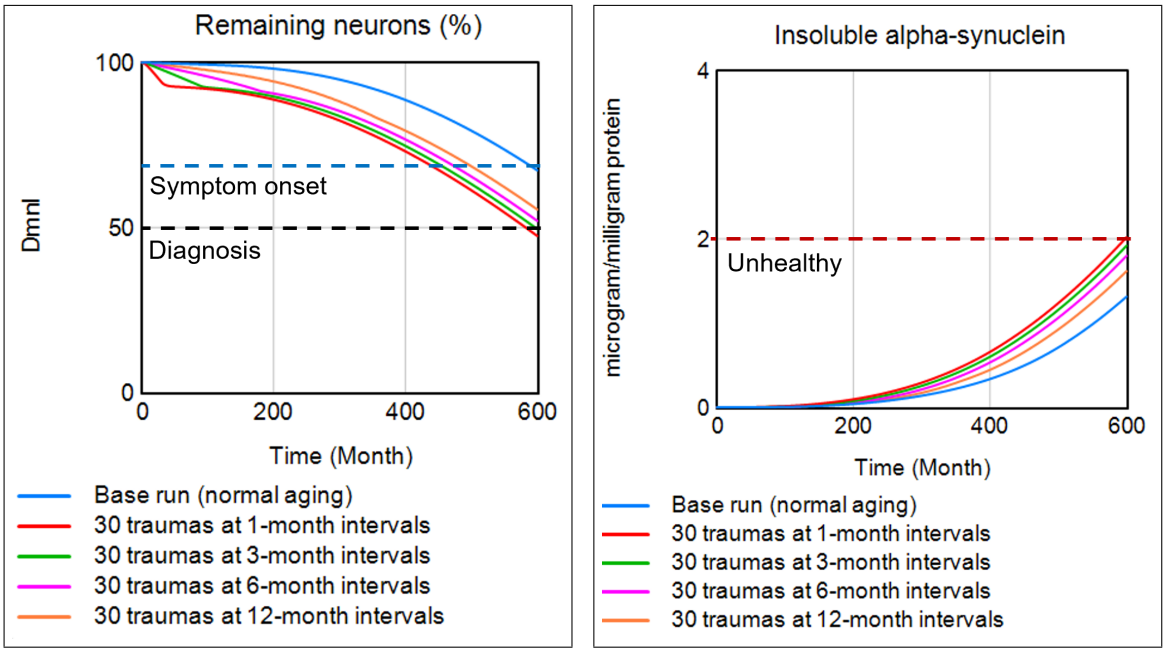


(a) Remaining neurons (%)

(b) Insoluble alpha-synuclein

Figure 8.10. Comparative plots of Scenario 3.

If the time interval between traumas is extended, people become older. Although the abilities of protective mechanisms become lower during aging, still earlier and more frequent traumas have a longer-term impact on PD vulnerability.

Table 8.3. Model outputs of Scenario 3.

| **Brain injury characteristics** | | | | **Final value** | |
|---|---|---|---|---|---|
| **Onset (age)** | **Affected area (%)** | **Total number** | **Interval (month)** | **Protein aggregation** | **Remaining neuron (%)** |
| 30 | 4% | 30 | 1 | **2.02** | **47.43** |
| | | | 3 | 1.92 | **49.52** |
| | | | 6 | 1.80 | 52.01 |
| | | | 12 | 1.62 | 55.46 |

### 8.1.4. Onset of Repetitive Traumatic Brain Injuries

The aim of this scenario is to investigate whether an age group is more vulnerable in terms of trauma-induced potential PD progression. Thus, a total of 30 repetitive traumas with an affected area of 5% are administered monthly to 30, 40, 50, and 60-year-old individuals. Elderly people who experience neuronal loss following brain injuries may develop neurological problems, however, alpha-synuclein accumulation is not seen in those individuals.

Table 8.4. Model outputs of Scenario 4.

| **Brain injury characteristics** | | | | **Final value** | |
|---|---|---|---|---|---|
| **Interval (month)** | **Affected area (%)** | **Total number** | **Onset (age)** | **Protein aggregation** | **Remaining neuron (%)** |
| 1 | 5% | 30 | 30 | **2.26** | **41.60** |
| | | | 40 | 1.90 | **48.47** |
| | | | 50 | 1.59 | 54.03 |
| | | | 60 | 1.35 | 57.70 |

The earlier the trauma begins, the greater the impact in terms of PD vulnerability. A certain period of time is required for PD to develop. According to simulation runs, it is not possible to observe immediate vulnerability after TBIs.

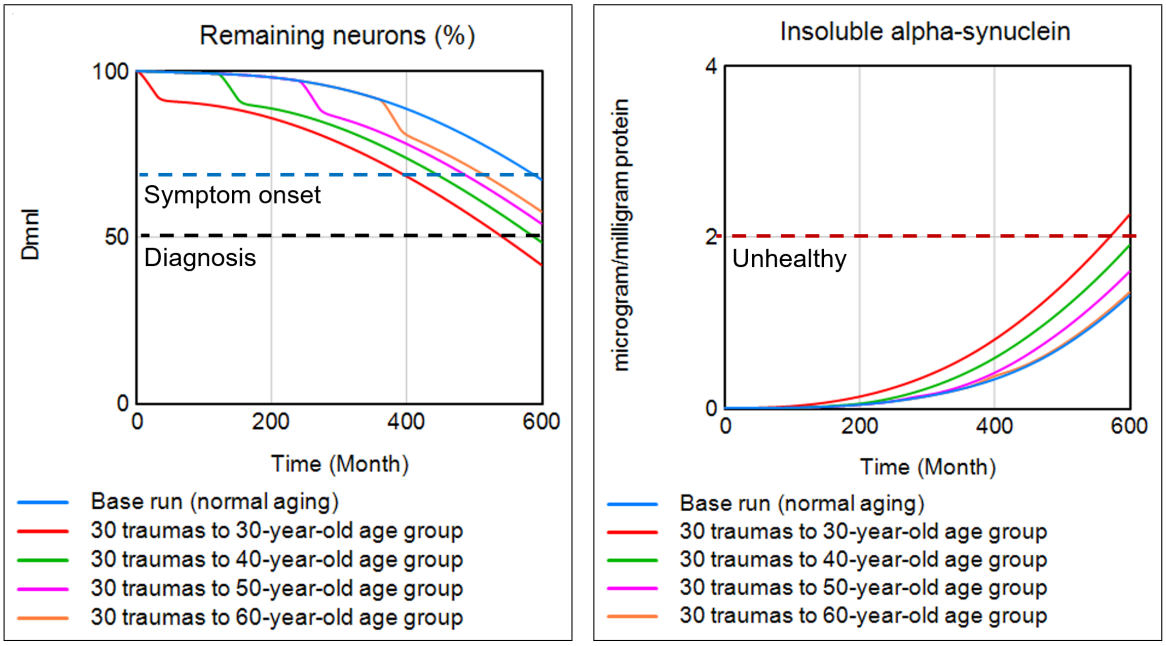


(a) Remaining neurons (%) (b) Insoluble alpha-synuclein

Figure 8.11. Comparative plots of Scenario 4.

### 8.1.5. Late Onset of Repetitive Traumatic Brain Injuries

The previous scenario demonstrates a higher PD vulnerability for the early onset of repetitive TBIs. In this scenario, we focus on the administration of traumas to elderly people to further investigate the underlying reasons. Thus, 50, 60, and 70 repetitive traumas with affected areas of 6%, 7%, and 8% are applied monthly to 60-year-old individuals. Table 8.5 shows the detailed results of simulation runs. We observed, interestingly, reduced amounts of insoluble alpha-synuclein aggregates for the affected areas of 7% and 8% compared to the base run (normal aging). Bold values for protein aggregation indicate those model outputs. The reason for this may be that a part of the activated microglia also degrades the toxic alpha-synuclein aggregates. This result also supports the outputs of the previous scenario. Repeated TBIs must start early in

life, be more severe than a certain threshold, and occur with a specific consistency to generate PD-like behaviors. Figure 8.12 compares normal aging and late-onset repetitive brain injuries with different severities and numbers.

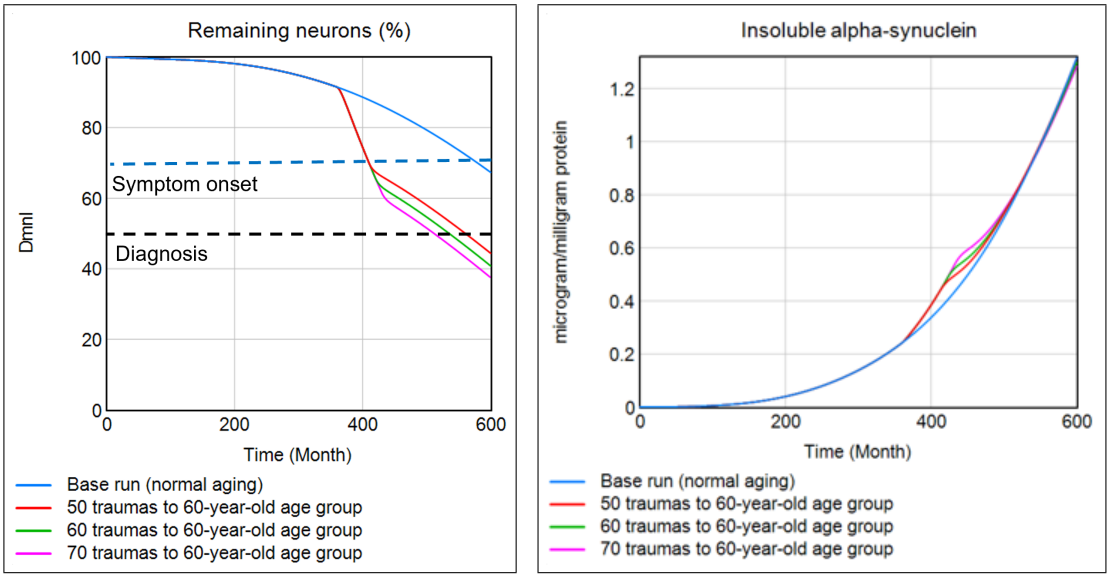


(a) Remaining neurons (%) (b) Insoluble alpha-synuclein

Figure 8.12. Comparative plots of Scenario 5.

Table 8.5. Model outputs of Scenario 5.

| **Brain injury characteristics** | | | | **Final value** | |
|---|---|---|---|---|---|
| **Interval (month)** | **Total number** | **Onset (age)** | **Affected area (%)** | **Protein aggregation** | **Remaining neuron (%)** |
| 1 | 50 | 60 | 6% | 1.33 | **49.51** |
| | | | 7% | 1.32 | **46.91** |
| | | | 8% | **1.31** | **44.39** |
| | 60 | | 6% | 1.32 | **46.60** |
| | | | 7% | **1.31** | **43.64** |
| | | | 8% | **1.30** | **40.80** |
| | 70 | | 6% | **1.31** | **43.87** |
| | | | 7% | **1.30** | **40.60** |
| | | | 8% | **1.28** | **37.48** |

The findings of this section are summarised below:

- Healthy individuals exposed to repetitive TBIs at younger ages (30 and 40) may produce PD-like outcomes in long-term. However, for those older than 40, there is a neuronal loss but no significant alpha-synuclein accumulation. Although they may have neurological problems more than their age counterparts, it cannot be concluded that they have PD.
- When elderly individuals experience repetitive TBIs, toxic protein accumulation is less than their healthy peers.
- The earlier the trauma begins, the greater the impact in terms of PD vulnerability. A certain period of time is required for the disease to develop. According to simulation runs, it is not realistic to expect immediate vulnerability after TBIs.
- The number and severity of trauma simultaneously affect the impact of injury both on alpha-synuclein aggregation and neuronal loss. Less severe injuries can produce PD when more repetitions occur. Similarly, more severe injuries may not produce PD with fewer repetitions.
- If the time interval between traumas is extended, people become older. Although the abilities of protective mechanisms become lower during aging, still earlier and more frequent traumas have a longer-term impact on PD vulnerability.
- To conclude, repeated TBIs must start early in life, be more severe than a certain threshold, and occur with a specific consistency to generate PD-like behaviors.

## 8.2. Protective Strategies

People's susceptibility to certain diseases may be determined by genetic factors. Varying degrees of interplay between genetic predisposition and environmental factors impose a risk for PD [156]. A better comprehension of the underlying causal links is necessary for the classification of patients and the development of advanced clinical trials, including causative therapies. We try to explore the protective impacts of genetic variance/treatment potentials and daily activities on TBI-induced PD-like outputs by implementing some improvements to the most essential variables from each sector.

Clinical studies indicate that dietary intake of natural antioxidants mitigates neurodegeneration by destroying oxidative compounds. Supplementation of foods with evidence of improving GSH levels is highly recommended for adults, such as lean protein sources, brassica vegetables, polyphenol-rich fruits and vegetables, herbs and spices, green tea, and omega-3 fatty acid rich foods [157].

Physical activity positively affects the expression of BDNF, because BDNF levels are activity-dependent [158]. Although the acute effect of exercise induces oxidative stress, regular exercise rises neuroprotection through increased BDNF levels, thus, preventing neurons from neurodegeneration [159]. Physical exercise is also vital for persons who already have PD, because, in comparison to their healthy counterparts, those individuals are more prone to become physically inactive which worsens the existing problems [160].

A healthy diet and regular exercise are effective strategies that target improved anti-oxidant capacity and neuroprotection mechanism by improving the levels of GSH and BDNF production. In addition, we aim to include the genetic variance and/or potential treatments promoting improved capabilities of mitochondria and protein degradation activity. Treatment strategies targeting those mechanisms are believed to be promising. Because the genes and mutations that contribute to hereditary PD vulnerability are particularly linked to protein aggregation and mitochondrial function [161].

### 8.2.1. Healthy Diet and Regular Exercise

For protective strategy 1, we hypothetically increase the initial value of GSH level and parameter value of BDNF production capacity by 15% to monitor the potential protective impact of a healthy diet and regular exercise. In the previous section, we observed that young individuals (30-year-old onset group) who experienced a total of 30 brain injuries at 1-month intervals with an affected area of 8% in the substantia nigra (SN) showed PD-like behavior. Thus, throughout this section, we refer to these individuals as PD-prone.

Protective strategy 1 reduces the insoluble alpha-synuclein levels by 8.6% while increasing the remaining neurons by 15.5%. A healthy diet and regular exercise alleviate the symptoms of individuals who are prone to Parkinson's disease by directly affecting the oxidative damage and dopaminergic neuron sectors, as well as indirectly benefiting the protein aggregation sector. Figure 8.13 illustrates the model behavior in response to protective strategy 1.

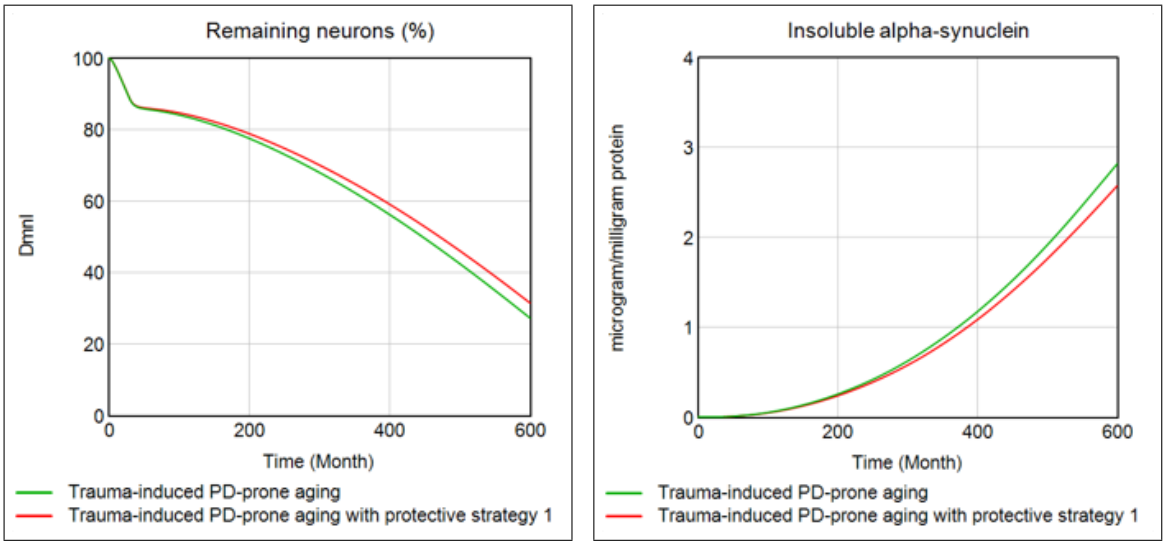


(a) Remaining neurons (%) (b) Insoluble alpha-synuclein

Figure 8.13. Comparative plots of Protective Strategy 1.

### 8.2.2. Genetic Variance

We increase the initial values of mitochondrial complex 1 activity and protein degradation by 15% to investigate the impact of possible genetic variance for potential treatment opportunities. Since healthy nutrition and exercise may be insufficient in terms of protein accumulation, such a complementary strategy is expected to offer longer-term benefits.

Protective strategy 2 exhibits a reduction in insoluble alpha-synuclein levels by 9.6% while simultaneously increasing the remaining dopaminergic neurons by 6.1%. This strategy directly influences the protein aggregation sector and is expected to have

a more pronounced impact on insoluble alpha-synuclein accumulation compared to other protective strategies. By targeting the mechanisms involved in protein aggregation, this strategy demonstrates its potential effectiveness in mitigating the pathological accumulation of insoluble alpha-synuclein. Additionally, the increase in the number of remaining neurons by 6.1% suggests a neuroprotective effect of this strategy. Preserving a higher percentage of neurons can contribute to maintaining neuronal function and integrity, which is crucial for overall brain health.

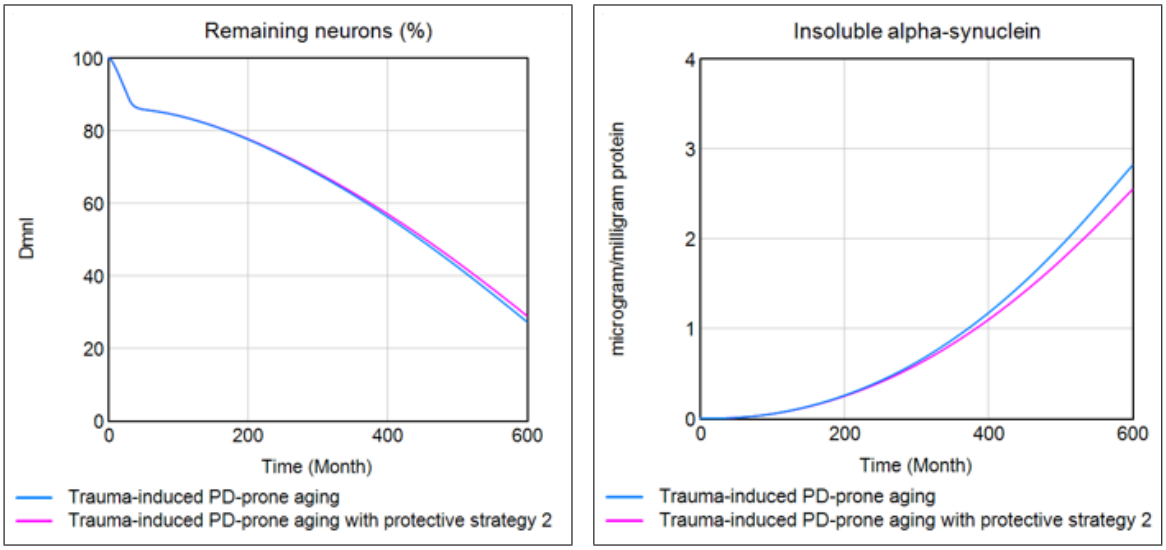


(a) Remaining neurons (%)

(b) Insoluble alpha-synuclein

Figure 8.14. Comparative plots of Protective Strategy 2.

### 8.2.3. Combined Protective Strategy

This strategy aims to combine the benefits of two previous approaches by integrating a diet rich in antioxidant nutrients and regular exercise with possible treatments and/or genetic variance that enhance protein degradation and mitochondrial activity to create a synergistic effect. This combined strategy seeks to leverage multiple factors to improve the dynamics of neuroprotection and overall brain health. By incorporating antioxidant-rich foods into the diet, this strategy aims to enhance the body's natural defense mechanisms against oxidative damage, potentially reducing the risk of protein

aggregation and neuronal loss. By engaging in regular physical activity, individuals can potentially enhance their neuronal resilience and support the maintenance of healthy brain function. Furthermore, the strategy suggests the integration of possible treatments and/or genetic variance that promote enhanced protein degradation and mitochondrial activity.

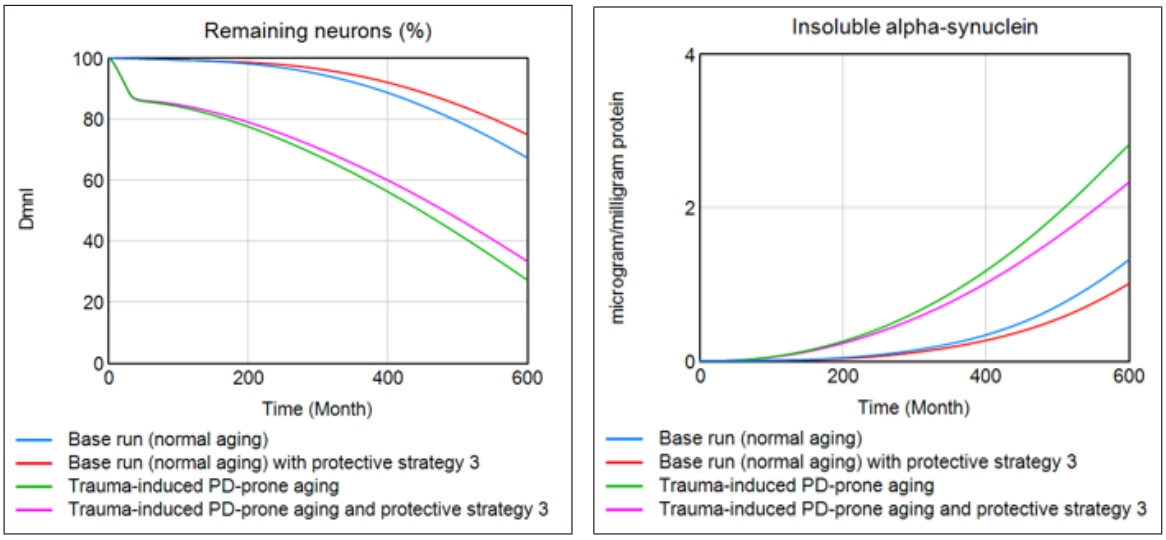


(a) Remaining neurons (%) (b) Insoluble alpha-synuclein

Figure 8.15. Comparative plots of protective strategy 3.

In addition to examining the impact of the combined protective strategy on trauma-induced PD-prone individuals, the investigation also extends to normal aging. The combined protective strategy demonstrates a restorative effect on both trauma-induced PD-prone individuals and individuals experiencing the natural aging process. Normal aging is associated with various non-motor and motor problems that arise due to natural changes in the brain. It is also important to identify potential therapeutic strategies that can alleviate or mitigate age-related non-motor and/or motor issues.

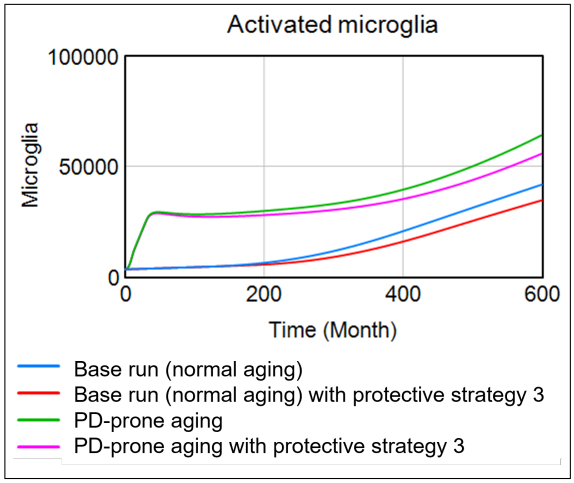


(a) Activated microglia

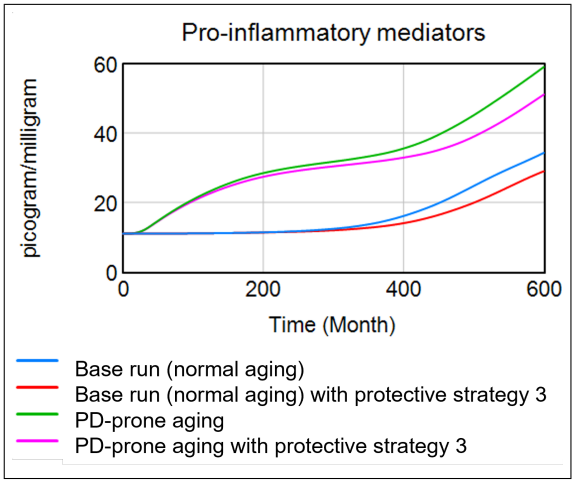


(b) Pro-inflammatory mediators

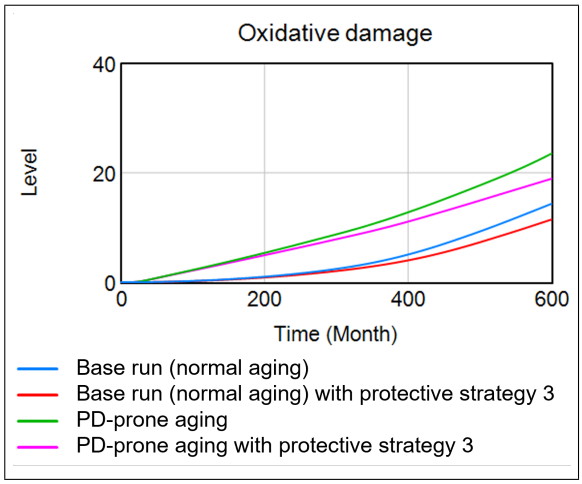


(c) Oxidative damage

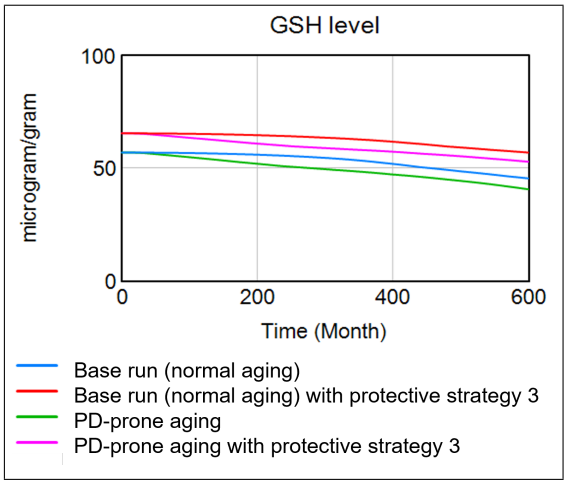


(d) GSH level

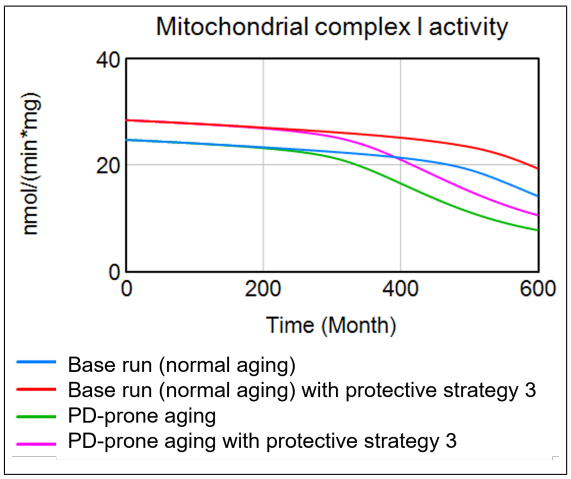


(e) Mitochondrial complex I activity

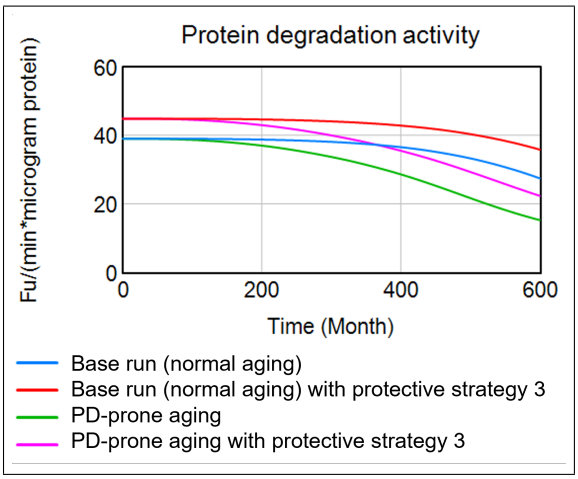


(f) Protein degradation activity

Figure 8.16. Final values of other stocks for protective strategy 3.

We further monitor the effect of protective strategy 3 on other important variables in the system. Individuals who have higher levels of protein degradation capacity genetically or due to possible treatments are less likely to have high levels of protein aggregation. GSH enhancement is a promising strategy for lowering oxidative damage. Better mitochondrial activity reduces oxidative damage, and, has an impact on both antioxidant function and neuroprotection by ATP-related pathways. BDNF is critical for neuronal survival but its impact on protein removal is not straightforward.

In Table 8.6 and Table 8.7, the percentage changes in remaining neurons and insoluble alpha-synuclein aggregates are summarized for the different protective strategies. The desired outcome is to reduce the levels of insoluble alpha-synuclein while simultaneously increasing the number of remaining dopaminergic neurons. The goal of these protective strategies is to achieve a dual effect: reducing insoluble alpha-synuclein levels, which are associated with neurodegenerative processes, while increasing the number of remaining dopaminergic neurons, which are essential for proper brain function. By examining the percentage changes in both parameters, researchers can assess the effectiveness of each protective strategy in achieving this desired outcome.

Table 8.6. Protective strategy comparisons for PD-prone aging.

| | **PD-prone aging** | |
|---|---|---|
| | **Insoluble alpha-synuclein** | **Remaining neurons (%)** |
| **Protective strategy 1** | -8.6% | 15.5% |
| **Protective strategy 2** | -9.6% | 6.1% |
| **Protective strategy 3** | -17.4% | 22.5% |

The protective strategy 3 demonstrates significant improvements in both PD-prone individuals and healthy aging individuals in terms of neuronal density and protein aggregation, ultimately leading to potential extensions in quality-adjusted life years (QALYs). For PD-prone individuals, protective strategy 3 shows a notable 22.5% improvement in neuronal density. This suggests that the strategy is effective in preserving

a higher number of neurons, which is crucial for maintaining proper brain function and delaying the onset of PD symptoms. Additionally, there is a 17.4% improvement in reducing insoluble alpha-synuclein protein aggregation. By targeting the underlying pathology of PD, the strategy aims to slow down disease progression and delay the manifestation of symptoms. Furthermore, protective strategy 3 demonstrates preventive effects for healthy aging individuals. It offers an 11.3% increase in neuronal density, indicating preservation of neurons and potentially mitigating age-related cognitive decline and motor impairments. Additionally, there is a significant 23.6% decrease in protein aggregation, suggesting a reduction in the accumulation of insoluble alpha-synuclein, which is associated with neurodegenerative processes.

Table 8.7. Protective strategy comparisons for normal aging.

| | **Normal aging** | |
|---|---|---|
| | **Insoluble alpha-synuclein** | **Remaining neurons (%)** |
| **Protective strategy 1** | -8.1% | 5.5% |
| **Protective strategy 2** | -16.1% | 5.6% |
| **Protective strategy 3** | -23.6% | 11.3% |

The time course of PD is postponed by roughly 4 years with this strategy. The median time taken between the stages of Hoehn and Yahr (H&Y), the most common and widely used scale to estimate disease severity [162], is approximately 2 years [163]. Thus, a 4-year interval is particularly significant for improving the quality of life for patients by reducing the disease symptoms and slowing down the transition between disease stages. Since people who are not exposed to TBIs also experience non-motor and motor problems during aging, it is also important to identify the effective possible therapeutic approaches for a healthier aging process.

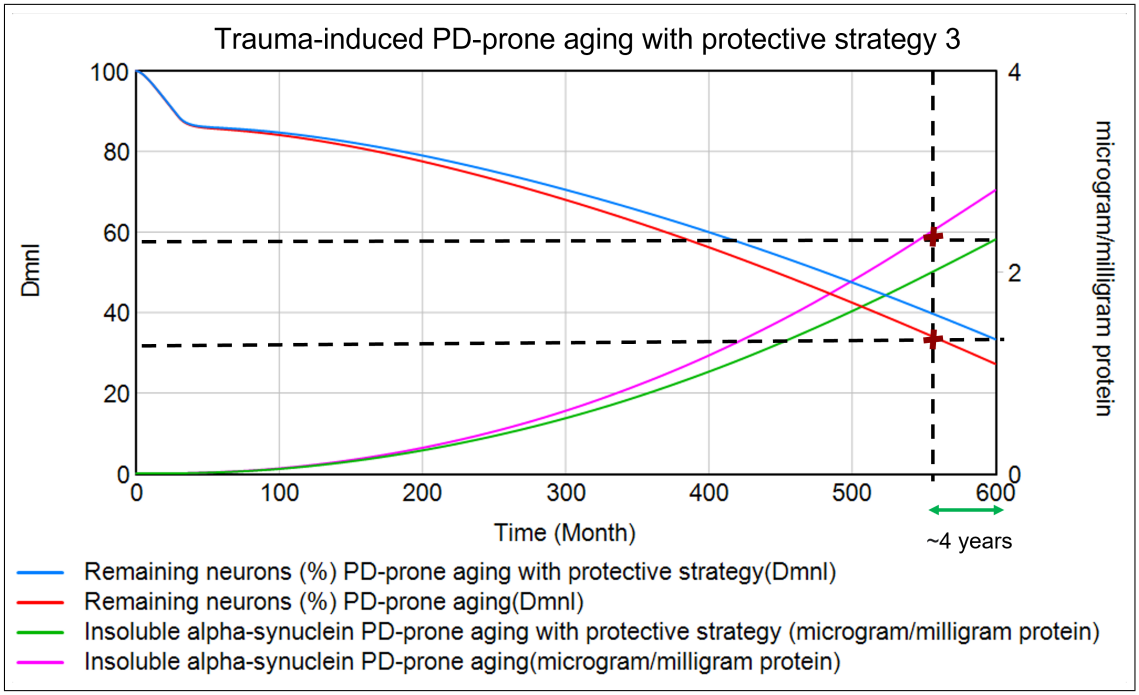


Figure 8.17. Potential disease symptom delay by protective strategy 3.

The findings of a study revealed that medical improvements that postpone the onset of Alzheimer's disease by 5 years result in 41% lower prevalence and 40% lower cost. This 5-year-delay leads to 2.7 additional life years which is approximately 5 disease-free years [164]. Treatment and prevention strategies delaying the onset of PD are also expected to generate significant economic and longevity benefits.

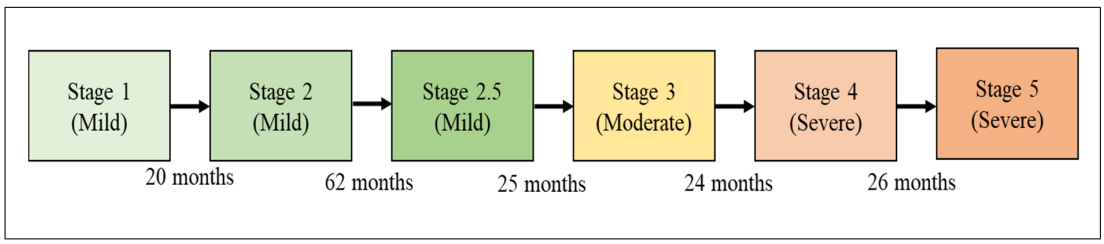


Figure 8.18. Median time between PD severity stages (reproduced from [163]).

# 9. CONCLUSION

There is an ongoing interest in fully understanding the underlying complex pathways leading to Parkinson's disease (PD). According to several studies, there is an important link between brain traumas and PD, mainly resulting from neuroinflammation-induced mechanisms. Due to the dynamic nature of the brain, many other sectors are also affected in the long-term. In this study, we have built a system dynamics model of a specific brain region where dopamine-producing neurons reside, to monitor the long-term dynamic effects of brain injury on potential mechanisms leading to PD development. The values of a 30-year-old healthy person are utilized as the initial parameters. Some age-related abnormalities (which are considered normal) are observed when these parameters are fed into the model. These changes are significantly pronounced in people with PD, as evidenced by toxic alpha-synuclein protein aggregation and the rapid depletion of dopaminergic neurons. After exploring the normal (healthy) aging dynamics, it is investigated whether individuals exhibit Parkinsonian-like output after having experienced repetitive brain injuries. Finally, potential positive impacts of genetic variance and/or healthy lifestyle factors are tested.

In the literature, there is no individual-level system dynamics model focusing on the relationship between PD and TBIs. The proposed mathematical models, mainly ordinary differential equations, for PD progression are far from a holistic approach. They are generally short-term and study the relationship of a few mechanisms within a limited scope. Also, these models tend to have a partial understanding of the system by only concentrating on the cause-and-effect relationship between two variables rather than circular causal loops. Besides, most models analyze the condition by developing hypothetical patients instead of examining pathways that lead to PD. Individual-level TBI-related system dynamics models are short-term. They focus on the dynamics in the acute and recovery phases post-injury and do not consider the potential connection between PD and TBI-induced neuroinflammation. The difficulties in monitoring, data

collection, and quantifying brain-related variables are the primary challenges for this research because only post-mortem analysis allows for neuropathological diagnosis. Thus, in the validation phase, qualitative and quantitative knowledge gained from autopsy reports and animal experimental studies are employed. Our model is validated by structure and behavior tests.

Using our model, we next analyzed different scenarios to investigate the association between PD and brain injury. To investigate the significance of age during the first trauma, four age groups are studied. Each age group is then exposed to repetitive brain injuries with varying numbers, intervals, and severities. Our findings suggest that healthy individuals who are subjected to brain trauma at an early age may produce PD-like outcomes later in life. Those over the age of 40 experience some neuronal loss, however, there is no substantial protein aggregation, the other pathological definition for PD. The earlier the trauma begins, the greater the impact in terms of PD susceptibility, indicating that PD takes some time to form after repetitive injuries. In summary, repeated TBIs must start early in life, be more severe than a threshold, and occur with a particular consistency with short intervals to produce PD-like behaviors in long-term. Otherwise, balancing mechanisms are able to compensate for the TBI-induced harm to the brain.

A diet rich in antioxidants nutrients and regular exercise are demonstrated to be a promising anti-PD strategy. Treatment methods or genetic variance that promote mitochondrial activity and protein degradation are also confirmed to be favorable for both PD and normal aging brains. Our combined strategy run reduces alpha-synuclein aggregation by 17.4% and increases remaining neurons by 22.5% in PD-prone people. Thus, the time course of PD is approximately postponed by 4 years. The quality-adjusted life year of potential PD patients can be extended by delaying symptoms and/or avoiding disease pathogenesis.

Overall, the model serves well our purposes in this study: it provides us with a quantitative tool to experiment with different brain injury scenarios to observe and

understand long-term impacts and potential treatment strategies. The ultimate aim of the research is to provide a comprehensive understanding of PD-related brain dynamics in interaction with external factors and to identify the most effective mechanisms for the treatment and prevention strategies. The work presented is naturally open to development by including discoveries from new field data and empirical studies.

# REFERENCES


1. Abbott, N. J., L. Rönnbäck and E. Hansson, "Astrocyte–Endothelial Interactions at the Blood–Brain Barrier", *Nature Reviews Neuroscience*, Vol. 7, No. 1, pp. 41–53, 2006.

2. Rachakonda, V., T. H. Pan and W. D. Le, "Biomarkers of Neurodegenerative Disorders: How Good Are They?", *Cell Research*, Vol. 14, No. 5, pp. 349–358, 2004.

3. Mrak, R. E., W. S. T. Griffin and D. I. Graham, "Aging-Associated Changes in Human Brain", *Journal of Neuropathology and Experimental Neurology*, Vol. 56, No. 12, pp. 1269–1275, 1997.

4. Peters, R., "Ageing and the Brain", *Postgraduate Medical Journal*, Vol. 82, No. 964, pp. 84–88, 2006.

5. Wang, Y., Y. Pan and H. Li, "What Is Brain Health and Why Is It Important?", *BMJ*, Vol. 371, 2020.

6. Agrawal, M. and A. Biswas, "Molecular Diagnostics of Neurodegenerative Disorders", *Frontiers in Molecular Biosciences*, Vol. 2, p. 54, 2015.

7. Abeliovich, A. and A. D. Gitler, "Defects in Trafficking Bridge Parkinson's Disease Pathology and Genetics", *Nature*, Vol. 539, No. 7628, pp. 207–216, 2016.

8. Canter, R. G., J. Penney and L. H. Tsai, "The Road to Restoring Neural Circuits for the Treatment of Alzheimer's Disease", *Nature*, Vol. 539, No. 7628, pp. 187–196, 2016.

9. Taylor, J. P., R. H. Brown and D. W. Cleveland, "Decoding ALS: From Genes to Mechanism", *Nature*, Vol. 539, No. 7628, pp. 197–206, 2016.

10. World Health Organization, "Neurological Disorders: Public Health Challenges", 2006, https://www.who.int/publications/i/item/9789241563369, accessed on December 28, 2022.

11. World Health Organization, "Parkinson Disease", 2022, https://www.who.int/news-room/fact-sheets/detail/parkinson-disease, accessed on December 28, 2022.

12. Chung, S., K. C. Sonntag, T. Andersson, L. M. Bjorklund, J. J. Park, D. W. Kim, U. J. Kang, O. Isacson and K. S. Kim, "Genetic Engineering of Mouse Embryonic Stem Cells by Nurr1 Enhances Differentiation and Maturation Into Dopaminergic Neurons", *The European Journal of Neuroscience*, Vol. 16, No. 10, pp. 1829–1838, 2002.

13. Sherer, T. B., S. Chowdhury, K. Peabody and D. W. Brooks, "Overcoming Obstacles in Parkinson's Disease", *Movement Disorders*, Vol. 27, No. 13, pp. 1606–1611, 2012.

14. Parkinson's Disease Foundation, "Statistics", 2022, https://www.parkinson.org/understanding-parkinsons/statistics, accessed on December 22, 2022.

15. Nussbaum, R. L. and C. E. Ellis, "Alzheimer's Disease and Parkinson's Disease", *The New England Journal of Medicine*, Vol. 348, No. 14, pp. 1356–1364, 2003.

16. de Lau, L. M. and M. M. Breteler, "Epidemiology of Parkinson's Disease", *The Lancet Neurology*, Vol. 5, No. 6, pp. 525–535, 2006.

17. Lampropoulos, I. C., F. Malli, O. Sinani, K. I. Gourgoulianis and G. Xiromerisiou, "Worldwide Trends in Mortality Related to Parkinson's Disease in the Period of 1994–2019: Analysis of Vital Registration Data From the WHO Mortality Database", *Frontiers in Neurology*, Vol. 13, p. 2217, 2022.

18. Poewe, W., K. Seppi, C. M. Tanner, G. M. Halliday, P. Brundin, J. Volkmann, A. E. Schrag and A. E. Lang, "Parkinson Disease", *Nature Reviews Disease Primers*, Vol. 3, No. 1, pp. 1–21, 2017.

19. GBD 2016 Parkinson's Disease Collaborators, "Global, Regional, and National Burden of Parkinson's Disease, 1990–2016: A Systematic Analysis for the Global Burden of Disease Study 2016", *The Lancet Neurology*, Vol. 17, No. 11, pp. 939–953, 2018.

20. Yang, W., J. L. Hamilton, C. Kopil, J. C. Beck, C. M. Tanner, R. L. Albin, E. R. Dorsey, N. Dahodwala, I. Cintina, P. Hogan and T. Thompson, "Current and Projected Future Economic Burden of Parkinson's Disease in the U.S.", *Npj Parkinson's Disease*, Vol. 6, No. 1, pp. 1–9, 2020.

21. Long-Smith, C. M., A. M. Sullivan and Y. M. Nolan, "The Influence of Microglia on the Pathogenesis of Parkinson's Disease", *Progress in Neurobiology*, Vol. 89, No. 3, pp. 277–287, 2009.

22. Cheng, H. C., C. M. Ulane and R. E. Burke, "Clinical Progression in Parkinson's Disease and the Neurobiology of Axons", *Annals of Neurology*, Vol. 67, No. 6, p. 715, 2010.

23. Chaudhuri, K. R. and N. Titova, "Societal Burden and Persisting Unmet Needs of Parkinson's Disease", *European Neurological Review*, Vol. 14, No. 1, pp. 28–35, 2019.

24. Beitz, J. M., "Parkinson's Disease: A Review", *Frontiers in Bioscience (Scholar edition)*, Vol. 6, No. 1, pp. 65–74, 2014.

25. Maiti, P., J. Manna, G. L. Dunbar, P. Maiti and G. L. Dunbar, "Current Understanding of the Molecular Mechanisms in Parkinson's Disease", *Translational Neurodegeneration*, Vol. 6, No. 1, pp. 1–35, 2017.

26. Dauer, W. and S. Przedborski, "Parkinson's Disease: Mechanisms and Models", *Neuron*, Vol. 39, No. 6, pp. 889–909, 2003.

27. Fujita, K. A., M. Ostaszewski, Y. Matsuoka, S. Ghosh, E. Glaab, C. Trefois, I. Crespo, T. M. Perumal, W. Jurkowski, P. M. A. Antony, N. Diederich, M. Burrini, A. Kodama, V. P. Satagopam, S. Eifes, A. del Sol, R. Schneider, H. Kirano and R. Balling, "Integrating Pathways of Parkinson's Disease in a Molecular Interaction Map", *Molecular Neurobiology*, Vol. 49, No. 1, pp. 88–102, 2014.

28. Goldman, S. M., K. Marek, R. Ottman, C. Meng, K. Comyns, P. Chan, J. Ma, C. Marras, J. W. Langston, G. W. Ross and C. M. Tanner, "Concordance for Parkinson's Disease in Twins: A 20-Year Update", *Annals of Neurology*, Vol. 85, No. 4, pp. 600–605, 2019.

29. Simon, D. K., C. M. Tanner and P. Brundin, "Parkinson Disease Epidemiology, Pathology, Genetics, and Pathophysiology", *Clinics in Geriatric Medicine*, Vol. 36, No. 1, pp. 1–12, 2020.

30. Delic, V., K. D. Beck, K. C. Pang and B. A. Citron, "Biological Links Between Traumatic Brain Injury and Parkinson's Disease", *Acta Neuropathologica Communications*, Vol. 8, No. 1, pp. 1–16, 2020.

31. Qian, L., P. M. Flood and J. S. Hong, "Neuroinflammation Is a Key Player in Parkinson's Disease and a Prime Target for Therapy", *Journal of Neural Transmission*, Vol. 117, No. 8, pp. 971–979, 2010.

32. Schimmel, S. J., S. Acosta and D. Lozano, "Neuroinflammation in Traumatic Brain Injury: A Chronic Response to an Acute Injury", *Brain Circulation*, Vol. 3, No. 3, p. 135, 2017.

33. Briggs, D. I., M. Angoa-Pérez and D. M. Kuhn, "Prolonged Repetitive Head Trauma Induces a Singular Chronic Traumatic Encephalopathy–Like Pathology in White Matter Despite Transient Behavioral Abnormalities", *The American*

*Journal of Pathology*, Vol. 186, No. 11, pp. 2869–2886, 2016.

34. Miller, I. N. and A. Cronin-Golomb, "Gender Differences in Parkinson's Disease: Clinical Characteristics and Cognition", *Movement Disorders*, Vol. 25, No. 16, pp. 2695–2703, 2010.

35. Taylor, C. A., J. M. Bell, M. J. Breiding and L. Xu, "Traumatic Brain Injury–Related Emergency Department Visits, Hospitalizations, and Deaths: United States, 2007 and 2013", *MMWR Surveillance Summaries*, Vol. 66, No. 9, p. 1, 2017.

36. Jordan, B. D., N. R. Relkin, L. D. Ravdin, A. R. Jacobs, A. Bennett and S. Gandy, "Apolipoprotein E $\in$4 Associated With Chronic Traumatic Brain Injury in Boxing", *JAMA*, Vol. 278, No. 2, pp. 136–140, 1997.

37. Hou, L., W. Chen, X. Liu, D. Qiao and F. Zhou, "Exercise-Induced Neuroprotection of the Nigrostriatal Dopamine Dystem in Parkinson's Disease", *Frontiers in Aging Neuroscience*, Vol. 9, p. 358, 2017.

38. Fischer, H. P., "Mathematical Modeling of Complex Biological Systems: From Parts Lists to Understanding Systems Behavior", *Alcohol Research and Health*, Vol. 31, No. 1, p. 49, 2008.

39. Lloret-Villas, A., T. M. Varusai, N. Juty, C. Laibe, N. L. Novere, H. Hermjakob and V. Chelliah, "The Impact of Mathematical Modeling in Understanding the Mechanisms Underlying Neurodegeneration: Evolving Dimensions and Future Directions", *CPT: Pharmacometrics and Systems Pharmacology*, Vol. 6, No. 2, p. 73, 2017.

40. Bakshi, S., V. Chelliah, C. Chen and P. H. van der Graaf, "Mathematical Biology Models of Parkinson's Disease", *CPT: Pharmacometrics and Systems Pharmacology*, Vol. 8, No. 2, pp. 77–86, 2019.

41. Morris, A. M. and R. G. Finke, "Alpha-Synuclein Aggregation Variable Temperature and Variable pH Kinetic Data: A Re-Analysis Using the Finke-Watzky 2-Step Model of Nucleation and Autocatalytic Growth", *Biophysical Chemistry*, Vol. 140, No. 1-3, pp. 9–15, 2009.

42. Bharathi, P., P. Nagabhushan and K. S. Rao, "Mathematical Approach to Understand the Kinetics of $\alpha$-Synuclein Aggregation: Relevance to Parkinson's Disease", *Computers in Biology and Medicine*, Vol. 38, No. 10, pp. 1084–1093, 2008.

43. Galvagnion, C., A. K. Buell, G. Meisl, T. C. Michaels, M. Vendruscolo, T. P. Knowles and C. M. Dobson, "Lipid Vesicles Trigger $\alpha$-Synuclein Aggregation by Stimulating Primary Nucleation", *Nature Chemical Biology*, Vol. 11, No. 3, pp. 229–234, 2015.

44. Flagmeier, P., G. Meisl, M. Vendruscolo, T. P. Knowles, C. M. Dobson, A. K. Buell and C. Galvagnion, "Mutations Associated With Familial Parkinson's Disease alter the Initiation and Amplification Steps of $\alpha$-Synuclein Aggregation", *Proceedings of the National Academy of Sciences of the United States of America*, Vol. 113, No. 37, pp. 10328–10333, 2016.

45. Raichur, A., S. Vali and F. Gorin, "Dynamic Modeling of Alpha-Synuclein Aggregation for the Sporadic and Genetic Forms of Parkinson's Disease", *Neuroscience*, Vol. 142, No. 3, pp. 859–870, 2006.

46. Vali, S., R. B. Mythri, B. Jagatha, J. Padiadpu, K. S. Ramanujan, J. K. Andersen, F. Gorin and M. M. Bharath, "Integrating Glutathione Metabolism and Mitochondrial Dysfunction With Implications for Parkinson's Disease: A Dynamic Model", *Neuroscience*, Vol. 149, No. 4, pp. 917–930, 2007.

47. Sneppen, K., L. Lizana, M. H. Jensen, S. Pigolotti and D. Otzen, "Modeling Proteasome Dynamics in Parkinson's Disease", *Physical Biology*, Vol. 6, No. 3, p. 036005, 2009.

48. Braak, H., J. R. Bohl, C. M. Müller, U. Rüb, R. A. de Vos and K. D. Tredici, "Stanley Fahn Lecture 2005: The Staging Procedure for the Inclusion Body Pathology Associated With Sporadic Parkinson's Disease Reconsidered", *Movement Disorders*, Vol. 21, No. 12, pp. 2042–2051, 2006.

49. Stefano, G. B., N. Pilonis, R. Ptacek, J. Raboch, M. Vnukova and R. M. Kream, "Gut, Microbiome, and Brain Regulatory Axis: Relevance to Neurodegenerative and Psychiatric Disorders", *Cellular and Molecular Neurobiology*, Vol. 38, No. 6, p. 1197, 2018.

50. Tomaskova, H., P. Maresova, D. Jun, M. Augustynek, J. Honegr and B. Klimova, "Dynamic Modeling of the Czech Republic Population With a Focus on Alzheimer's Disease Patients", *Intelligent Information and Database Systems: 10th Asian Conference*, pp. 347–356, Dong Hoi City, Vietnam, 2018.

51. Tomaskova, H., J. Kuhnova, R. Cimler, O. Dolezal and K. Kuca, "Prediction of Population With Alzheimer's Disease in the European Union Using a System Dynamics Model", *Neuropsychiatric Disease and Treatment*, Vol. 12, pp. 1589–1598, 2016.

52. Sabounchi, N. S., "A Systems Dynamic Approach to Alzheimer's Disease Prevention", *International Journal of Population Data Science*, Vol. 1, No. 1, 2017.

53. Ansah, J. P., V. Koh, C. T. Chiu, C. L. Chei, Y. Zeng, Z. X. Yin, X. M. Shi and D. B. Matchar, "Projecting the Number of Elderly With Cognitive Impairment in China Using a Multi-State Dynamic Population Model", *System Dynamics Review*, Vol. 33, No. 2, pp. 89–111, 2017.

54. Kenzie, E. S., E. L. Parks, N. Carney and W. Wakeland, "System Dynamics Modeling for Traumatic Brain Injury: Mini-Review of applications", *Frontiers in Bioengineering and Biotechnology*, Vol. 10, p. 1333, 2022.

55. Kochis, R. M., A. Ahota, H. B. Garcia, R. Z. Gottlieb, E. B. Ruelas and

G. Cauwenberghs, "Modeling the Dynamics of a Secondary Neurodegenerative Injury Following a Mild Traumatic Brain Injury", *43rd Annual International Conference of the IEEE Engineering in Medicine and Biology Society (EMBC)*, pp. 4469–4472, 2021.

56. Vaughan, L. E., P. R. Ranganathan, R. G. Kumar, A. K. Wagner and J. E. Rubin, "A Mathematical Model of Neuroinflammation in Severe Clinical Traumatic Brain Injury", *Journal of Neuroinflammation*, Vol. 15, No. 1, pp. 1–19, 2018.

57. Kenzie, E. S., E. L. Parks, E. D. Bigler, D. W. Wright, M. M. Lim, J. C. Chesnutt, G. W. Hawryluk, W. Gordon and W. Wakeland, "The Dynamics of Concussion: Mapping Pathophysiology, Persistence, and Recovery With Causal-Loop Diagramming", *Frontiers in Neurology*, Vol. 9, p. 203, 2018.

58. Wakeland, W. and E. Kenzie, "A Computational Model for Recovery From Traumatic Brain Injury", *Proceedings of the 63rd Annual Meeting of the ISSS-2019*, Corvallis, OR, USA, 2019.

59. Jones, P., L. Chalmers, S. Wells, S. Ameratunga, P. Carswell, T. Ashton, E. Curtis, P. Reid, J. Stewart, A. Harper and T. Tenbensel, "Implementing Performance Improvement in New Zealand Emergency Departments: The Six Hour Time Target Policy National Research Project Protocol", *BMC Health Services Research*, Vol. 12, No. 1, pp. 1–11, 2012.

60. Lee, L., M. Heffernan, G. McDonnell, S. D. Short and V. Naganathan, "A System Dynamics Modelling Approach to Studying the Increasing Prevalence of People With Intellectual Developmental Disorders in New South Wales", *Australian Health Review*, Vol. 40, No. 3, pp. 235–243, 2015.

61. DiSabato, D. J., N. Quan and J. P. Godbout, "Neuroinflammation: The Devil Is in the Details", *Journal of Neurochemistry*, Vol. 139, p. 136, 2016.

62. Beyer, K., "$\alpha$-Synuclein Structure, Posttranslational Modification and Alternative

Splicing as Aggregation Enhancers", *Acta Neuropathologica*, Vol. 112, No. 3, pp. 237–251, 2006.

63. Chinta, S. J. and J. K. Andersen, "Dopaminergic Neurons", *The International Journal of Biochemistry and Cell Biology*, Vol. 37, No. 5, pp. 942–946, 2005.

64. Dias, V., E. Junn and M. M. Mouradian, "The Role of Oxidative Stress in Parkinson's Disease", *Journal of Parkinson's disease*, Vol. 3, No. 4, p. 461, 2013.

65. Tretter, L., I. Sipos and V. Adam-Vizi, "Initiation of Neuronal Damage by Complex I Deficiency and Oxidative Stress in Parkinson's Disease", *Neurochemical Research*, Vol. 29, No. 3, pp. 569–577, 2004.

66. Yin, J., K. L. Valin, M. L. Dixon and J. W. Leavenworth, "The Role of Microglia and Macrophages in CNS Homeostasis, Autoimmunity, and Cancer", *Journal of Immunology Research*, Vol. 2017, 2017.

67. Picca, A., F. Guerra, R. Calvani, R. Romano, H. J. Coelho-Júnior, C. Bucci and E. Marzetti, "Mitochondrial Dysfunction, Protein Misfolding and Neuroinflammation in Parkinson's Disease: Roads to Biomarker Discovery", *Biomolecules*, Vol. 11, No. 10, p. 1508, 2021.

68. Goldberg, A. L., "Protein Degradation and Protection Against Misfolded or Damaged Proteins", *Nature*, Vol. 426, No. 6968, pp. 895–899, 2003.

69. Parnetti, L., L. Gaetani, P. Eusebi, S. Paciotti, O. Hansson, O. El-Agnaf, B. Mollenhauer, K. Blennow and P. Calabresi, "CSF and Blood Biomarkers for Parkinson's Disease", *The Lancet Neurology*, Vol. 18, No. 6, pp. 573–586, 2019.

70. Lee, H., X. Zhu, G. Liu, S. G. Chen, G. Perry, M. A. Smith and H. Lee, "Divalent Metal Transporter, Iron, and Parkinson's Disease: A Pathological Relationship", *Cell Research*, Vol. 20, No. 4, pp. 397–399, 2010.

71. Bharath, S., M. Hsu, D. Kaur, S. Rajagopalan and J. K. Andersen, "Glutathione, Iron and Parkinson's Disease", *Biochemical Pharmacology*, Vol. 64, No. 5-6, pp. 1037–1048, 2002.

72. Riederer, P., E. Sofic, W. Rausch, B. Schmidt, G. P. Reynolds, K. Jellinger and M. B. Youdim, "Transition Metals, Ferritin, Glutathione, and Ascorbic Acid in Parkinsonian Brains", *Journal of Neurochemistry*, Vol. 52, No. 2, pp. 515–520, 1989.

73. Hyman, C., M. Hofer, Y. Barde, M. Juhasz, G. D. Yancopoulos, S. P. Squinto and R. M. Lindsay, "BDNF Is a Neurotrophic Factor for Dopaminergic Neurons of the Substantia Nigra", *Nature*, Vol. 350, No. 6315, pp. 230–232, 1991.

74. Howells, D., M. Porritt, J. Wong, P. Batchelor, R. Kalnins, A. Hughes and G. Donnan, "Reduced BDNF mRNA Expression in the Parkinson's Disease Substantia Nigra", *Experimental Neurology*, Vol. 166, No. 1, pp. 127–135, 2000.

75. Sugimoto, M. A., L. P. Sousa, V. Pinho, M. Perretti and M. M. Teixeira, "Resolution of Inflammation: What Controls Its Onset?", *Frontiers in Immunology*, Vol. 7, p. 160, 2016.

76. Du, X., X. Xie and R. Liu, "The Role of $\alpha$-Synuclein Oligomers in Parkinson's Disease", *International Journal of Molecular Sciences*, Vol. 21, No. 22, p. 8645, 2020.

77. Paxinou, E., Q. Chen, M. Weisse, B. I. Giasson, E. H. Norris, S. M. Rueter, J. Q. Trojanowski, V. M. Y. Lee and H. Ischiropoulos, "Induction of $\alpha$-Synuclein Aggregation by Intracellular Nitrative Insult", *Journal of Neuroscience*, Vol. 21, No. 20, pp. 8053–8061, 2001.

78. Pajares, M., N. Jiménez-Moreno, I. H. Dias, B. Debelec, M. Vucetic, K. E. Fladmark, H. Basaga, S. Ribaric, I. Milisav and A. Cuadrado, "Redox Control of Protein Degradation", *Redox Biology*, Vol. 6, pp. 409–420, 2015.

79. Druzhyna, N. M., G. L. Wilson and S. P. LeDoux, "Mitochondrial DNA Repair in Aging and Disease", *Mechanisms of Ageing and Development*, Vol. 129, No. 7-8, pp. 383–390, 2008.

80. Dupré-Crochet, S., M. Erard and O. Nüβe, "ROS Production in Phagocytes: Why, When, and Where?", *Journal of Leukocyte Biology*, Vol. 94, No. 4, pp. 657–670, 2013.

81. Frank-Cannon, T. C., L. T. Alto, F. E. McAlpine and M. G. Tansey, "Does Neuroinflammation Fan the Flame in Neurodegenerative Diseases?", *Molecular Neurodegeneration*, Vol. 4, pp. 1–13, 2009.

82. Sian, J., D. Dexter, A. Lees, S. Daniel, P. Jenner and C. Marsden, "Glutathione-Related Enzymes in Brain in Parkinson's Disease", *Annals of Neurology: Official Journal of the American Neurological Association and the Child Neurology Society*, Vol. 36, No. 3, pp. 356–361, 1994.

83. Zecca, L., H. Wilms, S. Geick, J. H. Claasen, L. Brandenburg, C. Holzknecht, M. L. Panizza, F. A. Zucca, G. Deuschl, J. Sievers and R. Lucius, "Human Neuromelanin Induces Neuroinflammation and Neurodegeneration in the Rat Substantia Nigra: Implications for Parkinson's Disease", *Acta Neuropathologica*, Vol. 116, pp. 47–55, 2008.

84. Cianciulli, A., C. Porro, R. Calvello, T. Trotta, D. D. Lofrumento and M. A. Panaro, "Microglia Mediated Neuroinflammation: Focus on PI3K Modulation", *Biomolecules*, Vol. 10, No. 1, p. 137, 2020.

85. Bharath, S. and J. K. Andersen, "Glutathione Depletion in a Midbrain-Derived Immortalized Dopaminergic Cell Line Results in Limited Tyrosine Nitration of Mitochondrial Complex I Subunits: Implications for Parkinson's Disease", *Antioxidants and Redox Signaling*, Vol. 7, No. 7-8, pp. 900–910, 2005.

86. Toulorge, D., A. H. Schapira and R. Hajj, "Molecular Changes in the Postmortem

Parkinsonian Brain", *Journal of Neurochemistry*, Vol. 139, pp. 27–58, 2016.

87. Barnig, C., T. Bezema, P. C. Calder, A. Charloux, N. Frossard, J. Garssen, O. Haworth, K. Dilevskaya, F. Levi-Schaffer, E. Lonsdorfer, M. Wauben, A. D. Kraneveld and A. A. T. Velde, "Activation of Resolution Pathways to Prevent and Fight Chronic Inflammation: Lessons From Asthma and Inflammatory Bowel Disease", *Frontiers in Immunology*, Vol. 10, p. 1699, 2019.

88. Helmut, K., U. K. Hanisch, M. Noda and A. Verkhratsky, "Physiology of Microglia", *Physiological Reviews*, Vol. 91, No. 2, pp. 461–553, 2011.

89. Cianciulli, A., T. Dragone, R. Calvello, C. Porro, T. Trotta, D. D. Lofrumento and M. A. Panaro, "IL-10 Plays a Pivotal Role in Anti-Inflammatory Effects of Resveratrol in Activated Microglia Cells", *International Immunopharmacology*, Vol. 24, No. 2, pp. 369–376, 2015.

90. Brodacki, B., J. Staszewski, B. Toczyłowska, E. Kozłowska, N. Drela, M. Chalimoniuk and A. Stepien, "Serum Interleukin (IL-2, IL-10, IL-6, IL-4), TNF$\alpha$, and INF$\gamma$ Concentrations Are Elevated in Patients With Atypical and Idiopathic parkinsonism", *Neuroscience Letters*, Vol. 441, No. 2, pp. 158–162, 2008.

91. VanGuilder, H. D., G. V. Bixler, R. M. Brucklacher, J. A. Farley, H. Yan, J. P. Warrington, W. E. Sonntag and W. M. Freeman, "Concurrent Hippocampal Induction of MHC II Pathway Components and Glial Activation With Advanced Aging Is Not Correlated With Cognitive Impairment", *Journal of Neuroinflammation*, Vol. 8, No. 1, pp. 1–21, 2011.

92. Henry, C. J., Y. Huang, A. M. Wynne and J. P. Godbout, "Peripheral Lipopolysaccharide (LPS) Challenge Promotes Microglial Hyperactivity in Aged Mice That Is Associated With Exaggerated Induction of Both Pro-Inflammatory IL-1$\beta$ and Anti-Inflammatory IL-10 Cytokines", *Brain, Behavior, and Immunity*, Vol. 23, No. 3, pp. 309–317, 2009.

93. Timmer, M., K. Cesnulevicius, C. Winkler, J. Kolb, E. Lipokatic-Takacs, J. Jungnickel and C. Grothe, "Fibroblast Growth Factor (FGF)-2 and FGF Receptor 3 Are Required for the Development of the Substantia Nigra, and FGF-2 Plays a Crucial Role for the Rescue of Dopaminergic Neurons After 6-Hydroxydopamine Lesion", *Journal of Neuroscience*, Vol. 27, No. 3, pp. 459–471, 2007.

94. Lawson, L. J., V. H. Perry, P. Dri and S. Gordon, "Heterogeneity in the Distribution and Morphology of Microglia in the Normal Adult Mouse Brain", *Neuroscience*, Vol. 39, No. 1, pp. 151–170, 1990.

95. Pakkenberg, B., A. Møller, H. Gundersen, A. M. Dam and H. Pakkenberg, "The Absolute Number of Nerve Cells in Substantia Nigra in Normal Subjects and in Patients With Parkinson's Disease Estimated With an Unbiased Stereological Method", *Journal of Neurology, Neurosurgery and Psychiatry*, Vol. 54, No. 1, pp. 30–33, 1991.

96. Mogi, M., M. Harada, P. Riederer, H. Narabayashi, K. Fujita and T. Nagatsu, "Tumor Necrosis Factor-$\alpha$ (TNF-$\alpha$) Increases Both in the Brain and in the Cerebrospinal Fluid From Parkinsonian Patients", *Neuroscience Letters*, Vol. 165, No. 1-2, pp. 208–210, 1994.

97. Porcher, L., S. Bruckmeier, S. D. Burbano, J. E. Finnell, N. Gorny, J. Klett, S. K. Wood and M. P. Kelly, "Aging Triggers an Upregulation of a Multitude of Cytokines in the Male and Especially the Female Rodent Hippocampus but More Discrete Changes in Other Brain Regions", *Journal of Neuroinflammation*, Vol. 18, pp. 1–19, 2021.

98. Akundi, R. S., Z. Huang, J. Eason, J. D. Pandya, L. Zhi, W. A. Cass, P. G. Sullivan and H. Büeler, "Increased Mitochondrial Calcium Sensitivity and Abnormal Expression of Innate Immunity Genes Precede Dopaminergic Defects in Pink1-Deficient Mice", *PloS One*, Vol. 6, No. 1, p. e16038, 2011.

99. Conway, K. A., J. D. Harper and P. T. Lansbury, "Accelerated in Vitro Fibril

Formation by a Mutant $\alpha$-Synuclein Linked to Early-Onset Parkinson Disease", *Nature Medicine*, Vol. 4, No. 11, pp. 1318–1320, 1998.

100. Venda, L. L., S. J. Cragg, V. L. Buchman and R. Wade-Martins, "$\alpha$-Synuclein and Dopamine at the Crossroads of Parkinson's Disease", *Trends in Neurosciences*, Vol. 33, No. 12, pp. 559–568, 2010.

101. Hashimoto, M., L. J. Hsu, Y. Xia, A. Takeda, A. Sisk, M. Sundsmo and E. Masliah, "Oxidative Stress Induces Amyloid-Like Aggregate Formation of NACP/$\alpha$-Synuclein in Vitro", *Neuroreport*, Vol. 10, No. 4, pp. 717–721, 1999.

102. Walsh, D. M., A. Lomakin, G. B. Benedek, M. M. Condron and D. B. Teplow, "Amyloid $\beta$-Protein Fibrillogenesis: Detection of a Protofibrillar Intermediate", *Journal of Biological Chemistry*, Vol. 272, No. 35, pp. 22364–22372, 1997.

103. Kalia, L. V., S. K. Kalia, P. J. McLean, A. M. Lozano and A. E. Lang, "$\alpha$-Synuclein Oligomers and Clinical Implications for Parkinson Disease", *Annals of Neurology*, Vol. 73, No. 2, pp. 155–169, 2013.

104. Kourtis, N. and N. Tavernarakis, "Cellular Stress Response Pathways and Ageing: Intricate Molecular Relationships", *The EMBO Journal*, Vol. 30, No. 13, pp. 2520–2531, 2011.

105. Chu, Y. and J. H. Kordower, "Age-Associated Increases of $\alpha$-Synuclein in Monkeys and Humans Are Associated With Nigrostriatal Dopamine Depletion: Is This the Target for Parkinson's Disease?", *Neurobiology of Disease*, Vol. 25, No. 1, pp. 134–149, 2007.

106. Martins Branco, D., D. M. Arduino, A. R. Esteves, D. F. Silva, S. M. Cardoso and C. Oliveira, "Cross-Talk Between Mitochondria and Proteasome in Parkinson's Disease Pathogenesis", *Frontiers in Aging Neuroscience*, p. 17, 2010.

107. Goedert, M., M. G. Spillantini, K. Del Tredici and H. Braak, "100 Years of Lewy

Pathology", *Nature Reviews Neurology*, Vol. 9, No. 1, pp. 13–24, 2013.

108. Chartier, S. and C. Duyckaerts, "Is Lewy Pathology in the Human Nervous System Chiefly an Indicator of Neuronal Protection or of Toxicity?", *Cell and Tissue Research*, Vol. 373, No. 1, pp. 149–160, 2018.

109. Kumar, V., N. Sami, T. Kashav, A. Islam, F. Ahmad and M. I. Hassan, "Protein Aggregation and Neurodegenerative Diseases: From Theory to Therapy", *European Journal of Medicinal Chemistry*, Vol. 124, pp. 1105–1120, 2016.

110. Sweeney, P., H. Park, M. Baumann, J. Dunlop, J. Frydman, R. Kopito, A. McCampbell, G. Leblanc, A. Venkateswaran, A. Nurmi and R. Hodgson, "Protein Misfolding in Neurodegenerative Diseases: Implications and Strategies", *Translational Neurodegeneration*, Vol. 6, pp. 1–13, 2017.

111. Chondrogianni, N. and E. S. Gonos, "Proteasome Dysfunction in Mammalian Aging: Steps and Factors Involved", *Experimental Gerontology*, Vol. 40, No. 12, pp. 931–938, 2005.

112. McNaught, K. S. P., R. Belizaire, O. Isacson, P. Jenner and C. W. Olanow, "Altered Proteasomal Function in Sporadic Parkinson's Disease", *Experimental Neurology*, Vol. 179, No. 1, pp. 38–46, 2003.

113. Conway, K. A., S. J. Lee, J. C. Rochet, T. T. Ding, R. E. Williamson and P. T. Lansbury Jr, "Acceleration of Oligomerization, Not Fibrillization, Is a Shared Property of Both $\alpha$-Synuclein Mutations Linked to Early-Onset Parkinson's Disease: Implications for Pathogenesis and Therapy", *Proceedings of the National Academy of Sciences*, Vol. 97, No. 2, pp. 571–576, 2000.

114. Chinta, S. J. and J. K. Andersen, "Dopaminergic Neurons", *The International Journal of Biochemistry and Cell biology*, Vol. 37, No. 5, pp. 942–946, 2005.

115. Franco, R., I. Reyes-Resina and G. Navarro, "Dopamine in Health and Disease:

Much More Than a Neurotransmitter", *Biomedicines*, Vol. 9, No. 2, p. 109, 2021.

116. Rudow, G., R. O'Brien, A. V. Savonenko, S. M. Resnick, A. B. Zonderman, O. Pletnikova, L. Marsh, T. M. Dawson, B. J. Crain, M. J. West and J. C. Troncoso, "Morphometry of the Human Substantia Nigra in Ageing and Parkinson's Disease", *Acta Neuropathologica*, Vol. 115, pp. 461–470, 2008.

117. Reeve, A., E. Simcox and D. Turnbull, "Ageing and Parkinson's Disease: Why Is Advancing Age the Biggest Risk Factor?", *Ageing Research Reviews*, Vol. 14, pp. 19–30, 2014.

118. Goldman, J. E., S. Yen, F. Chiu and N. S. Peress, "Lewy Bodies of Parkinson's Disease Contain Neurofilament Antigens", *Science*, Vol. 221, No. 4615, pp. 1082–1084, 1983.

119. Hartmann, A., "Postmortem Studies in Parkinson's Disease", *Dialogues in Clinical Neuroscience*, 2022.

120. Frazzitta, G., R. Maestri, M. F. Ghilardi, G. Riboldazzi, M. Perini, G. Bertotti, N. Boveri, S. Buttini, F. L. Lombino, D. Uccellini, M. Turla, G. Pezzoli and C. Comi, "Intensive Rehabilitation Increases BDNF Serum Levels in Parkinsonian Patients: A Randomized Study", *Neurorehabilitation and Neural Repair*, Vol. 28, No. 2, pp. 163–168, 2014.

121. Palasz, E., A. Wysocka, A. Gasiorowska, M. Chalimoniuk, W. Niewiadomski and G. Niewiadomska, "BDNF as a Promising Therapeutic Agent in Parkinson's Disease", *International Journal of Molecular Sciences*, Vol. 21, No. 3, p. 1170, 2020.

122. Lima Giacobbo, B., J. Doorduin, H. C. Klein, R. A. Dierckx, E. Bromberg and E. F. de Vries, "Brain-Derived Neurotrophic Factor in Brain Disorders: Focus on Neuroinflammation", *Molecular Neurobiology*, Vol. 56, pp. 3295–3312, 2019.

123. Howells, D., M. Porritt, J. Wong, P. Batchelor, R. Kalnins, A. Hughes and G. Donnan, "Reduced BDNF mRNA Expression in the Parkinson's Disease Substantia Nigra", *Experimental Neurology*, Vol. 166, No. 1, pp. 127–135, 2000.

124. Greffard, S., M. Verny, A. M. Bonnet, D. Seilhean, J.-J. Hauw and C. Duyckaerts, "A Stable Proportion of Lewy Body Bearing Neurons in the Substantia Nigra Suggests a Model in Which the Lewy Body Causes Neuronal Death", *Neurobiology of Aging*, Vol. 31, No. 1, pp. 99–103, 2010.

125. Johnson, W. M., A. L. Wilson-Delfosse and J. J. Mieyal, "Dysregulation of Glutathione Homeostasis in Neurodegenerative Diseases", *Nutrients*, Vol. 4, No. 10, pp. 1399–1440, 2012.

126. Naqvi, S., M. Samim, M. Abdin, F. J. Ahmad, A. Maitra, A. K. Dinda and C. Prashant, "Concentration-Dependent Toxicity of Iron Oxide Nanoparticles Mediated by Increased Oxidative Stress [Retraction]", *International Journal of Nanomedicine*, Vol. 17, pp. 1459–1460, 2022.

127. Sun, Y., A. N. Pham, D. J. Hare and T. D. Waite, "Kinetic Modeling of pH-Dependent Oxidation of Dopamine by Iron and Its Relevance to Parkinson's Disease", *Frontiers in Neuroscience*, Vol. 12, p. 859, 2018.

128. Beckman, K. B. and B. N. Ames, "The Free Radical Theory of Aging Matures", *Physiological Reviews*, 1998.

129. Parihar, M., A. Parihar, M. Fujita, M. Hashimoto and P. Ghafourifar, "Mitochondrial Association of Alpha-Synuclein Causes Oxidative Stress", *Cellular and Molecular Life Sciences*, Vol. 65, pp. 1272–1284, 2008.

130. Ďuračková, Z., "Some Current Insights Into Oxidative Stress.", *Physiological Research*, Vol. 59, No. 4, 2010.

131. Poon, H. F., V. Calabrese, G. Scapagnini and D. A. Butterfield, "Free Radicals:

Key to Brain Aging and Heme Oxygenase as a Cellular Response to Oxidative Stress", *The Journals of Gerontology Series A: Biological Sciences and Medical Sciences*, Vol. 59, No. 5, pp. M478–M493, 2004.

132. Yoritaka, A., N. Hattori, K. Uchida, M. Tanaka, E. R. Stadtman and Y. Mizuno, "Immunohistochemical Detection of 4-Hydroxynonenal Protein Adducts in Parkinson Disease.", *Proceedings of the National Academy of Sciences*, Vol. 93, No. 7, pp. 2696–2701, 1996.

133. Venkateshappa, C., G. Harish, R. B. Mythri, A. Mahadevan, M. Srinivas Bharath and S. Shankar, "Increased Oxidative Damage and Decreased Antioxidant Function in Aging Human Substantia Nigra Compared to Striatum: Implications for Parkinson's Disease", *Neurochemical Research*, Vol. 37, pp. 358–369, 2012.

134. Ferrer, I., A. Martinez, R. Blanco, E. Dalfó and M. Carmona, "Neuropathology of Sporadic Parkinson Disease Before the Appearance of Parkinsonism: Preclinical Parkinson Disease", *Journal of Neural Transmission*, Vol. 118, pp. 821–839, 2011.

135. Trist, B. G., D. J. Hare and K. L. Double, "Oxidative Stress in the Aging Substantia Nigra and the Etiology of Parkinson's Disease", *Aging Cell*, Vol. 18, No. 6, p. e13031, 2019.

136. Mischley, L. K., R. C. Lau, E. G. Shankland, T. K. Wilbur and J. M. Padowski, "Phase IIb Study of Intranasal Glutathione in Parkinson's Disease", *Journal of Parkinson's Disease*, Vol. 7, No. 2, pp. 289–299, 2017.

137. Wallace, D. C., "A Mitochondrial Paradigm of Metabolic and Degenerative Diseases, Aging, and Cancer: A Dawn for Evolutionary Medicine", *Annual Review of Genetics*, Vol. 39, pp. 359–407, 2005.

138. Dölle, C., I. Flønes, G. S. Nido, H. Miletic, N. Osuagwu, S. Kristoffersen, P. K. Lilleng, J. P. Larsen, O.-B. Tysnes, K. Haugarvoll, L. A. Bindoff and C. Tzoulis, "Defective Mitochondrial DNA Homeostasis in the Substantia Nigra in Parkinson

Disease", *Nature Communications*, Vol. 7, No. 1, p. 13548, 2016.

139. Mimaki, M., X. Wang, M. McKenzie, D. R. Thorburn and M. T. Ryan, "Understanding Mitochondrial Complex I Assembly in Health and Disease", *Biochimica et Biophysica Acta (BBA)-Bioenergetics*, Vol. 1817, No. 6, pp. 851–862, 2012.

140. Barlas, Y., "Formal Aspects of Model Validity and Validation in System Dynamics", *System Dynamics Review*, Vol. 12, No. 3, pp. 183–210, 1996.

141. Eyolfson, E., A. Khan, R. Mychasiuk and A. W. Lohman, "Microglia Dynamics in Adolescent Traumatic Brain Injury", *Journal of Neuroinflammation*, Vol. 17, No. 1, pp. 1–19, 2020.

142. Koellhoffer, E. C., L. D. McCullough and R. M. Ritzel, "Old Maids: Aging and Its Impact on Microglia Function", *International Journal of Molecular Sciences*, Vol. 18, No. 4, p. 769, 2017.

143. Quinn, J. G., D. T. Coulson, S. Brockbank, N. Beyer, R. Ravid, J. Hellemans, G. B. Irvine and J. A. Johnston, "$\alpha$-Synuclein mRNA and Soluble $\alpha$-Synuclein Protein Levels in Post-Mortem Brain From Patients With Parkinson's Disease, Dementia With Lewy Bodies, and Alzheimer's Disease", *Brain Research*, Vol. 1459, pp. 71–80, 2012.

144. Sharon, R., I. Bar-Joseph, M. P. Frosch, D. M. Walsh, J. A. Hamilton and D. J. Selkoe, "The Formation of Highly Soluble Oligomers of $\alpha$-Synuclein Is Regulated by Fatty Acids and Enhanced in Parkinson's Disease", *Neuron*, Vol. 37, No. 4, pp. 583–595, 2003.

145. Wills, J., J. Jones, T. Haggerty, V. Duka, J. N. Joyce and A. Sidhu, "Elevated Tauopathy and Alpha-Synuclein Pathology in Postmortem Parkinson's Disease Brains With and Without Dementia", *Experimental Neurology*, Vol. 225, No. 1, pp. 210–218, 2010.

146. Hwang, J. S., J. S. Hwang, I. Chang and S. Kim, "Age-Associated Decrease in Proteasome Content and Activities in Human Dermal Fibroblasts: Restoration of Normal Level of Proteasome Subunits Reduces Aging Markers in Fibroblasts From Elderly Persons", *The Journals of Gerontology Series A: Biological Sciences and Medical Sciences*, Vol. 62, No. 5, pp. 490–499, 2007.

147. Zecca, L., D. Tampellini, M. Gerlach, P. Riederer, R. Fariello and D. Sulzer, "Substantia Nigra Neuromelanin: Structure, Synthesis, and Molecular Behaviour", *Molecular Pathology*, Vol. 54, No. 6, p. 414, 2001.

148. Parker Jr, W. D., S. J. Boyson and J. K. Parks, "Abnormalities of the Electron Transport Chain in Idiopathic Parkinson's Disease", *Annals of Neurology*, Vol. 26, No. 6, pp. 719–723, 1989.

149. Ferrer, I., E. Perez, E. Dalfó and M. Barrachina, "Abnormal Levels of Prohibitin and ATP Synthase in the Substantia Nigra and Frontal Cortex in Parkinson's Disease", *Neuroscience Letters*, Vol. 415, No. 3, pp. 205–209, 2007.

150. Rabini, R., E. Petruzzi, R. Staffolani, M. Tesei, P. Fumelli, M. Pazzagli and L. Mazzanti, "Diabetes Mellitus and Subjects' Ageing: A Study on the ATP Content and ATP-Related Enzyme Activities in Human Erythrocytes", *European Journal of Clinical Investigation*, Vol. 27, No. 4, pp. 327–332, 1997.

151. Von Linstow, C. U., M. DeLano-Taylor, J. H. Kordower and P. Brundin, "Does Developmental Variability in the Number of Midbrain Dopamine Neurons Affect Individual Risk for Sporadic Parkinson's Disease?", *Journal of Parkinson's Disease*, Vol. 10, No. 2, pp. 405–411, 2020.

152. Brain Injury Association of America, "ABI vs. TBI: What is the Difference?", 2023, `https://www.biausa.org/brain-injury/about-brain-injury/nbiic/what-is-the-difference-between-an-acquired-brain-injury-and-a-traumatic-brain-injury`, accessed on January 19, 2023.

153. McKee, C. A. and J. R. Lukens, "Emerging Roles for the Immune System in Traumatic Brain Injury", *Frontiers in Immunology*, Vol. 7, p. 556, 2016.

154. Ramlackhansingh, A. F., D. J. Brooks, R. J. Greenwood, S. K. Bose, F. E. Turkheimer, K. M. Kinnunen, S. Gentleman, R. A. Heckemann, K. Gunanayagam, G. Gelosa and D. J. Sharp, "Inflammation After Trauma: Microglial Activation and Traumatic Brain Injury", *Annals of Neurology*, Vol. 70, No. 3, pp. 374–383, 2011.

155. Xiong, Y., A. Mahmood and M. Chopp, "Animal Models of Traumatic Brain Injury", *Nature Reviews Neuroscience*, Vol. 14, No. 2, pp. 128–142, 2013.

156. Shulman, J. M., P. L. De Jager and M. B. Feany, "Parkinson's Disease: Genetics and Pathogenesis", *Annual Review of Pathology: Mechanisms of Disease*, Vol. 6, pp. 193–222, 2011.

157. Zandi, P. P., J. C. Anthony, A. S. Khachaturian, S. V. Stone, D. Gustafson, J. T. Tschanz, M. C. Norton, K. A. Welsh-Bohmer, J. C. S. Breitner and for the Cache County Study Group, "Reduced Risk of Alzheimer Disease in Users of Antioxidant Vitamin Supplements: The Cache County Study", *Archives of Neurology*, Vol. 61, No. 1, pp. 82–88, 2004.

158. Tuon, T., S. Valvassori, G. Dal Pont, C. Paganini, B. Pozzi, T. Luciano, P. Souza, J. Quevedo, C. Souza and R. Pinho, "Physical Training Prevents Depressive Symptoms and a Decrease in Brain-Derived Neurotrophic Factor in Parkinson's Disease", *Brain Research Bulletin*, Vol. 108, pp. 106–112, 2014.

159. Monteiro-Junior, R. S., T. Cevada, B. R. Oliveira, E. Lattari, E. M. Portugal, A. Carvalho and A. C. Deslandes, "We Need to Move More: Neurobiological Hypotheses of Physical Exercise as a Treatment for Parkinson's Disease", *Medical Hypotheses*, Vol. 85, No. 5, pp. 537–541, 2015.

160. van Nimwegen, M., A. D. Speelman, E. J. Hofman-van Rossum, S. Overeem, D. J.

Deeg, G. F. Borm, M. H. van der Horst, B. R. Bloem and M. Munneke, "Physical Inactivity in Parkinson's Disease", *Journal of Neurology*, Vol. 258, pp. 2214–2221, 2011.

161. Deng, H., P. Wang and J. Jankovic, "The genetics of Parkinson disease", *Ageing Research Reviews*, Vol. 42, pp. 72–85, 2018.

162. Hoehn, M. M. and M. D. Yahr, "Parkinsonism: Onset, Progression, and Mortality", *Neurology*, Vol. 50, No. 2, pp. 318–318, 1998.

163. Zhao, Y. J., H. L. Wee, Y.-H. Chan, S. H. Seah, W. L. Au, P. N. Lau, E. C. Pica, S. C. Li, N. Luo and L. C. Tan, "Progression of Parkinson's Disease as Evaluated by Hoehn and Yahr Stage Transition Times", *Movement Disorders*, Vol. 25, No. 6, pp. 710–716, 2010.

164. Zissimopoulos, J., E. Crimmins and P. St.Clair, "The Value of Delaying Alzheimer's Disease Onset", *Forum for Health Economics and Policy*, Vol. 18, No. 1, pp. 25–39, 2015.

165. Umare, M., N. Wankhede, K. Bajaj, R. Trivedi, B. Taksande, M. Umekar, J. Mahore and M. Kale, "Interweaving of Reactive Oxygen Species and Major Neurological and Psychiatric Disorders", *Annales Pharmaceutiques Françaises*, pp. 409–425, 2022.

166. Bisaglia, M., "Mediterranean Diet and Parkinson's Disease", *International Journal of Molecular Sciences*, Vol. 24, No. 1, p. 42, 2022.

# APPENDIX A: MODEL EQUATIONS

There are 22 flow and 15 stock variables in the model. Lookup graphs are used in the formulation of 17 effect functions. Other components of the model include 60 constant parameters and 27 auxiliary variables.

Accumulated mtDNA deletions: INTEG (mtDNA deletions, mtDNA deletions at age 30)
Units: Level
Activated microglia: INTEG (microglial activation - microglial resolution, activated microglia at age 30)
Units: Microglia
Antiinflammatory mediators: INTEG (antiinf increase - antiinf decrease, antiinf at age 30)
Units: pg/ milligram
ATP synthesis level: INTEG (- ATP decrease, ATP synthesis at age 30)
Units: Level
Damaged neurons: INTEG (neuronal damage - neuronal death - neuronal protection, damaged neurons at age 30)
Units: Neuron
Dead neurons: INTEG (neuronal death - neuronal phagocytosis, dead neurons at age 30)
Units: Neuron
GSH level : INTEG (GSH increase - GSH decrease, GSH level at age 30)
Units: microgram/ gram
Healthy neurons : INTEG (neuronal protection - neuronal damage, healthy neurons at age 30)
Units: Neuron

Insoluble alphasyn: INTEG (fibrillization - phagocytosis, alphasyn insoluble toxic at age 30)

Units: microgram/ milligram protein

Mitochondrial Complex I Activity : INTEG (- MCIA reduction, MCIA at age 30)

Units: nmol/ (min*mg)

Oxidative damage : INTEG (oxidative damage increase - oxidative damage decrease, xidative damage at age 30)

Units: Level

Proinflammatory mediators : INTEG (proinf increase - proinf decrease, proinf at age 30)

Units: pg/ milligram

Protein degradation activity : INTEG (- degradation activity decrease, protein degradation at age 30)

Units: Fu/min/ microgram protein

Resting microglia : INTEG (microglial resolution - microglial activation, resting microglia at age 30)

Units: Microglia

Soluble alphasyn : INTEG (oligomerization – degradation - fibrillization, alphasyn soluble at age 30)

Units: Microgram /milligram protein

activated microglia graph for oxidative damage: ([(0, 0)-(10, 10)], (0,0), (0.08,0), (0.1388, 0.0416), (0.1973, 0.1098), (0.2485, 0.2159), (0.3070, 0.3446), (0.3654, 0.4734), (0.4203, 0.625), (0.5007, 0.7727), (0.6140, 0.8825), (0.7346, 0.9507), (0.8479, 0.9734), (1.0368, 0.9962), (3, 1))

Units: Dmnl

activated microglia graph for proinf mediators: ([(0, 0)-(10, 10)], (0,0), (0.08, 0), (0.1752, 0.0167), (0.2886, 0.0446), (0.3814, 0.0865), (0.4793, 0.1452), (0.5755, 0.2033), (0.6891, 0.3106), (0.7913, 0.3939), (0.8776, 0.4734), (0.9640, 0.5757), (1.046, 0.6818), (1.1379, 0.7651), (1.2300, 0.8371), (1.3667, 0.8977), (1.5375, 0.9507), (1.7631, 0.9810), (2.1042, 1), (2.4900, 0.9962), (3, 1))

Units: Dmnl

activated microglia graph for resolution: ([(0, 0)-(10, 10)], (0, 0), (0.0672, 0.0075), (0.1553, 0.0492), (0.2394, 0.125), (0.3300, 0.2234), (0.4128, 0.3371), (0.4682, 0.4280), (0.5231, 0.5340), (0.6049, 0.6742), (0.6784, 0.7765), (0.8010, 0.875), (0.9564, 0.9356), (1.1035, 0.9621), (1.2752, 0.9810), (1.4550, 0.9886), (1.6716, 1), (1.9639, 1), (2.3837, 1), (3, 1))

Units: Dmnl

antiinf sensitivity graph: ([(0, 0)-(10, 10)], (0, 0), (1, 0), (1.0830, 0.0029), (1.1687, 0.0037), (1.3112, 0.0037), (1.4702, 0.0151), (1.6085, 0.0340), (1.8042, 0.0795), (1.9404, 0.1287), (2.0395, 0.1931), (2.1017, 0.2462), (2.1529, 0.2916), (2.2338, 0.3863), (2.3108, 0.4886), (2.3768, 0.5833), (2.4374, 0.6780), (2.5415, 0.8106), (2.6344, 0.8863), (2.7358, 0.9393), (2.8746, 0.9734), (3, 0.9962), (6, 1))

Units: Dmnl

insoluble alphasyn graph for MCIA: ([(0, 0)-(10, 10)], (0, 0), (0.0378, 0.0084), (0.0860, 0.0254), (0.1342, 0.0651), (0.1703, 0.1076), (0.1996, 0.1784), (0.2289, 0.2577), (0.2598, 0.3512), (0.2943, 0.4419), (0.3342, 0.5189), (0.3842, 0.6060), (0.4447, 0.6893), (0.5155, 0.7765), (0.6062, 0.8484), (0.7025, 0.9128), (0.8158, 0.9583), (0.9178, 0.9810), (1.0266, 1), (1.5, 1))

Units: Dmnl

MCIA compensation graph: ([(0, 0)-(10, 10)], (0, 0), (0.0679, 0.00378), (0.1359, 0.0113), (0.2039, 0.0340), (0.2577, 0.0719), (0.3229, 0.1287), (0.3739, 0.1856),(1, 1))

Units: Dmnl

MCIA graph for ATP synthesis: ([(0, 0)-(10, 10)], (0, 1), (0.0906, 0.9696), (0.1643, 0.9393), (0.2436, 0.8977), (0.3399, 0.8522), (0.4305, 0.7992), (0.5155, 0.7386), (0.5977, 0.6704), (0.6657, 0.6060), (0.7252, 0.5416), (0.7903, 0.4583), (0.8668, 0.3295),(0.9178, 0.2310), (0.9660, 0.1098), (1, 0))

Units: Dmnl

mtDNA graph for MCIA: ([(0, 0)-(10, 10)], (0, 0), (0.1104, 0.0037), (0.2124, 0.0075), (0.3271, 0.0189), (0.4249, 0.0416), (0.5141, 0.0681), (0.5736, 0.1136), (0.6373, 0.1893), (0.6883, 0.2651), (0.7308, 0.3560), (0.7818, 0.4659), (0.8158, 0.5795), (0.8498, 0.6780), (0.8923, 0.7462), (0.9688, 0.8371), (1.0708, 0.9053), (1.1813, 0.9469), (1.3215, 0.9810), (1.5, 1))

Units: Dmnl

oxidative damage graph for GSH: ([(0, 0)-(10, 10)], (0, 0), (0.3, 0.3), (0.4305, 0.4128), (0.6118, 0.5151), (0.8385, 0.6136), (1.1104, 0.7007), (1.4277, 0.7840), (1.7790, 0.8598), (2.1983, 0.9242), (2.6855, 0.9734), (3.1954, 0.9924), (4, 1), (5, 1))

Units: Dmnl

oxidative damage graph for GSH capacity: ([(0, 0)-(10, 10)], (0, 0), (0.1082, 0.0037), (0.2460, 0.01515), (0.3739, 0.0378), (0.4920, 0.0681), (0.5707, 0.1060), (0.6888, 0.1704), (0.8019, 0.2537), (0.9151, 0.3522), (1.0135, 0.4356), (1.1316, 0.5378), (1.2538, 0.6363), (1.3817, 0.7121), (1.5558, 0.7840), (1.8055, 0.8484), (2.1248, 0.9128), (2.4905, 0.9621), (2.7372, 0.9810), (3.2381, 1),(5,1))

Units: Dmnl

oxidative damage graph for mtDNA: ([(0, 0)-(10, 10)], (0, 0), (0.0642, 0.0037), (0.1375, 0.0265), (0.20057, 0.0568), (0.2808, 0.1022), (0.3610, 0.1628), (0.4412, 0.2537), (0.5214, 0.3446), (0.6067, 0.4659), (0.6719, 0.5568), (0.7571, 0.6401), (0.8524, 0.7234), (0.9711, 0.7916), (1.0731, 0.8371), (1.2134, 0.8901), (1.3839, 0.9318), (1.6597, 0.9659), (2.0007, 0.9848), (2.3796, 0.9962), (2.8280, 0.9962), (3.1841, 1), (3.5, 1), (5,1))

Units: Dmnl

oxidative damage graph for neuronal damage: ([(0, 0)-(10, 10)], (0, 1), (0.0386, 1.2575), (0.0717, 1.4697), (0.1103, 1.7121), (0.1544, 1.9545), (0.2096, 2.1969), (0.2758, 2.4242), (0.3475, 2.6515), (0.4303, 2.8333), (0.5073, 2.9848), (0.6725, 3.2424), (0.7387, 3.33333), (0.8554, 3.4697), (0.9498, 3.5606), (1.0501, 3.6363), (1.1858, 3.7272), (1.3156, 3.8030), (1.4670, 3.8636), (1.6675, 3.9090), (1.8786, 3.9393), (2.3937, 3.9697), (3.5807, 4), (5, 4))

Units: Dmnl

oxidative damage graph for oligomerization: ([(0, 0)-(10, 10)], (0, 0), (0.5 ,0.5), (0.6458, 0.6534), (0.8498, 0.8238), (1.0991, 0.9943), (1.3371, 1.1193), (1.5750, 1.1988), (1.9263, 1.2897), (2.2889, 1.3465), (2.6515, 1.3920), (3.0363, 1.4261), (3.4447, 1.4602), (5,1.5))

Units: Dmnl

oxidative damage graph for protein degradation: ([(0,0)-(10,10)], (0,0), (0.1359, 0.0189), (0.3399, 0.0568), (0.5892, 0.1174), (0.8158, 0.2007), (1.0198, 0.3106), (1.2011, 0.4204), (1.3711, 0.5151), (1.5410, 0.6060), (1.7337, 0.6931), (1.9943, 0.7803), (2.3116, 0.8484),

(2.6289, 0.9015), (2.9801, 0.9393), (3.3087, 0.9621),(3.6713, 0.9886), (4, 1), (7,1))
Units: Dmnl
proinf graph for antiinf: ([(0,0)-(10,10)], (0,0), (1,0), (1.2070, 0.0140), (1.5300, 0.0492), (1.9694, 0.1060), (2.5018, 0.1856), (2.8887, 0.2575), (3.2498, 0.3522), (3.7141, 0.4659), (4.0752, 0.5833), (4.3847, 0.6969), (4.6942, 0.7916), (5.0295, 0.875), (5.4164, 0.9356), (5.9065, 0.9659), (6.5255, 0.9886), (9.1048, 1), (15,1))
Units: Dmnl
proinf sensitivity graph: ([(0,0)-(10,10)], (0,0), (1,0), (1.1275, 0.0037), (1.3568, 0.0140), (1.5671, 0.0335), (1.7910, 0.0670), (2.0149, 0.1173), (2.2024, 0.1704), (2.3901, 0.2348), (2.5481, 0.3143), (2.6963, 0.3939), (2.8740, 0.4924), (3.0682, 0.5757), (3.3994, 0.6628), (3.7270, 0.7310), (4.0793, 0.7916), (4.5325, 0.8522), (5.0764, 0.9053), (5.7563, 0.9431), (6.3909, 0.9696), (7.1161, 0.9848), (8, 1), (15,1))
Units: Dmnl
protein degradation sensitivity graph: ([(0,0)-(10,10)], (0,0), (0.0679, 0.0037), (0.1359, 0.0189), (0.2011, 0.0416), (0.2549, 0.0719), (0.3314, 0.1325), (0.3994, 0.2007), (1,1))
Units: Dmnl
antiinf decrease: MIN(antiinf discrepancy/adj time for antiinf decrease,possible antiinf decrease)
Units: pg/ milligram/Month
antiinf increase: antiinf increase fraction*effect of proinf on antiinf
Units: pg/ milligram/Month
ATP decrease: effect of MCIA on ATP*ATP decrease fraction
Units: Level/ Month
degradation: Soluble alphasyn*degradation efficiency/adj time for degradation
Units: microgram/ milligram protein/ Month
degradation activity decrease: degradation decrease*effect of oxidative damage on protein degradation*protein degradation sensitivity
Units: Fu/(min* microgram protein)/ Month
fibrillization: Soluble alphasyn/fibrillization delay
Units: microgram/ (Month* milligram protein)

GSH decrease: MIN(GSH level/adj time for GSH decrease, oxidative damage effect on GSH*GSH decrease fraction)

Units: microgram/(Month* gram)

GSH increase: GSH discrepancy*ATP efficiency/GSH increase delay

Units: microgram/gram/ Month

MCIA reduction: MCIA reduction fraction*(effect of mtDNA on MCIA+effect of insoluble alphasyn on MCIA)*MCIA compensation

Units: nmol/ (Month* min*mg)

microglial activation: MIN(Resting microglia/adj time for activation,(activation by dead neurons+activation by alphasyn))

Units: Microglia/Month

microglial resolution: MIN(microglial discrepancy/adj time for resolution, Antiinflammatory mediators*microglial resolution fraction*effect of activated microglia on resolution)

Units: Microglia/Month

mtDNA deletions: (other sources of deletions+mtDNA deletion fraction*effect of oxidative damage on mtDNA)*mtDNA deletion posibility

Units: Level/ Month

neuronal damage: min neuronal damage*effect of oxidative damage on neurons*neuronal damage availability+brain injury

Units: Neuron/ Month

neuronal death: Damaged neurons/neuronal death delay

Units: Neuron/ Month

neuronal phagocytosis: MIN(Dead neurons/adj time for neuronal phagocytosis,Activated microglia*(1-microglial activation by protein fraction)*microglia phagocytosis capacity)

Units: Neuron/ Month

neuronal protection: MIN(BDNF neuroprotection capacity,Damaged neurons/adj time for neuronal protection)

Units: Neuron /Month

oligomerization: effect of oxidative damage on oligomerization*oligomerization fraction

Units: microgram/milligram protein/ Month

oxidative damage decrease: MIN(Oxidative damage/adj time for oxidative damage, GSH level*GSH capacity for oxidative reduction*oxidative damage effect on GSH capacity)

Units: Level/ Month

oxidative damage increase: mitochondrial OD+microglial OD

Units: Level /Month

phagocytosis: MIN(Insoluble alphasyn/adj time for phagocytosis,Activated microglia*microglial activation by protein fraction*phagocytosis capacity)

Units: microgram/(Month* milligram protein)

proinf decrease: MIN(proinf discrepancy/adj time for proinf decrease,possible proinf decrease)

Units: pg/milligram/Month

proinf increase: release fraction*effect of MA on proinf mediators

Units: pg/milligram/Month

antiinf sensitivity: antiinf sensitivity graph(antiinf ratio)

Units: Dmnl

effect of activated microglia on resolution: activated microglia graph for resolution(microglia density)

Units: Dmnl

effect of insoluble alphasyn on MCIA: insoluble alphasyn graph for MCIA(Insoluble alphasyn/reference insoluble alphasyn)

Units: Dmnl

effect of MA on proinf mediators: activated microglia graph for proinf mediators(Activated microglia/reference activated microglia)

Units: Dmnl

effect of MCIA on ATP: MCIA graph for ATP synthesis(Mitochondrial Complex I Activity/MCIA at age 30)

Units: Dmnl

effect of microglia on oxidative damage: activated microglia graph for oxidative damage(Activated microglia/reference activated microglia)
Units: Dmnl
effect of mtDNA on MCIA: mtDNA graph for MCIA(Accumulated mtDNA deletions/reference mtDNA deletions)
Units: Dmnl
effect of oxidative damage on mtDNA: oxidative damage graph for mtDNA(Oxidative damage/reference oxidative damage)
Units: Dmnl
effect of oxidative damage on neurons: oxidative damage graph for neuronal damage(Oxidative damage/reference oxidative damage)
Units: Dmnl
effect of oxidative damage on oligomerization: oxidative damage graph for oligomerization(Oxidative damage/reference oxidative damage)
Units: Dmnl
effect of oxidative damage on protein degradation: oxidative damage graph for protein degradation(Oxidative damage/reference oxidative damage)
Units: Dmnl
effect of proinf on antiinf: proinf graph for antiinf(proinf ratio)
Units: Dmnl
MCIA compensation: MCIA compensation graph(Mitochondrial Complex I Activity/MCIA at age 30)
Units: Dmnl
oxidative damage effect on GSH: oxidative damage graph for GSH(Oxidative damage/reference oxidative damage)
Units: Dmnl
oxidative damage effect on GSH capacity: oxidative damage graph for GSH capacity(oxidative damage ratio)
Units: Dmnl
proinf sensitivity: proinf sensitivity graph(proinf ratio)
Units: Dmnl

protein degradation sensitivity: protein degradation sensitivity graph(Protein degradation activityprotein degradation at age 30)

Units: Dmnl

activated microglia at age 30: 3319

Units: Microglia

activation per alphasyn: 45

Units: Microglia/ (microgram/milligram protein)/ Month

activation per neuron: 0.4

Units: Microglia/Neuron/ Month

adj time for activation: 1

Units: Month

adj time for antiinf decrease: 1

Units: Month

adj time for degradation: 1

Units: Month

adj time for GSH decrease: 1

Units: Month

adj time for neuronal phagocytosis: 1

Units: Month

adj time for neuronal protection: 1

Units: Month

adj time for oxidative damage: 1

Units: Month

adj time for phagocytosis: 1

Units: Month

adj time for proinf decrease: 1

Units: Month

adj time for resolution: 1

Units: Month

alphasyn insoluble toxic at age 30: 0

Units: microgram/milligram protein

alphasyn soluble at age 30: 0

Units: microgram/milligram protein

antiinf at age 30: 11

Units: picogram/milligram

antiinf increase fraction: 0.45

Units: picogram/milligram/Month

antiinf mediators decrease: 0.48

Units: picogram/milligram/Month

ATP decrease fraction: 0.125

Units: Level/ Month

ATP synthesis at age 30: 100

Units: Level

BDNF production capacity: 0.00044

Units: 1/Month

BDNF production reduction: 0.2

Units: Dmnl

brain injury duration: 0

Units: Month

brain injury interval: Determined according to TBI scenario

Units: Month

brain injury number: Determined according to TBI scenario

Units: Dmnl

brain injury onset: Determined according to TBI scenario

Units: Month

damaged neurons at age 30: 170

Units: Neuron

dead neurons at age 30: 28

Units: Neuron

degradation decrease: 0.45

Units: Fu/(min* microgram protein)/ Month

fibrillization delay: 2.5

Units: Month

GSH capacity for oxidative reduction: 0.004

Units: Level/ Month/ (microgram/gram)

GSH decrease fraction: 4.7

Units: microgram/gram/ Month

GSH increase delay: 3

Units: Month

GSH level at age 30: 56.8

Units: microgram/gram

healthy neurons at age 30: 450000

Units: Neuron

MCIA at age 30: 24.7

Units: nmol/min/mg

MCIA reduction fraction: 0.14

Units: nmol/ (Month* min*mg)

microglia phagocytosis capacity: 0.2

Units: Neuron/ Microglia/Month

microglial oxidative damage production: 0.000001

Units: Level/ Microglia/Month

microglial resolution fraction: 9

Units: (Microglia/Month)/ (picogram/milligram)

min neuronal damage: 200

Units: Neuron/ Month

mitochondrial oxidative damage production: 0.19

Units: Level/ Month

mtDNA deletion fraction: 0.055

Units: Level/ Month

mtDNA deletion upper limit: 100

Units: Level

mtDNA deletions at age 30: 20

Units: Level

neuronal death delay: 6

Units: Month

oligomerization fraction: 0.045

Units: microgram/milligram protein/ Month

other sources of deletions: 0.012

Units: Level/ Month

oxidative damage at age 30: 0

Units: Level

phagocytosis capacity: 0.0000009

Units: microgram/(Month* milligram protein)/ Microglia

proinf at age 30: 11

Units: picogram/milligram

proinf mediators decrease: 0.3

Units: picogram/milligram/Month

protein degradation at age 30: 39

Units: Fu/(min* microgram protein)

reference activated microglia: 41900

Units: Microglia

reference insoluble alphasyn: 3.1

Units: microgram/milligram protein

reference mtDNA deletions: 45

Units: Level

reference oxidative damage: 15

Units: Level

release fraction: 0.45

Units: picogram/milligram/Month

resting microglia at age 30: Total microglia-activated microglia at age 30

Units: Microglia

Total microglia: 200000

Units: Microglia

activation by alphasyn: Insoluble alphasyn*activation per alphasyn

Units: Microglia/Month

activation by dead neurons: Dead neurons*activation per neuron

Units: Microglia/Month

actual microglial oxidative damage production: microglial oxidative damage production*effect of microglia on oxidative damage

Units: Level/ (Microglia*Month)

antiinf discrepancy: MAX(0,Antiinflammatory mediators-antiinf at age 30)

Units: picogram/milligram

antiinf ratio: Antiinflammatory mediators/antiinf at age 30

Units: Dmnl

ATP efficiency: ATP synthesis level/ATP synthesis at age 30

Units: Dmnl

BDNF neuroprotection capacity: ((Healthy neurons*BDNF production capacity)+BDNF production capacity*(1-BDNF production reduction)*Damaged neurons)*ATP efficiency

Units: Neuron/ Month

brain injury: brain injury pulse*Healthy neurons*affected area

Units: Neuron/ Month

affected area: Determined according to TBI scenario

Units: 1/Month

brain injury pulse: PULSE TRAIN(brain injury onset,brain injury duration,brain injury interval,last brain injury)

Units: Dmnl

degradation efficiency: Protein degradation activity/protein degradation at age 30

Units: Dmnl

GSH discrepancy: GSH level at age 30-GSH level

Units: microgram/gram

last brain injury: brain injury onset+(brain injury number-1)*brain injury interval

Units: Month

MCIA efficiency: Mitochondrial Complex I Activity/MCIA at age 30

Units: Dmnl

microglia density: Activated microglia/reference activated microglia

Units: Dmnl

microglial activation by protein fraction: ZIDZ(activation by alphasyn,(activation by dead neurons+activation by alphasyn))

Units: Dmnl

microglial discrepancy: (Activated microglia-activated microglia at age 30)

Units: Microglia

microglial OD: Activated microglia*actual microglial oxidative damage production

Units: Level/ Month

mitochondrial OD: MIN((1-MCIA efficiency), 1) *mitochondrial oxidative damage production

Units: Level/ Month

mtDNA deletion posibility: (mtDNA deletion upper limit-Accumulated mtDNA deletions)/mtDNA deletion upper limit

Units: Dmnl

neuronal damage availability: Healthy neurons/(Healthy neurons+Dead neurons+Damaged neurons)

Units: Dmnl

oxidative damage ratio: Oxidative damage/reference oxidative damage

Units: Dmnl

possible antiinf decrease: antiinf sensitivity*antiinf mediators decrease

Units: picogram/milligram/Month

possible proinf decrease: proinf sensitivity*proinf mediators decrease

Units: picogram/milligram/Month

proinf discrepancy: MAX(0, Proinflammatory mediators-proinf at age 30)

Units: picogram/milligram

proinf ratio: Proinflammatory mediators/proinf at age 30

Units: Dmnl

remaining neurons: (Healthy neurons+Damaged neurons/healthy neurons at age 30*100

Units: Dmnl

# APPENDIX B: SENSITIVITY ANALYSIS RUNS

Table B.1 shows the final values of key outputs (insoluble alpha-synuclein aggregation and remaining neurons) at age 80 for different initial values of stocks.

Table B.1. Final values of key outputs for different initial values.

| Variables | Values | Protein aggregation | Remaining neurons (%) |
|---|---|---|---|
| **Oxidative damage** | 0.5 | 1.57 | 62.1 |
| | 1 | 2.14 | 51.2 |
| | 1.5 | 1.86 | 56.3 |
| | 2 | 2.40 | 47.0 |
| **Activated microglia** | 0 | 1.28 | 68.0 |
| | 10,000 | 1.57 | 63.1 |
| | 20,000 | 2.46 | 49.0 |
| | 30,000 | 2.99 | 41.2 |
| **MCIA** | 20 | 3.91 | 32.6 |
| | 22 | 3.19 | 40.8 |
| | 23 | 2.65 | 47.3 |
| | 26 | 0.46 | 84.5 |
| **Insoluble alpha-synuclein** | 0.1 | 1.38 | 66.2 |
| | 0.2 | 1.48 | 64.8 |
| | 0.3 | 1.61 | 62.9 |
| | 0.4 | 1.81 | 59.9 |
| **Healthy neurons** | 300,000 | 1.54 | 34.6 |
| | 350,000 | 1.46 | 49.0 |
| | 500,000 | 1.26 | 73.1 |
| | 600,000 | 1.18 | 81.1 |
| **mtDNA deletions** | 5 | 0.08 | 93.4 |
| | 10 | 0.23 | 88.3 |
| | 15 | 0.64 | 78.5 |
| | 25 | 2.34 | 54.7 |

Table B.2 shows the final values of key outputs (insoluble alpha-synuclein aggregation and remaining neurons) at age 80 for different parameter values of constants. Test values are determined by multiplying the base value by 0.2, 0.5, 1.5, and 2.

Table B.2. Final values of key outputs for different parameter values.

| **Variables** | **Values** | **Protein aggregation** | **Remaining neurons (%)** |
|---|---|---|---|
| **MCIA reduction** | 0.028 | 0.20 | 89.0 |
| | 0.07 | 0.63 | 78.3 |
| | 0.21 | 1.89 | 60.3 |
| | 0.28 | 2.37 | 55.3 |
| **Oligomerization fraction** | 0.009 | 0.23 | 68.3 |
| | 0.0225 | 0.59 | 68.0 |
| | 0.0675 | 2.23 | 66.4 |
| | 0.09 | 3.32 | 65.5 |
| **Neuronal death delay** | 1 | 1.52 | 59.7 |
| | 3 | 1.36 | 65.4 |
| | 12 | 1.28 | 69.1 |
| | 18 | 1.26 | 70.5 |
| **Fibrillization delay** | 1 | 2.60 | 66.0 |
| | 3 | 1.13 | 67.5 |
| | 6 | 0.61 | 68.0 |
| | 12 | 0.32 | 68.2 |
| **BDNF production capacity** | 0.000088 | 1.87 | 42.8 |
| | 0.00022 | 1.66 | 51.8 |
| | 0.00066 | 1.14 | 77.1 |
| | 0.00088 | 1.01 | 84.1 |
| **Microglial OD production** | 0.0000002 | 0.99 | 69.8 |
| | 0.0000005 | 1.11 | 68.9 |
| | 0.0000015 | 1.52 | 66.0 |
| | 0.000002 | 1.72 | 64.7 |

# APPENDIX C: TRAUMATIC BRAIN INJURY SCENARIO RUNS

In total 1152 scenario runs are conducted via Vensim subscript feature. We provide the final values of key outputs at age 80 for the 30-year-old onset group.

Table C.1. Final values of key outputs for brain injuries with 1% affected area.

| **Interval (month)** | **Affected area (%)** | **Number** | **Onset (age)** | **Protein aggregation** | **Remaining neurons (%)** |
|---|---|---|---|---|---|
| **CONTROL** | | | | **1.32** | **67.33** |
| 1 | 1 | 1 | 30 | 1.32 | 67.28 |
| 3 | 1 | 1 | 30 | 1.32 | 67.28 |
| 6 | 1 | 1 | 30 | 1.32 | 67.28 |
| 12 | 1 | 1 | 30 | 1.32 | 67.28 |
| 1 | 1 | 5 | 30 | 1.32 | 66.93 |
| 3 | 1 | 5 | 30 | 1.32 | 66.98 |
| 6 | 1 | 5 | 30 | 1.32 | 67.07 |
| 12 | 1 | 5 | 30 | 1.32 | 67.08 |
| 1 | 1 | 10 | 30 | 1.34 | 66.42 |
| 3 | 1 | 10 | 30 | 1.33 | 66.56 |
| 6 | 1 | 10 | 30 | 1.33 | 66.78 |
| 12 | 1 | 10 | 30 | 1.33 | 66.67 |
| 1 | 1 | 20 | 30 | 1.37 | 65.30 |
| 3 | 1 | 20 | 30 | 1.36 | 65.62 |
| 6 | 1 | 20 | 30 | 1.35 | 65.79 |
| 12 | 1 | 20 | 30 | 1.36 | 65.58 |
| 1 | 1 | 30 | 30 | 1.40 | 64.07 |
| 3 | 1 | 30 | 30 | 1.39 | 64.48 |
| 6 | 1 | 30 | 30 | 1.38 | 64.63 |
| 12 | 1 | 30 | 30 | 1.38 | 64.73 |

Table C.2. Final values of key outputs for brain injuries with 2% affected area.

| **Interval (month)** | **Affected area (%)** | **Number** | **Onset (age)** | **Protein aggregation** | **Remaining neurons (%)** |
|---|---|---|---|---|---|
| **CONTROL** | | | | **1.32** | **67.33** |
| 1 | 2 | 1 | 30 | 1.32 | 67.20 |
| 3 | 2 | 1 | 30 | 1.32 | 67.20 |
| 6 | 2 | 1 | 30 | 1.32 | 67.20 |
| 12 | 2 | 1 | 30 | 1.32 | 67.20 |
| 1 | 2 | 5 | 30 | 1.34 | 66.38 |
| 3 | 2 | 5 | 30 | 1.34 | 66.44 |
| 6 | 2 | 5 | 30 | 1.33 | 66.54 |
| 12 | 2 | 5 | 30 | 1.33 | 66.65 |
| 1 | 2 | 10 | 30 | 1.37 | 65.21 |
| 3 | 2 | 10 | 30 | 1.36 | 65.37 |
| 6 | 2 | 10 | 30 | 1.36 | 65.60 |
| 12 | 2 | 10 | 30 | 1.36 | 65.66 |
| 1 | 2 | 20 | 30 | 1.45 | 62.56 |
| 3 | 2 | 20 | 30 | 1.43 | 62.94 |
| 6 | 2 | 20 | 30 | 1.43 | 63.18 |
| 12 | 2 | 20 | 30 | 1.42 | 63.41 |
| 1 | 2 | 30 | 30 | 1.56 | 59.30 |
| 3 | 2 | 30 | 30 | 1.53 | 59.97 |
| 6 | 2 | 30 | 30 | 1.50 | 60.66 |
| 12 | 2 | 30 | 30 | 1.45 | 61.76 |

Table C.3. Final values of key outputs for brain injuries with 3% affected area.

| **Interval (month)** | **Affected area (%)** | **Number** | **Onset (age)** | **Protein aggregation** | **Remaining neurons (%)** |
|---|---|---|---|---|---|
| **CONTROL** | | | | **1.32** | **67.33** |
| 1 | 3 | 1 | 30 | 1.32 | 67.11 |
| 3 | 3 | 1 | 30 | 1.32 | 67.11 |
| 6 | 3 | 1 | 30 | 1.32 | 67.11 |
| 12 | 3 | 1 | 30 | 1.32 | 67.11 |
| 1 | 3 | 5 | 30 | 1.35 | 65.80 |
| 3 | 3 | 5 | 30 | 1.35 | 65.86 |
| 6 | 3 | 5 | 30 | 1.35 | 65.96 |
| 12 | 3 | 5 | 30 | 1.34 | 66.14 |
| 1 | 3 | 10 | 30 | 1.41 | 63.88 |
| 3 | 3 | 10 | 30 | 1.40 | 64.05 |
| 6 | 3 | 10 | 30 | 1.39 | 64.31 |
| 12 | 3 | 10 | 30 | 1.39 | 64.48 |
| 1 | 3 | 20 | 30 | 1.56 | 59.15 |
| 3 | 3 | 20 | 30 | 1.54 | 59.69 |
| 6 | 3 | 20 | 30 | 1.52 | 60.20 |
| 12 | 3 | 20 | 30 | 1.49 | 61.03 |
| 1 | 3 | 30 | 30 | 1.78 | 53.50 |
| 3 | 3 | 30 | 30 | 1.72 | 54.82 |
| 6 | 3 | 30 | 30 | 1.65 | 56.38 |
| 12 | 3 | 30 | 30 | 1.53 | 58.64 |

Table C.4. Final values of key outputs for brain injuries with 4% affected area.

| **Interval (month)** | **Affected area (%)** | **Number** | **Onset (age)** | **Protein aggregation** | **Remaining neurons (%)** |
|---|---|---|---|---|---|
| **CONTROL** | | | | **1.32** | **67.33** |
| 1 | 4 | 1 | 30 | 1.32 | 67.01 |
| 3 | 4 | 1 | 30 | 1.32 | 67.01 |
| 6 | 4 | 1 | 30 | 1.32 | 67.01 |
| 12 | 4 | 1 | 30 | 1.32 | 67.01 |
| 1 | 4 | 5 | 30 | 1.37 | 65.18 |
| 3 | 4 | 5 | 30 | 1.37 | 65.24 |
| 6 | 4 | 5 | 30 | 1.36 | 65.35 |
| 12 | 4 | 5 | 30 | 1.36 | 65.57 |
| 1 | 4 | 10 | 30 | 1.45 | 62.45 |
| 3 | 4 | 10 | 30 | 1.44 | 62.64 |
| 6 | 4 | 10 | 30 | 1.43 | 62.92 |
| 12 | 4 | 10 | 30 | 1.43 | 63.16 |
| 1 | 4 | 20 | 30 | 1.71 | 55.29 |
| 3 | 4 | 20 | 30 | 1.67 | 56.05 |
| 6 | 4 | 20 | 30 | 1.63 | 57.00 |
| 12 | 4 | 20 | 30 | 1.57 | 58.49 |
| 1 | 4 | 30 | 30 | 2.02 | 47.43 |
| 3 | 4 | 30 | 30 | 1.92 | 49.52 |
| 6 | 4 | 30 | 30 | 1.80 | 52.01 |
| 12 | 4 | 30 | 30 | 1.62 | 55.46 |

Table C.5. Final values of key outputs for brain injuries with 5% affected area.

| **Interval (month)** | **Affected area (%)** | **Number** | **Onset (age)** | **Protein aggregation** | **Remaining neurons (%)** |
|---|---|---|---|---|---|
| **CONTROL** | | | | **1.32** | **67.33** |
| 1 | 5 | 1 | 30 | 1.32 | 66.91 |
| 3 | 5 | 1 | 30 | 1.32 | 66.91 |
| 6 | 5 | 1 | 30 | 1.32 | 66.91 |
| 12 | 5 | 1 | 30 | 1.32 | 66.91 |
| 1 | 5 | 5 | 30 | 1.39 | 64.51 |
| 3 | 5 | 5 | 30 | 1.39 | 64.58 |
| 6 | 5 | 5 | 30 | 1.38 | 64.70 |
| 12 | 5 | 5 | 30 | 1.38 | 64.93 |
| 1 | 5 | 10 | 30 | 1.50 | 60.81 |
| 3 | 5 | 10 | 30 | 1.50 | 61.04 |
| 6 | 5 | 10 | 30 | 1.48 | 61.36 |
| 12 | 5 | 10 | 30 | 1.47 | 61.70 |
| 1 | 5 | 20 | 30 | 1.87 | 51.17 |
| 3 | 5 | 20 | 30 | 1.82 | 52.27 |
| 6 | 5 | 20 | 30 | 1.75 | 53.70 |
| 12 | 5 | 20 | 30 | 1.65 | 55.88 |
| 1 | 5 | 30 | 30 | 2.26 | 41.60 |
| 3 | 5 | 30 | 30 | 2.12 | 44.44 |
| 6 | 5 | 30 | 30 | 1.94 | 47.83 |
| 12 | 5 | 30 | 30 | 1.70 | 52.27 |

Table C.6. Final values of key outputs for brain injuries with 6% affected area.

| **Interval (month)** | **Affected area (%)** | **Number** | **Onset (age)** | **Protein aggregation** | **Remaining neurons (%)** |
|---|---|---|---|---|---|
| **CONTROL** | | | | **1.32** | **67.33** |
| 1 | 6 | 1 | 30 | 1.33 | 66.80 |
| 3 | 6 | 1 | 30 | 1.33 | 66.80 |
| 6 | 6 | 1 | 30 | 1.33 | 66.80 |
| 12 | 6 | 1 | 30 | 1.33 | 66.80 |
| 1 | 6 | 5 | 30 | 1.41 | 63.83 |
| 3 | 6 | 5 | 30 | 1.41 | 63.90 |
| 6 | 6 | 5 | 30 | 1.40 | 64.03 |
| 12 | 6 | 5 | 30 | 1.39 | 64.27 |
| 1 | 6 | 10 | 30 | 1.60 | 58.52 |
| 3 | 6 | 10 | 30 | 1.56 | 59.27 |
| 6 | 6 | 10 | 30 | 1.54 | 59.66 |
| 12 | 6 | 10 | 30 | 1.52 | 60.15 |
| 1 | 6 | 20 | 30 | 2.08 | 46.37 |
| 3 | 6 | 20 | 30 | 1.97 | 48.48 |
| 6 | 6 | 20 | 30 | 1.88 | 50.37 |
| 12 | 6 | 20 | 30 | 1.73 | 53.30 |
| 1 | 6 | 30 | 30 | 2.47 | 36.38 |
| 3 | 6 | 30 | 30 | 2.28 | 39.97 |
| 6 | 6 | 30 | 30 | 2.07 | 43.92 |
| 12 | 6 | 30 | 30 | 1.79 | 49.13 |

Table C.7. Final values of key outputs for brain injuries with 7% affected area.

| **Interval (month)** | **Affected area (%)** | **Number** | **Onset (age)** | **Protein aggregation** | **Remaining neurons (%)** |
|---|---|---|---|---|---|
| **CONTROL** | | | | **1.32** | **67.33** |
| 1 | 7 | 1 | 30 | 1.33 | 66.69 |
| 3 | 7 | 1 | 30 | 1.33 | 66.69 |
| 6 | 7 | 1 | 30 | 1.33 | 66.69 |
| 12 | 7 | 1 | 30 | 1.33 | 66.69 |
| 1 | 7 | 5 | 30 | 1.44 | 63.01 |
| 3 | 7 | 5 | 30 | 1.43 | 63.21 |
| 6 | 7 | 5 | 30 | 1.42 | 63.33 |
| 12 | 7 | 5 | 30 | 1.41 | 63.58 |
| 1 | 7 | 10 | 30 | 1.74 | 55.42 |
| 3 | 7 | 10 | 30 | 1.63 | 57.41 |
| 6 | 7 | 10 | 30 | 1.61 | 57.85 |
| 12 | 7 | 10 | 30 | 1.58 | 58.56 |
| 1 | 7 | 20 | 30 | 2.32 | 41.27 |
| 3 | 7 | 20 | 30 | 2.12 | 44.69 |
| 6 | 7 | 20 | 30 | 2.00 | 47.12 |
| 12 | 7 | 20 | 30 | 1.82 | 50.75 |
| 1 | 7 | 30 | 30 | 2.65 | 31.57 |
| 3 | 7 | 30 | 30 | 2.41 | 35.99 |
| 6 | 7 | 30 | 30 | 2.19 | 40.24 |
| 12 | 7 | 30 | 30 | 1.86 | 46.09 |

Table C.8. Final values of key outputs for brain injuries with 8% affected area.

| **Interval (month)** | **Affected area (%)** | **Number** | **Onset (age)** | **Protein aggregation** | **Remaining neurons (%)** |
|---|---|---|---|---|---|
| **CONTROL** | | | | **1.32** | **67.33** |
| 1 | 8 | 1 | 30 | 1.33 | 66.58 |
| 3 | 8 | 1 | 30 | 1.33 | 66.58 |
| 6 | 8 | 1 | 30 | 1.33 | 66.58 |
| 12 | 8 | 1 | 30 | 1.33 | 66.58 |
| 1 | 8 | 5 | 30 | 1.48 | 61.97 |
| 3 | 8 | 5 | 30 | 1.45 | 62.48 |
| 6 | 8 | 5 | 30 | 1.44 | 62.61 |
| 12 | 8 | 5 | 30 | 1.44 | 62.87 |
| 1 | 8 | 10 | 30 | 1.90 | 51.98 |
| 3 | 8 | 10 | 30 | 1.70 | 55.45 |
| 6 | 8 | 10 | 30 | 1.68 | 55.99 |
| 12 | 8 | 10 | 30 | 1.64 | 56.92 |
| 1 | 8 | 20 | 30 | 2.50 | 37.04 |
| 3 | 8 | 20 | 30 | 2.25 | 41.40 |
| 6 | 8 | 20 | 30 | 2.11 | 44.12 |
| 12 | 8 | 20 | 30 | 1.89 | 48.27 |
| 1 | 8 | 30 | 30 | 2.81 | 27.24 |
| 3 | 8 | 30 | 30 | 2.53 | 32.29 |
| 6 | 8 | 30 | 30 | 2.29 | 36.77 |
| 12 | 8 | 30 | 30 | 1.94 | 43.13 |